Physiology of Electrically Excitable Cells

David McKinnon

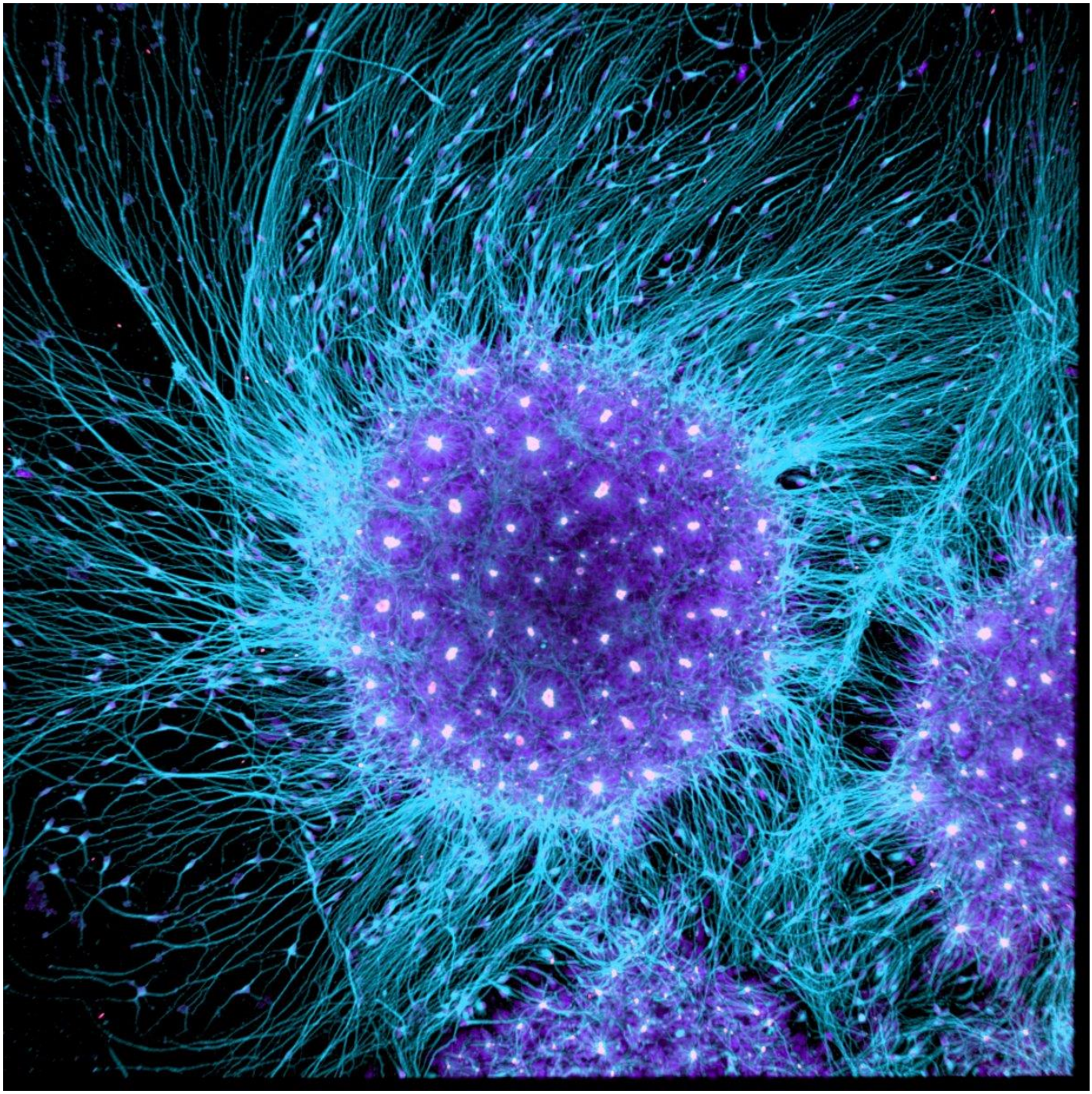

Contents

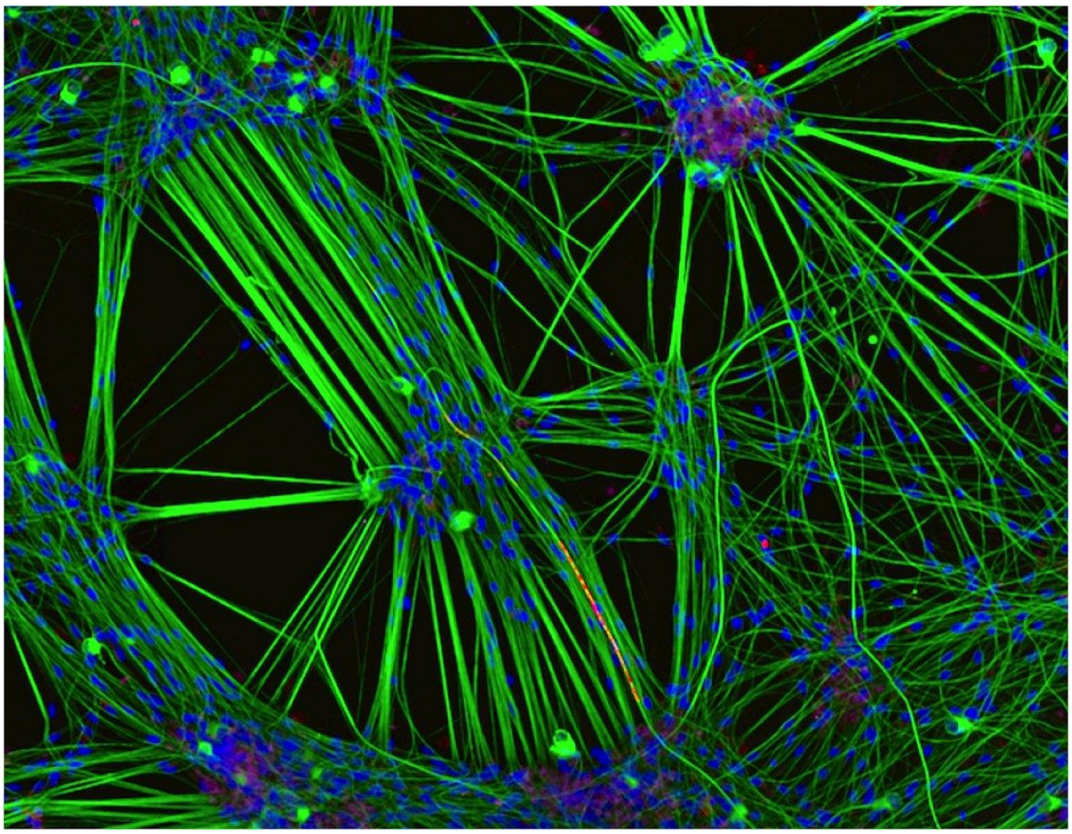

Preamble

Why should a student invest time and effort in learning the information contained in this text? There is no shortage of other, potentially more interesting or enjoyable things to do. There are waves to catch, bands to hear, potential mates to chase and a seemingly endless array of alternative subjects to learn. Any one of these other subjects might be more useful than the topic of this particular text. So why bother? There are two good reasons to continue, one intellectual and one practical.

The two greatest unsolved mysteries in science are the origin of life and how a collection of cells in the brain can give rise to consciousness, emotion and the myriad of other sensations that collectively give us the feeling of being a human being. The origin of life is a historical event, which is not now and may never be subject to experimental analysis. Consequently, understanding of this problem may be forever out of our reach. In contrast, brain function is amenable to experimental study at every level. The current impediment to understanding appears to be the massive complexity of neural systems, a more extreme example of a general problem in understanding biological systems. There is complexity at the molecular, cellular and anatomical/circuitry levels as well as complexity at the organizational/algorithmic levels. It is currently believed that this complexity is not necessarily out of reach of human understanding. Admittedly, scientists have held this belief for some time with only modest progress to show for their efforts but, given the rate of technical advances in the field, this belief is not purely a product of their irrational hopes and dreams. Even partial success will have an impact on a broad range of human endeavors, from the understanding of mental diseases to questions about free will and the relationship between the individual and society.

This text focuses primarily on the 'nuts and bolts' of the nervous system, the electrical and biochemical functions of neurons. Unlike a computer program, where there is an overarching algorithmic design that can potentially be instantiated in multiple, very different hardware implementations, nervous system function is a tightly integrated product of evolution. The higher level functions of the nervous system are strongly constrained by the long evolutionary history of the underlying molecular and cellular biology. Brain function is intimately tied to the particularities and peculiarities of this biology. For the brain, the computer engineering dichotomy between hardware and software does not existent. There is an intermingling of functions at every level of organization. Cognitive function, in all its forms, has a material basis that is directly knowable, subject to description and experimentation. Theories of brain function must ultimately be tied into our understanding of the material basis of neural function. A failure to recognize this simple reality has contributed to many of the more egregious failures to describe cognitive function and treat mental illness.

The second reason is practical, there is very little information in this text that will not be useful to anyone engaged in the clinical sciences - from why it is not a good idea to eat too many bananas to understanding how local anesthetics work.

1 Cell Physiology

Many cells in the body have highly sophisticated electrical signaling mechanisms. These mechanisms allow electrical impulses to travel within and between the cells of the nervous system. Electrical signaling translates 'thought' into action by triggering contractions in muscle and facilitates the control of organs within the body by triggering the release of hormones from various endocrine organs.

The proteins that underlie these specialized electrical signaling functions are evolutionarily ancient. In most cases considerable similarity can be found between proteins used by the human brain for electrical signaling and proteins found in single cell prokaryotes. This is because cells, of all kinds, have to solve a common set of basic cell physiological problems. These problems include maintenance of salt balance, maintenance of osmotic balance, transport of useful solutes into the cell and transport of waste products out of the cell. The proteins that underlie these basic cellular functions have been elaborated and modified during the course of evolution to support other complex functions, including the electrical excitability of neurons and muscle cells. This elaboration of protein function by evolution has limits, however, and the molecular complexity of a neuron in a fruit fly brain and one in a human brain is similar. The much larger repertoire of behaviors seen in humans compared to flies is primarily a function of a more complex nervous system rather than the product of significantly more complex molecular and cellular physiology. Neural development in humans has accreted enormous complexity during the course of evolution, largely due to the evolution and elaboration of gene regulatory function.

1. Evolution of Cellular Life

The events leading to the evolution of cellular life are very poorly understood. This ancient, apparently unique, historical event cannot be readily replicated, making it inaccessible for systematic study. Consequently, most writing on this topic remains highly speculative, if not hopelessly deluded. Even a fundamental question such as whether the pathway towards life began first with replicating nucleic acids or from a protein based origin currently remains unresolved.

The evolution of the first protocells, small cells with a continuous cell membrane, was a major step in the evolution of life. Before the existence of membrane delimited structures it would have been difficult, or impossible, to define discrete individuals, whatever their biochemical basis. The cell membrane creates the basic delineation between self and non-self, creating the potential for competition between individuals. From the time when individual protocells appeared it is reasonable to believe that the theory of evolution can explain all the subsequent pathways to more complex and diverse life forms. Evolution of the cell membrane represents the dividing line between life, as it is commonly understood, and non-living biochemical processes.

The cell membrane's critical role in the evolution of single cells comes about because it performs functions that are somewhat analogous to the property and patent laws of a capitalist economy. Like the property laws, the cell membrane distinguishes private property, what is inside the cell, from common property, everything outside the cell. This allows the cell to concentrate useful resources inside the cell (e.g. ATP, glucose) restricting them for the private use of the cell.

An even more important property is that the cell membrane allows the cell to effectively patent any novel innovations occurring in that cell's genetic material by restricting the sharing of novel

proteins and metabolic products. If a cell has an advantageous mutation in its genetic material, that cell and its progeny will retain sole rights to the benefits afforded by that mutation for some time, potentially conferring a competitive advantage to cells in this lineage relative to other cells. The cell membrane can function in this way because it is an effective barrier to the transport of charged and polar molecules.

Physical Constraints on Cellular Physiology

Although the steps leading to the evolution of membrane bound, cell based life are not well understood there are several well defined physical constraints that definitely had to be resolved before this could occur. Three particular problems were:

1. Transport of metabolites across the cell membrane
2. Regulation of internal calcium concentration
3. Regulation of osmotic balance/cell volume

The solutions selected for these problems set the basic plan for all subsequent cellular life and reverberate to the present day. Much of the particular functionality of the neurons in your brain derive from the solutions selected several billion years ago to resolve these narrow apparently simple physical problems. The rest of this chapter and the next describe the basic solutions to these problems.

2. Water

It is difficult to ignore the central role of water in virtually every aspect of cell physiology. Water is essential for life, as we understand the term. The human body is composed primarily of water molecules, which make up about 60% of the total body weight and 99% of the total number of molecules.

Water is a polar molecule, meaning that there is an uneven distribution of charge within the water molecule. The bonds between the oxygen and two hydrogen atoms are polar covalent bonds. The polarity of the covalent bonds results from the high **electronegativity** of the oxygen atom relative to the hydrogen atom. As a consequence, a partial charge distribution exists such that there is a local positive charge on each hydrogen atom and a partial negative charge on the oxygen atom. The uneven distribution of electrons due to the nature of the H-O bond causes the water molecule to act as a **dipole**, meaning that the molecule has a positive and negative pole (Figure 1).

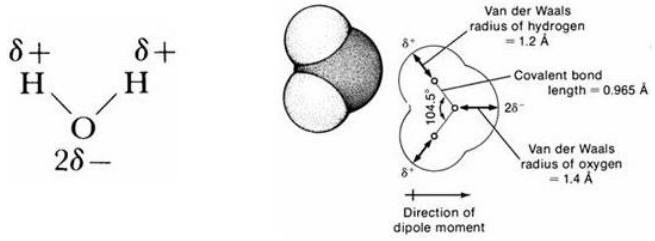

Figure 1 Dipole nature of water, a polar molecule. There is a partial negative charge (2δ-) on the oxygen atom and partial positive charges (δ+) on the two hydrogen atoms.

Water can form hydrogen bonds between the positively charged hydrogen atoms and negatively charged oxygen atoms in the neighboring water molecules. Since the angle between the two covalent bonds of water is about 105°, groups of hydrogen-bonded water molecules form tetrahedral arrangements (Figure 2).

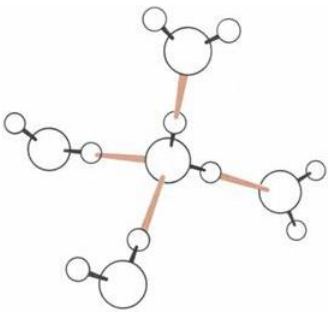

Figure 2 Hydrogen bonding between water molecules.

By itself pure water is not a good conductor of electricity. The conduction of electrical current by an aqueous solution depends primarily on the number and nature of the charged ions found in that solution. These ions can dissolve in water because of the polar nature of water molecules. Water is generally a good **solvent** for ionic compounds, which include salts, acids and bases. These solutes all share the property of **dissociating** into ions when dissolved in water.

3. Ions

Ions in Solution

Two of the most common ions in the body are Na^+ and Cl^-. NaCl is common table salt. The need to replenish these ions in the body is one reason why salty foods are perceived by animals as tasty. The NaCl molecule is uncharged and cannot carry a current in its undissociated form. In the NaCl crystal, the Na^+ and Cl^- ions are firmly held together by ionic bonds between the positively charged Na^+ ions and the negatively charged Cl^- ions (Figure 3).

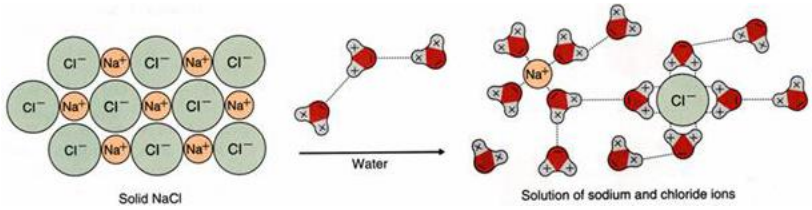

Figure 3 Dissociation of Na^+ and Cl^- ions in water.

Water can dissolve the NaCl crystal, just as it can dissolve most other ionic compounds (salts, acids, bases), because the dipolar water molecules can overcome the electrostatic interactions between the individual ions. The partial negative charge of the oxygen allows weak electrostatic binding with the positively charged Na^+ ion and the partial positive charge on the hydrogen allows weak electrostatic binding with the negatively charged Cl^- ion. The water molecules surround the ions, orienting themselves so that their positive poles face anions and their negative poles face cations. These shells of water molecules are known as **hydration shells** (Figure 3).

Dissociated ions are the primary current carriers in the body. They are known collectively as **electrolytes**, because of their ability to conduct electricity. Ions that have a net positive charge are called **cations**, while those that have a net negative charge are called **anions**. A failure of athletes to replenish electrolytes during endurance or other sporting events can produce disruption of the electrical activity in some of their electrically excitable cells, with potentially tragic effect if cardiac function is disrupted.

Distribution of Ions in the Body

The water in the body can be divided into two main compartments: intracellular and extracellular. These two compartments are separated by the cell membranes of individual cells. Typical values for the concentration of the most common ions in these two compartments are given in Table 1. These specific values will vary among different species and between different cells in the body but the general principle is that all animal cells have a relatively high intracellular concentration of K^+ ions, a low intracellular concentration of Na^+ ions and a very low intracellular concentration of Ca^{2+} ions. The high concentration of NaCl in the extracellular fluid is similar to sea water and reflects our origins as ocean living organisms. There is a relatively high concentration of fixed anions inside the cell. These comprise all the organic compounds synthesized or sequestered by the cell, which have a net negative charge.

Table 1. Ion concentrations in the intracellular and extracellular fluids of a typical mammalian cell

Ion	Intracellular Concentration (mM)	Extracellular Concentration (mM)
K^+	125	5
Na^+	12	120
Cl^-	5	125
Ca^{2+}	1 x10^{-4} (100 nM)	2
A^-	108	0

A^- = the fixed anions, sum of all the proteins, amino acids (aspartate and glutamate), inorganic ions (sulfate and phosphate), nucleotides, DNA, RNA that are located inside the cell.

Maintenance of this unequal distribution of ions between the inside and outside of the cell is a primary function of the cell and dictates much of the basic cellular physiology of every cell.

4. Cell Membrane

The role of the cell membrane in distinguishing the intracellular fluid from the extracellular fluid is made possible by the fact that it is such an effective barrier to the transport of ions and polar molecules.

Lipid Bilayer Structure

Cell membranes are composed of lipids and proteins. The predominant lipids in the cell membrane are **phospholipids**. Phospholipids have two distinct regions (Figure 4). A polar region that is **hydrophilic** (water loving) that interacts with water molecules and a nonpolar region that is **hydrophobic** (water hating). Molecules that have a mixed chemical nature like this are known as **amphipathic** molecules.

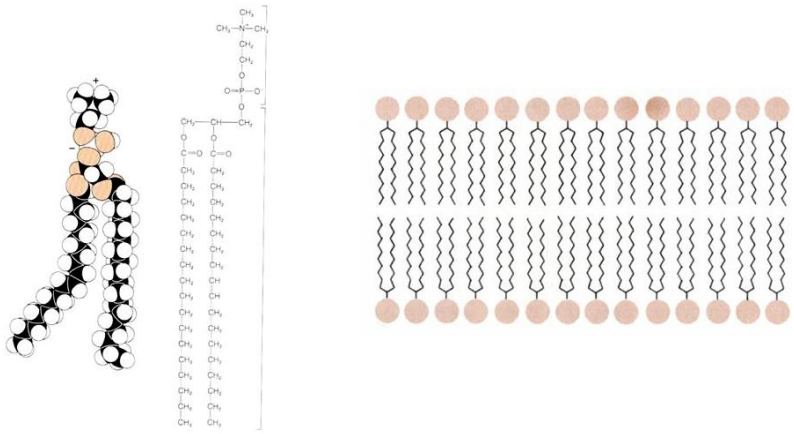

Figure 4 (Left panel) Structure of a phospholipid molecule. Note the charged head of the molecule and the two long hydrophobic tails. (right panel) Arrangement of phospholipids in a lipid bilayer, with the heads pointing out to the aqueous solution and the hydrophobic heads sequestered in the interior of the membrane.

The lipids assemble into a **lipid bilayer** (Figure 4), which is the lowest energy arrangement for phospholipid molecules. In this arrangement the hydrophobic tails point in towards the center of the bilayer, minimizing their interaction with water molecules. The hydrophilic heads interact with the water molecules surrounding the membrane.

Although the lipid bilayer is very thin, it is a very effective barrier to the diffusion of many biologically important molecules. The interior of the lipid bilayer functions like a very thin layer of oil presenting an almost impermeable barrier to the diffusion of polar or charged molecules. In contrast, hydrophobic molecules can pass easily because they can dissolve into the hydrophobic core of the lipid bilayer.

Charged molecules like ions are only stable in a highly polarizable media such as water. It is essentially impossible for a charged molecule to cross the lipid bilayer because the core of the bilayer is non-polarizable. In electrical terms, it has a low dielectric constant.

If the cell membrane was composed only of a lipid bilayer only hydrophobic molecules could enter and leave the cell, which would greatly limit the function of the cell. Real cell membranes also contain proteins, and a major function of these proteins is to facilitate the movement of ions and polar molecules across the membrane.

Cell Membrane Structure

Current ideas about how the cell membrane functions originate with the fluid mosaic model of Singer and Nicolson. In their model a class of proteins, known as **integral membrane proteins**, are sequestered within the lipid bilayer, something like icebergs floating in a lipid sea (Figure 5). These proteins have amphipathic properties, meaning that they have both nonpolar portions, which are buried in the hydrocarbon core of the bilayer, and polar or charged portions, which protrude from the bilayer to form a hydrophilic surface that interacts with the aqueous phase. Typically, charged residues in the protein are only found in regions that contact the aqueous solution.

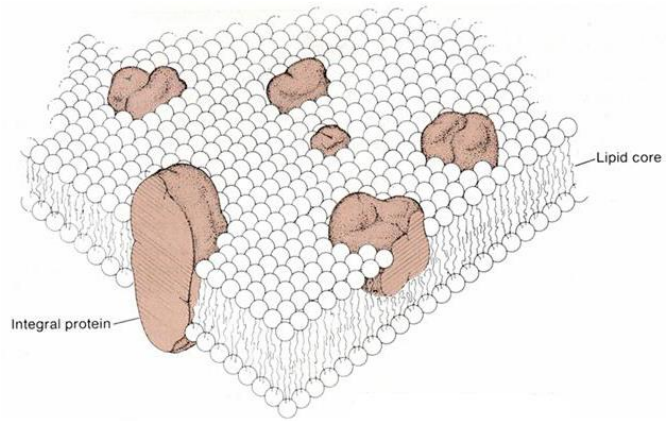

Figure 5 Fluid mosaic model of the cell membrane, showing the integral proteins and the lipid bilayer.

In addition to integral membrane proteins there are also **peripheral membrane proteins**, which are typically located on the inner surface of the cell membrane (Figure 6). These are often linked to **cytoskeletal proteins**, which control cell shape and motility. In the original model, the integral membrane proteins were considered to move freely within the plane of the lipid bilayer. In fact, the majority of proteins are tethered to a dense network of other proteins, forming large protein complexes.

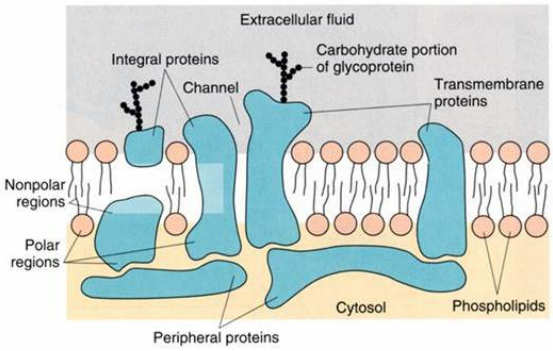

Figure 6 Multiple types of proteins contribute to the formation of the cell membrane.

Typically, the **transmembrane proteins** (those that cross the cell membrane to the extracellular surface) have covalently linked carbohydrates on their extracellular surface (Figure 6) and are known as **glycoproteins**, a term that reflects the contribution of carbohydrate moieties to the protein structure.

Synthesis of Membrane Proteins

Synthesis of integral membrane proteins, with one or more membrane spanning regions, is a complex problem for the cell, particularly achieving the correct topology of the protein in the membrane. Integral membrane proteins are synthesized by ribosomes that become tethered to a translocator complex (translocon) located in the endoplasmic reticulum (ER) membrane (**Figure 7**). Typically, the first transmembrane (TM) domain of the nascent peptide functions as a targeting sequence. This transmembrane sequence is recognized by the signal recognition particle (SRP), which in turn binds to the SRP receptor in the ER membrane. Following successful targeting to the ER membrane, the complex of ribosome and nascent peptide is transferred to the translocon. For proteins such as

voltage-gated channels the amino terminus of the protein is located intracellularly and the first membrane spanning domain functions as a start-transfer signal, causing the translocon to mediate the translocation of the peptide trailing this transmembrane sequence through the translocon pore. This displaces the intralumenal plug that normally gates the translocon channel. Transfer of the peptide continues until the translocon encounters a stop-transfer signal (typically the second membrane spanning domain) causing the translocon to stop transferring the peptide across the membrane, thereby allowing the peptide to accumulate on the cytoplasmic side. In general, alternating start and stop-transfer signals in the protein's peptide sequence will combine to allow the channel to assemble with the correct membrane topology. This topology signaling can include cues from regions of the polypeptide outside the transmembrane domain of the protein and more complex schemes may be required to ensure that proteins with non-canonical transmembrane domains, such as voltage sensors and channel pores, can achieve the correct topology.

In addition to having a trans-membrane pore for movement of the peptide across the membrane, the translocator complex is hinged and can open to allow the hydrophobic membrane spanning domains of the ion channel-forming protein to partition into the hydrophobic core of the membrane (**Figure 7**). By this means, the channel-forming protein is integrated into the lipid bilayer of the membrane.

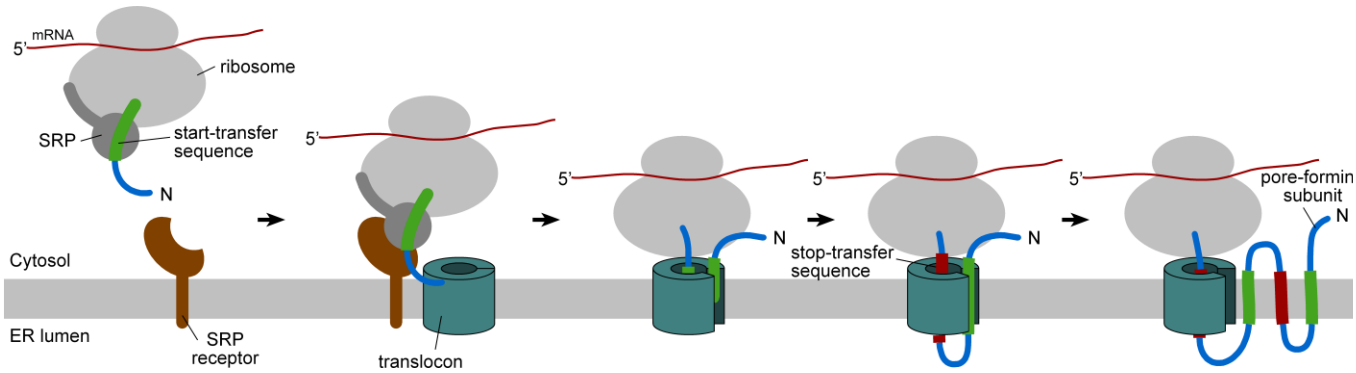

Figure 7 Most integral membrane proteins have hydrophobic transmembrane (TM) domains of 20–25 residues in length that form membrane spanning α-helices in the fully assembled protein (marked with red and green in the figure). The first of these TM domains acts as a targeting sequence to target the nascent peptide to the translocon in the ER membrane. This sequence is recognized by the signal recognition particle (SRP), which targets the entire complex to the ER membrane by binding to the SRP receptor. The ribosome and nascent peptide then attach directly to the translocon. The first TM domain is recognized as a start-transfer sequence by the translocon. This initiates movement of the downstream peptide through the translocon pore into the ER lumen. During subsequent translation of the protein the TM domains each signal to the translocon to start or stop transfer of the peptide across the ER membrane. The translocon has a lateral gate that can open to allow lateral transfer of each of the hydrophobic TM domains into the lipid bilayer.

Translocation of the growing peptide occurs co-translationally, meaning that the transfer of the protein into the ER lumen and membrane occurs at the same time as the protein is being synthesized. In general, the pore-forming subunit will first undergo further maturation, aided by proteins associated with the translocon complex such as oligosaccharyl transferase as well as by ER resident

membrane chaperones (such as calnexin). Glycosylation of the channel peptide by oligosaccharyl transferase also occurs cotranslationally and can contribute to establishing the correct topology.

Diffusion of Hydrophobic Molecules through the Lipid Bilayer

There are several ways in which a **solute** can either enter or leave the cell. If the solute is hydrophobic (lipophilic) and can dissolve into the lipid membrane, it can cross the cell membrane by diffusion since the lipid bilayer does not present a diffusion barrier. Many key molecules can act like this: oxygen, carbon dioxide, fatty acids and steroid hormones are all examples of nonpolar molecules that diffuse rapidly through the lipid portions of membranes.

The majority of molecules in the cell cannot diffuse through the membrane, or diffuse only poorly. For example, most of the molecules that make up the intermediate stages of the various metabolic pathways are ionized or polar molecules that cannot cross the cell membrane. There is a good reason for this, it is inefficient for the cell to expend energy producing metabolic intermediates that can then simply diffuse out of the cell in an uncontrolled manner. For the typical polar and charged molecules found inside the cell the lipid bilayer represents an almost complete barrier to passive diffusion.

5. Membrane Transport

A diverse set of proteins facilitate the movement of polar and charged molecules in various ways across the cell membrane. These proteins fall into three major classes:

Table 2. Classes of integral membrane proteins involved in transport of ions and polar molecules	
Pumps	require energy in the form of ATP to move ions up their concentration gradients
Transporters	do not directly use energy in the form of ATP, are often linked to ion gradients that indirectly provide energy
Ion channels	facilitate diffusion of ions by creating pores across the cell mem-brane

6. Membrane Transport – Pumps

Most of the solutes distributed across the cell membrane are not in equilibrium. In particular, the major inorganic ions have steep distribution gradients across the cell membrane (Table 1). As a consequence, energy must be expended in order to maintain those transmembrane concentration gradients. Typically, the source of energy is chemical energy in the form of ATP. If the cell is poisoned so that ATP is no longer produced, then the transmembrane gradients dissipate and the cell dies.

The proteins that actively transport solutes against their concentration gradients are known as membrane pumps. Four pumps have been identified, each is an ATPase and each is involved in transporting one or more of the following ions: Na^+, K^+, H^+ or Ca^{2+}.

Table 3. Membrane pumps	
Na,K-ATPase	maintains the Na^+, K+ ion gradients across the cell membrane
Ca-ATPase	maintains the very low intracellular Ca^{2+} ion concentration
H-ATPase	maintains intracellular pH (H^+ ion concentration)
H,K-ATPase	acid secretion in stomach and kidneys

Na,K-ATPase

An argument can be made that the Na,K-ATPase pump is the most important protein in the cell because, in most cells, it is the single largest consumer of cellular energy. Surprisingly, the maintenance of ion gradients is the most energetically demanding process within many cells. More expensive than many other apparently more sophisticated functions, such as protein synthesis.

The Na,K-ATPase pump actively pumps Na^+ ions out of the cell against their concentration gradient. It simultaneously pumps K^+ ions into the cell and the metabolic energy for both of these functions is provided by the hydrolysis of ATP to ADP (Figure 8). Two K^+ ions from outside the cell are exchanged for three Na^+ ions from inside the cell.

The pump is known as an **electrogenic** pump because there is an associated electrical current, the net movement of one positive ion out of the cell for every cycle of the pump. This current is generally very small relative to other ion currents in electrically excitable cells.

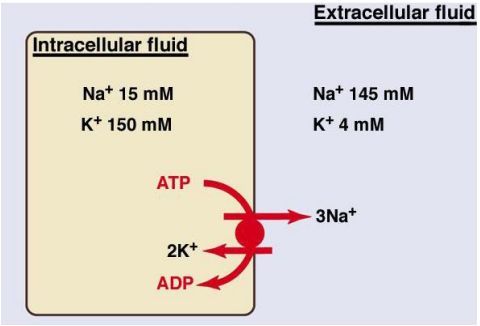

Figure 8 Movement of metabolites and ions during one cycle of the Na,K-ATPase pump .

The Na,K-ATPase is present in the plasma membranes of all animal cells. It is responsible for the fact that all animal cells have a relatively high intracellular concentration of potassium ions and a low intracellular concentration of sodium ions.

The pump can be poisoned or inhibited with the drug **ouabain**, which ultimately results in the death of the cell. Ouabain was originally isolated from plants in Africa and was used to poison arrow tips. Surprisingly, similar compounds are used in modern medicine to block the pump in the treatment of some forms of congestive heart failure.

Other pumps

The Ca-ATPase is found in both the cell membrane and in the membrane of several organelles within the cell. As shown in Table 1, the internal concentration of Ca^{2+} ions is very low compared with the extracellular Ca^{2+} ion concentration, in large part due to active pumping of Ca^{2+} ions out of the cell. There is an approximately 1:20,000 gradient in Ca^{2+} ion concentration gradient between the interior of the cell and the extracellular fluid.

The other two pumps move hydrogen ions, controlling intracellular or extracellular acidity. The H-ATPase helps regulate intracellular pH in all cells. The H,K-ATPase is involved in acid secretion by specialized cells in the stomach and kidneys.

Structure and Function of Membrane Pumps

All four pumps work similarly and have similar structures. They function by translocating an ion binding surface from inside the cell to outside the cell and then a modified surface from outside back to the inside of the cell. The movement of this surface is produced by a **conformational change** in the shape of the protein. The hydrolysis of ATP provides the energy for this change in protein

shape. The kinase function of the pump is used to phosphorylate the pump protein, which then induces the first conformational change (Figure 9). Dephosphorylation of the pump, to remove the covalently linked phosphate group, results in the reversion of the pump to its original conformation.

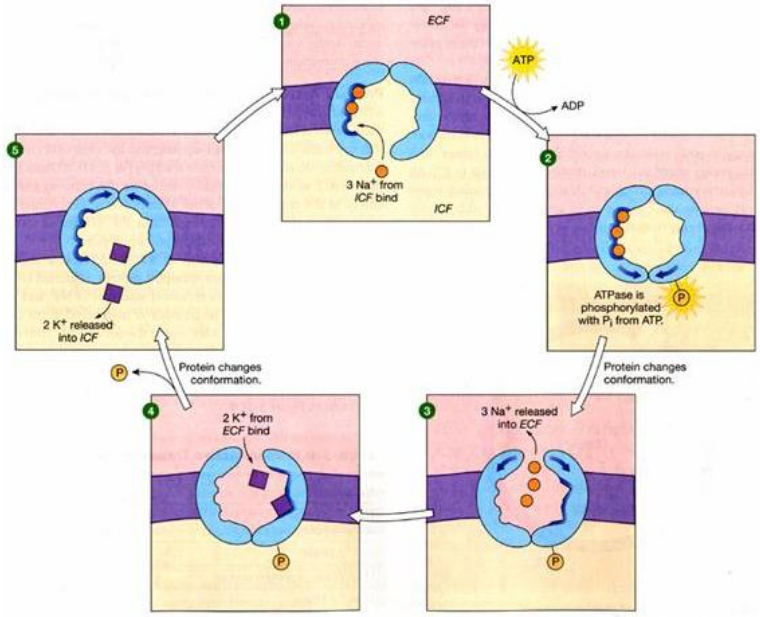

Figure 9 Cycle of Na^+ and K^+ binding and movement during one cycle of the Na,K-ATPase pump.

The detailed structure of the Ca-ATPase pump has been solved. It is a large protein and has ten membrane spanning domains (Figure 10). There are two binding sites for Ca^{2+} ions within the membrane and it has a very large intracellular domain, which contains the ATPase enzyme that hydrolyzes ATP. The pump undergoes large rearrangements upon phosphorylation and dephosphorylation of the ATPase site (Figure 10). This results in the rearrangement of the alpha helices in the membrane so that the Ca^{2+} binding sites are moved from facing the intracellular region of the membrane to facing the extracellular region and also causes a reduction of the affinity for Ca^{2+} ion binding so that the ions are released into the extracellular fluid or the interior of membrane bound organelles.

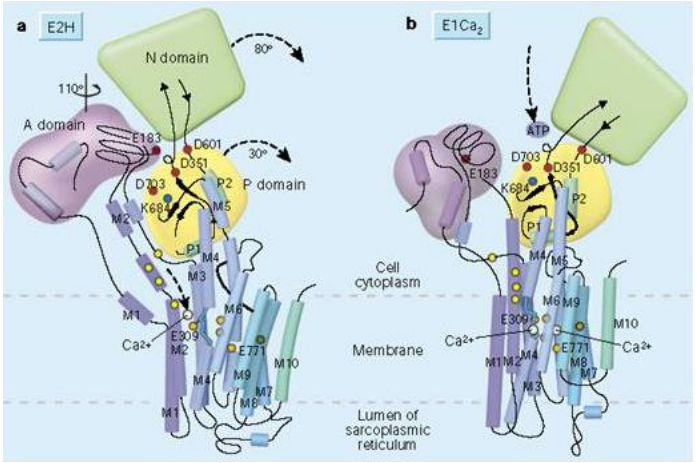

Figure 10 Conformational changes of the Ca-ATPase before and after phosphorylation.

This requirement for a large conformational change limits the rate at which ion pumps can move ions across the membrane. In general, the pumps are continuously active in order to keep up with the flux of ions through the membrane's ion channels, which allow ions to move very rapidly down their ion concentration gradients. In most cells the ion channels turn on for only brief periods of time in order to limit the amount of work required of the pumps. An exception to this is found in cardiac myocytes, where the Ca^{2+} pumps have to return Ca^{2+} ions back to the lumen of the sarcoplasmic reticulum after it has escaped through Ca^{2+} channels that remain open for the duration of the cardiac contraction. In this case, very high concentrations of the Ca-ATPase pump are required in the SR membrane in order to keep up with the calcium release and this protein makes up a large fraction of the total membrane protein in cardiac cells. This is one reason why we are so vulnerable to ischemia during a heart attack. When blood flow stops even for a short period of time there can be significant damage to the cardiac muscle because it fails to meet the energy demands of the Ca-ATPase pump.

Ion Gradients as Sources of Cellular Energy

The generation of ion gradients by pumps is one way in which the cell can convert chemical energy, stored in the form of ATP, into another form of chemical energy, in this case a concentration gradient of ions. The gradient of ions acts as a source of chemical energy that can be used for other cellular functions such as **secondary active transport**.

The generation of ion gradients can also function to convert chemical energy into electrical energy. The ion gradients created by the pumps allow the generation of an electrical potential across the cell membrane, known as the **membrane potential**.

7. Membrane Transport - Transporters

Pumps and ion channels only move ions across the cell membrane. All cells, however, have to transport a large number of solutes in addition to ions. These solutes belong to a diverse set of biochemical molecules that are useful to the cell, including amino acids and glucose. In general, the different chemical natures of these solutes requires that there are specialized transport systems for each type, or at least class, of molecule that is transported. There are two types of transport systems, those that facilitate the movement of solutes down their concentration gradients and those that actively transport the solute up a concentration gradient (Figure 11). As mentioned earlier, hydrophobic molecules can move freely cross the membrane without the requirement of a specific transport system. It would be self-defeating to actively transport these molecules since their movement is not limited by the cell membrane and they could easily diffuse back across the membrane.

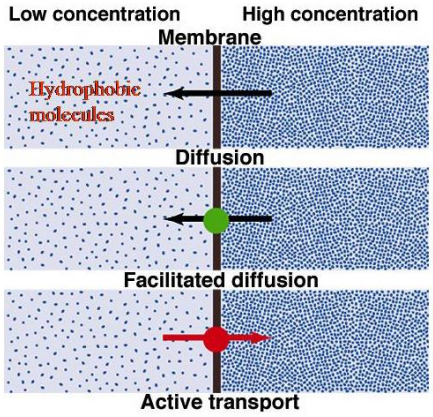

Figure 11 Hydrophobic molecules can diffuse down their concentration gradient without any specialized transport system. Facilitated diffusion transport systems allow the movement of hydrophilic solutes down their concentration gradients. Active transport can move hydrophilic solutes across the membrane up a concentration gradient.

Facilitated Diffusion

The simplest of all the membrane transport mechanisms is known as **facilitated diffusion**. It does not require any energy input. Solutes simply diffuse down their concentration gradients. The facilitated transporter proteins provide a wrapper to allow hydrophilic molecules to pass across the cell membrane by avoiding contact with the lipid bilayer (Figure 12).

An important example of facilitated transport is the **passive glucose transporter**, which is found in the membrane of most cells. This transporter facilitates the movement of glucose from the blood stream into the cells of most organs, where it is used as an energy source. A transporter is required because glucose is a polar molecule that cannot otherwise cross the cell membrane. Without this transporter most cells would not be able to use the glucose produced by the breakdown of ingested food.

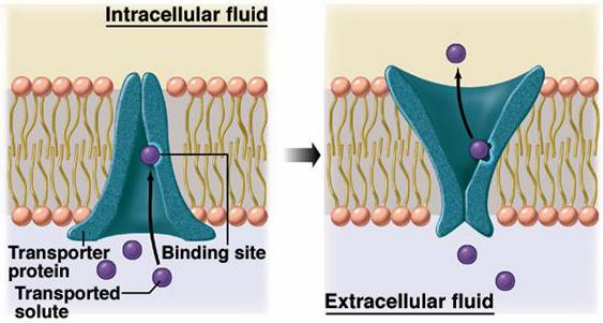

Figure 12 The solute binding site of a facilitated transporter flips from one side of the membrane to the other allowing solutes to move down their concentration gradient.

Secondary Active Transport

The gradient of sodium ions across the cell membrane generated by the Na,K-ATPase pump is a form of stored energy. This energy can be used by transport proteins to move solutes up their concentration gradients. These transport proteins are known as **secondary active transporters**. They are called secondary because they use chemical energy stored in the form of an ion gradient rather

than directly use ATP. They are active transporters, like pumps, in that they move solutes up a concentration gradient.

An important example of a secondary active transporter is the **Na^+/glucose transporter** (Figure 13). In addition to having a binding site for glucose the glucose transporter has an additional binding site for a Na^+ ion. The binding of the Na^+ ion to the transporter alters the affinity of the binding site for glucose. The change is brought about through allosteric modification of the protein's conformation as a result of ion binding. One glucose molecule is translocated up its concentration gradient at the cost of one Na^+ ion moving down its concentration gradient.

The Na^+/glucose transporter is used to actively transport glucose out of the intestines and into the blood stream and also out of the kidney tubules and back into the blood.

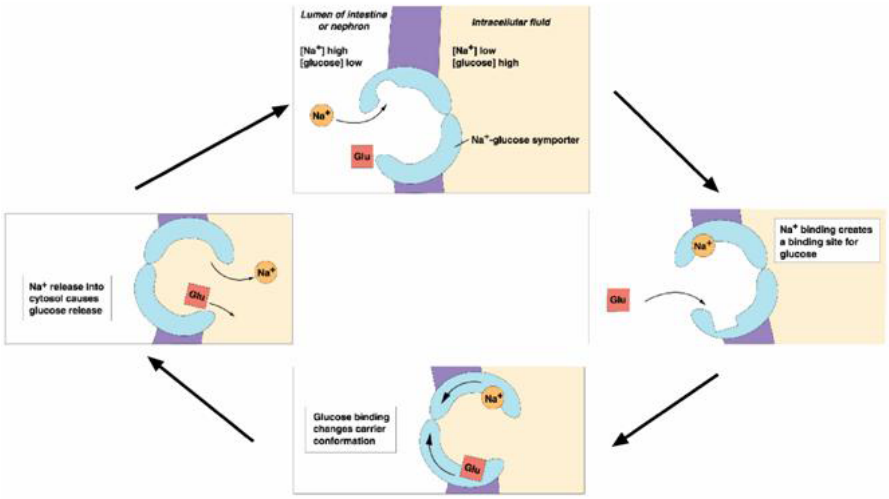

Figure 13 Na^+/glucose transporter.

During secondary active transport a solute can be transported either into the cell (**cotransport**) or out of the cell (**countertransport**). In both cases, however, Na^+ ions move into the cell, down their concentration gradient (Figure 14).

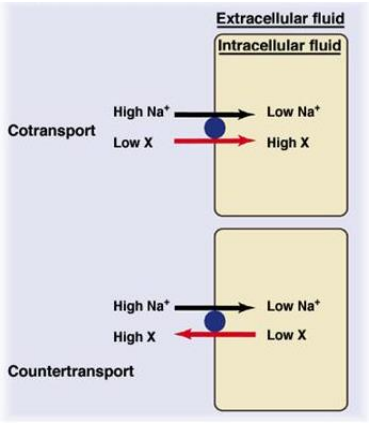

Figure 14 Cotransport and countertransport.

Another important secondary active transporter is the Na-Ca countertransporter, or **Na-Ca exchanger**. This uses downhill movement of sodium ions into the cell to move calcium ions out of the cell by secondary active transport. Other transporters linked to the sodium ion gradient move **amino**

acids. Amino acids can be actively transported out of the kidney tubules and into the blood by sodium-driven transporters. Related transporters mediate the reuptake of some neurotransmitters from the synaptic cleft in the nervous system.

Structure of Secondary Active Transporters

The LacY transporter is the prototype for transporter proteins. The LacY transporter mediates the coupled cotransport of lactose and protons (H^+) down a proton gradient in prokaryotyes. It has a roughly symmetrical clamshell-like structure with twelve membrane spanning domains (Figure 15).

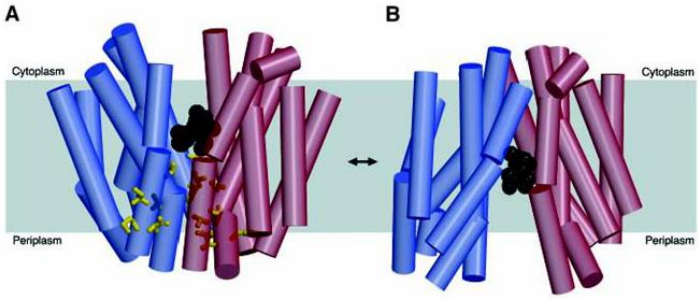

Figure 15 Structure of lactose permease (LacY). Note the two different conformations of the transporter

Relatively large movements of the protein are required to produce the translocation of the solute binding site. Like pumps, active transporters move solutes slowly compared to the movement of ions through ion channels.

8. Membrane Transport - Ion channels

The function of ion channel proteins is captured almost perfectly by their name, they are channels through which ions can pass across the membrane. Ion channels are integral membrane proteins and they shield the charged ions from the hydrophobic lipid bilayer as the ions cross the cell membrane (Figure 16). One key feature of ion channels is that they show **ion selectivity**. There are channels that only let K^+ ions to pass and channels that only let Na^+ ions to pass.

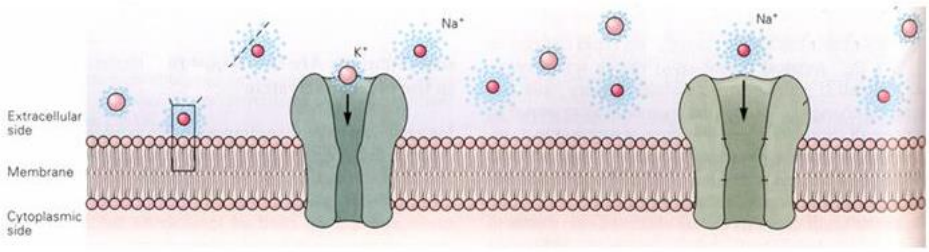

Figure 16 A K^+ selective ion channel and a Na^+ selective ion channel in the cell membrane.

At rest, in a typical cell, only a small number of channels are open and available to pass ions at any one time. Collectively, the channels open in a resting cell are known as the **leak channels** and these leak channels are predominantly K^+ selective with few or no Na^+ channels open. As a consequence, at rest, the cell membrane is predominantly permeable to K^+ ions.

Ion channels are found in the cell membrane of all cells in the human body and in the cell membranes of almost all living organisms, and many viruses. Ion channels are of particular interest in electrically excitable cells because of their key role in generating electrical excitation. The other two types of transporters are also ubiquitous and create the basic cellular environment necessary to

support electrical activity, as well as many other cell functions. The structure and function of ion channels will be described in detail in Chapter 2.

9. Summary of Mediated Membrane Transport Systems

Figure 17 provides an overview of all the different mediated transport systems found in a typical cell membrane. Mediated transport implies the use of a protein molecule for the movement of a solute across the cell membrane, as opposed to simple diffusion of hydrophobic solutes through the lipid bilayer.

As noted, the Na,K-ATPase is arguably the single most important transport system in mammalian cells. It creates the nonequilibrium ion distributions, which produce electrical potential energy in the form of the membrane potential, so important in electrically excitable cells, and the sodium ion gradient, which provides the chemical energy source for the secondary active transporters. Only the facilitated diffusion systems function independently of the Na,K-ATPase pump.

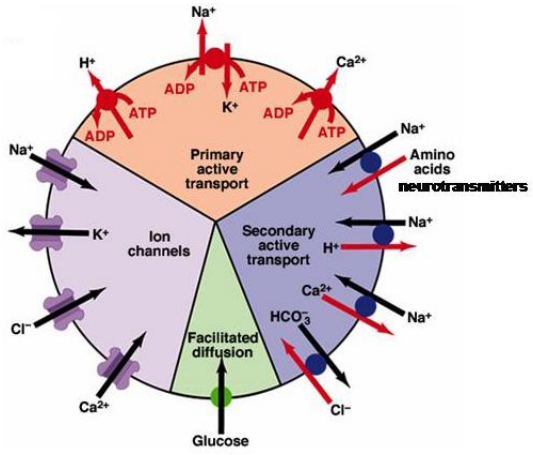

Figure 17 Summary of mediated membrane transport systems.

10. Regulation of Internal Ca^{2+} Ion Concentration

Intracellular Ca^{2+} ion concentrations are maintained at very low levels inside the cell and there is a very large concentration gradient of Ca^{2+} ions across the cell membrane (Table 4).

Table 4. Intracellular and Extracellular Calcium Ion Concentrations

	Intracellular	Extracellular
Ca^{2+} concentration	100 nM	2 mM

There are a multitude of transport systems that contribute to the regulation of the internal Ca^{2+} ion concentration (Figure 18). The Ca-ATPase pump is found in the cell membrane and several organelle membranes. It actively pumps Ca^{2+} ions out of the cell or into intracellular organelles (mitochondria and endoplasmic reticulum), where the Ca^{2+} ions are sequestered. In addition, there is the Na-Ca exchanger that uses the energy of the Na^+ ion gradient to transport Ca^{2+} ions out of the cell. Calcium binding proteins are another important part of the system. These proteins bind Ca^{2+} ions and act like buffers, rapidly reducing Ca^{2+} ion concentrations following an influx of Ca^{2+} ions through open calcium channels. These buffers give the more slowly acting pump and transporters some time to

remove the ions from the intracellular fluid. The buffers limit the duration and extent of the change in free Ca^{2+} ion concentration within the cell.

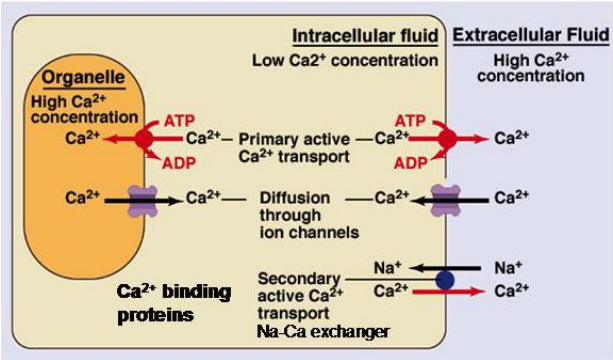

Figure 18 Summary of the various systems for handling Ca^{2+} ions within the cell.

Ca^{2+} Ions as Second Messengers

Perhaps oddly, given the effort that cells expend in keeping internal Ca^{2+} ion concentrations low, Ca^{2+} ions have an important role as intracellular signaling molecules. Although an apparently unlikely candidate, given the simple nature of these molecules, Ca^{2+} ions modulate the function of a myriad of proteins and a wide variety of cellular functions are sensitive to changes in intracellular Ca^{2+} ion concentrations.

Typically, increases in Ca^{2+} ion concentrations are triggered by the opening of Ca^{2+} channels, either in the cell membrane or in the membranes of the organelles that sequester Ca^{2+} ions. These calcium fluxes produce a transient increase in the free calcium ion concentration in the cell that triggers downstream cell signaling pathways. This signaling system is used by all cells but is particularly important for electrically excitable cells because it provides a means of converting an electrical signal into a biochemical one. Examples of important cellular functions dependent on Ca^{2+} signaling include synaptic transmission and muscle contraction.

Internal Ca^{2+} Concentration and Cell Death

Maintenance of a low intracellular Ca^{2+} ion concentration is critical for normal cell function. In most cells, a prolonged increase in intracellular Ca^{2+} ion concentrations rapidly leads to cell death.

Blockade of blood flow (and thus oxygen) in the brain or the heart quickly leads to **ischemic tissue damage** in these organs. The brain and the heart are very metabolically active tissues and as a consequence use up their local energy supplies very quickly. This makes them particularly vulnerable to ischemic tissue damage because the maintenance of low Ca^{2+} ion concentrations inside the cell is strongly dependent on maintained cellular energy levels. The decrease in local oxygen tension during ischemia results in a rapid fall in ATP levels inside the cell, which leads to a rise in calcium levels. The rise in intracellular calcium levels can trigger cellular processes that lead to the destruction of the cell.

11. Maintenance of Cell Volume

The most abundant molecules both inside the cell and in the extracellular solution are water molecules, which make the major contribution to the volume of the intracellular and extracellular solutions. As a consequence, the flow of water into or out of the cell across the cell membrane is the primary determinant of changes in cell volume.

Water Channels

The cell membrane is highly permeant to water molecules. For much of the history of cellular physiolgy the high permeability of the cell membrane to water was something of a mystery because H_2O is a highly polar molecule that cannot easily cross the lipid bilayer. It was ultimately determined that there are specialized membrane transport proteins for water molecules known as **water channels** (or **aquaporins**).

Water channels are integral membrane proteins, analogous to ion channels, that provide a low resistance pathway for the movement of water molecules across the cell membrane.

Osmolarity

Osmolarity is a measure of the concentration of osmotically active particles in a solution, typically expressed as osmoles of solute per liter of solution. For molecules such as glucose, sucrose and urea that do not dissociate, a solution containing 1 mole of dissolved molecules in 1 liter of water is a 1 osmole/liter solution. For salts or acids dissolved in solution the situation is slightly more complex because these compounds dissociate into two or more ions in solution. For NaCl, which dissociates into two dissolved particles, the Na^+ and Cl^- ions, a 1M NaCl solution is a 2 osmole/l solution. For $CaCl_2$, which dissociates into three ions, a 1M $CaCl_2$ solution is a 3 osmole/l solution.

Regulation of Cell Volume

Maintaining a balance between the osmolarity inside the cell versus the osmolarity of the extracellular solution is critical to maintain the integrity of the cell membrane. To limit potential damage to the cell membrane, the osmolarity of extracellular solution is kept within relatively tight limits, in the range 275-295 mosmole/l in mammals.

To understand the effect of changes in intracellular or extracellular osmolarity on cell volume it is important to recognize that water has a concentration (number of molecules per unit volume) just like the solutes dissolved in a solution. The concentration of H_2O molecules in pure water is approximately 55.5M. If sugar molecules are dissolved into water the volume of the resulting solution increases because the sugar molecules take up some volume in the solution. Assuming that each solute molecule takes up the space of one water molecule, for a 1 M glucose solution, the water concentration falls to approximately 54.5M, significantly less that the 55.5M value for pure water. As a consequence, the concentration of water molecules in a sugar solution is lower than it is in pure water.

Water can flow down its concentration gradient across the cell membrane, just like membrane permeable solutes. If the concentration of water outside of a cell is higher than it is inside the cell, water will flow into the cell across the cell membrane until the concentration of water is equal on each side of the membrane. An extreme example of this is if a cell is placed in distilled water (water containing no ions or other solvents). In this case the cell rapidly expands and dies, because the osmolarity inside the cell is much higher than outside and water flows rapidly into the cell, down its concentration gradient.

2 Ion Channels

Ion channels are membrane proteins that form continuous channels from one side of the membrane to the other through which ions can pass into or out of the cell. All ion channels have two key properties: **ion permeation**, they provide a pathway for ions to permeate across the membrane, and **ion selectivity**, they allow some ions to pass more easily than others. These properties are intimately related and will be discussed together.

Most ion channels have a third property known as **gating**. Gating means the opening and closing of the pore of the ion channel. The gating mechanism shows marked differences between different channels. Some aspects of gating will be described in the final section of this chapter.

The crystal structure of several K^+ channels has been solved and ion permeation, selectivity and gating are now well understood for this channel. For this reason, much of this discussion will focus on K^+ channels. The general principles are valid for other ion channels.

1. Ion Permeation and Ion Selectivity

Typically, the pores of K^+ channels are highly selective, favoring K^+ ions over Na^+ ions by a ratio of 10,000:1. Potassium channels are also very efficient, allowing approximately 10^8 ions to pass per second. Essentially, K^+ ions can pass through the channel at the same rate at which they arrive at the mouth of the channel. Energetically, the channel appears to be almost transparent to the ions as they pass through it.

Quaternary Structure of K^+ Channels

Most K^+ channels are **tetramers**, meaning that they are assembled from four protein subunits. The simplest K^+ channel subunits have two membrane spanning domains (Figure 1A). The amino- and carboxyl-terminals of these subunits are located on the cytoplasmic side of the membrane. The four subunits co-assemble around a central ion pore something like the staves of a barrel (Figure 1B).

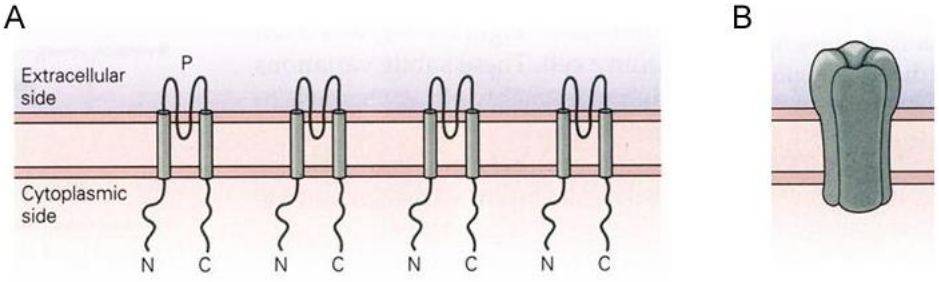

Figure 1 (A) K^+ channel subunits with two membrane spanning domains. (B) Subunits assembled into a channel.

The crystal structure for a simple K^+ channel is shown in Figure 2. The channel has three prominent alpha helices per subunit: an inner and outer helix, which are both membrane spanning, and a pore helix located near the extracellular surface of the channel. The inner helix is more closely associated with the channel pore than the outer helix.

This simple form of the K^+ channel is a relatively small protein that sits largely within the boundaries of the membrane's lipid bilayer (Figure 2C)

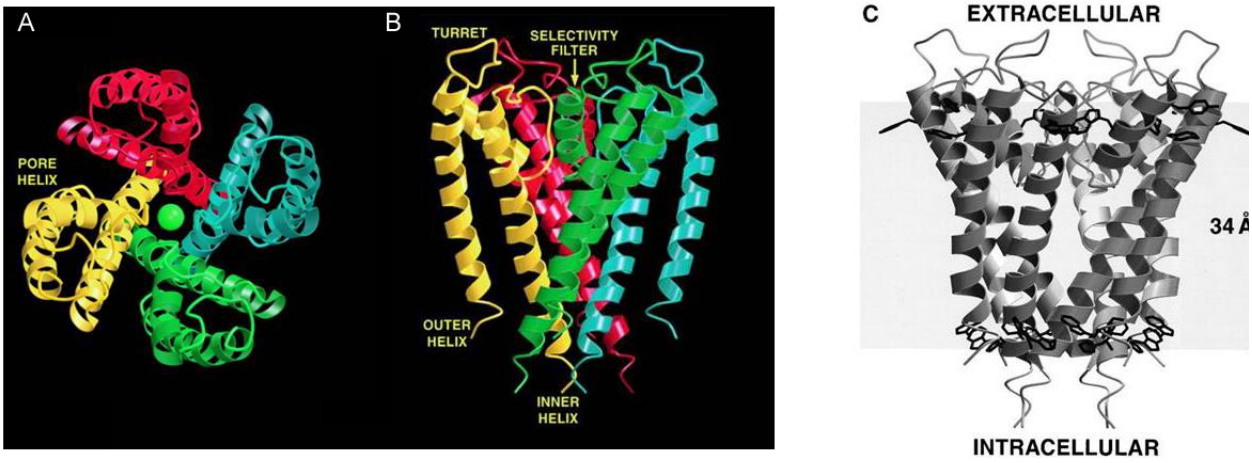

Figure 2 Crystal structure of a simple K^+ channel. (A) The four subunits of a K^+ channel arranged around a central pore. Each subunit is shown in a different color and a K^+ ion (green ball) is located within the pore. (B) Side view of the channel showing the two membrane spanning domains of each subunit. (C) Location of channel protein within the lipid bilayer of the membrane.

Quaternary Structure of K^+ Channels

The pore is 45 Å long and has a narrow **selectivity filter** close to the extracellular surface, with a relatively wide water-filled pore connecting this to the intracellular surface (Figure 3). Potassium ions can traverse from the intracellular solution through the internal pore to the selectivity filter while retaining their hydration shell. Essentially, they remain in an aqueous environment until they enter the selectivity filter, which is much narrower.

In principle, the primary energy barrier for ion movement will be greatest at the center of the channel where it should be most difficult for the ion to polarize the surrounding channel protein due to the hydrophobic nature of the protein in the lipid bilayer. The channel solves this problem by surrounding the ion with polarizable water molecules for much of its journey through the channel. In addition, the pore helices are positioned to maximize the helix-dipole effect, allowing the protein itself to be polarized by the ion. Essentially the cavity acts as a well of polarizable water, and ions can move freely from the intracellular solution to the cavity and back out again.

The selectivity filter is much narrower, however, and the ion must shed most of its hydration shell in order to pass through the filter.

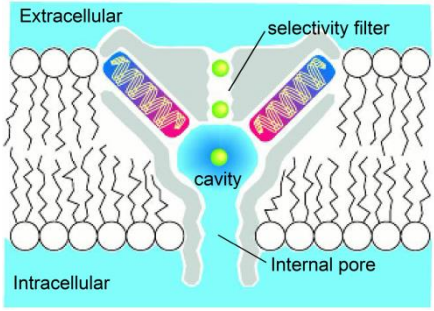

Figure 3 Cartoon showing the pore domains, the long internal pore leading to the cavity adjacent to the narrow selectivity filter that separates the water filled pore from the extracellular solution.

Structure of the Selectivity Filter

The amino acid sequence of the selectivity filter is conserved in all known types of potassium channels from bacterial potassium channels to plant and animal channels. During the course of evolution, a mechanism to selectively catalyze the movement of K^+ ions across the cell membrane has evolved only once.

The conserved amino acid sequence of the selectivity filter is (T/S)(V/I)G(Y/F)G. The last three residues GYG are absolutely conserved in almost every potassium channel, with only a few rare exceptions having the alternate GFG sequence. This short sequence of amino acids lines the surface of the selectivity filter (Figure 4).

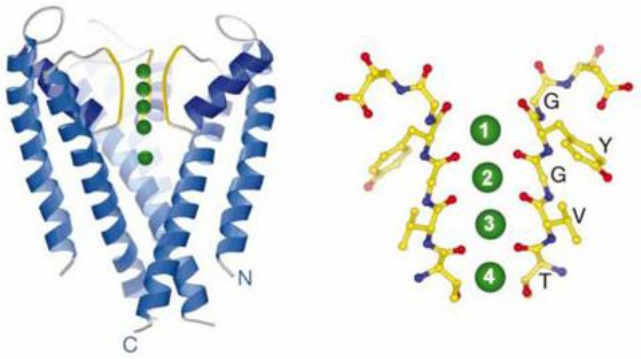

Figure 4 (left panel) The K^+ channel with the front subunit removed. The yellow region corresponds to the selectivity filter and the green spheres correspond to K^+ ions. (right panel) High resolution image of the selectivity filter showing the TVGYG amino acid sequence. Only two of the four subunits are shown. Each red dot corresponds to a carbonyl oxygen atom. There are five rings of carbonyl oxygen atoms each containing four oxygen atoms, one from each subunit. These oxygen atoms are positioned within the pore to mimic the position of oxygen atoms of the water molecules of the inner hydration shell.

The structure of the TVGYG sequence is highly unusual. The amino acids are arranged to form an almost straight line running up the sides of the pore and the side chains of the residues are turned away from the pore so that the closest contact point between the ion and the channel protein is with the carbonyl oxygen atoms, which are part of the peptide backbone. It is the arrangement of these carbonyl oxygen atoms that is critical to understanding the function of the pore.

In solution, K^+ ions are surrounded by a tight shell of water molecules, known as the inner hydration shell. The oxygen atoms of these water molecules are oriented to face the positively charged K^+ ion. The selectivity filter replaces the shell of oxygen atoms provided by the water molecules with the rings of carbonyl oxygen atoms. These five rings of oxygen atoms replicate the position of the oxygen atoms of the water molecules of the inner hydration shell. In this way the channel mimics the normal aqueous environment of the K^+ ions and there is almost no energy barrier for the movement of the K^+ ions from the aqueous solution into the selectivity filter and back out again.

Ion Selectivity

The structure of the selectivity filter explains in a very simple and elegant way how the K^+ channel can show such great selectivity for K^+ ions over Na^+ ions.

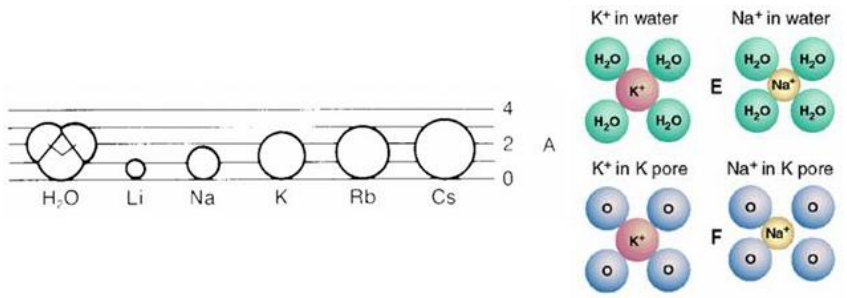

Figure 5 (left panel) Comparison of the ionic radii of different alkali-metal atoms. (right panel) The relationship between oxygen atoms of water molecules and K^+ and Na^+ ions and between oxygen atoms of the selectivity filter and K^+ and Na^+ ions.

There is relatively little difference between a K^+ ion and a Na^+ ion. They have the same charge and relatively similar ionic radiuses: K^+ 1.33 Å and Na^+ 0.95 Å (Figure 5). In solution, the oxygen atoms of the water molecules move freely and can adjust to the different ionic radiuses so that both atoms can easily dissolve in an aqueous environment. In the selectivity filter of the K^+ channel, the oxygen atoms are held in a relatively rigid spatial arrangement into which the K^+ ion fits well but the Na^+ ion less well (Figure 5). This relatively small geometrical difference translates into a large difference in the ease with which the two ions can move into the selectivity filter. Potassium ions partition easily into the filter whereas sodium ions cannot move as readily into the selectivity filter. This difference in the energy state of the two ions in the pore is the source of the differential selectivity of the channel to the two ions.

Ion Permeation

The selectivity filter has five oxygen rings that result in four binding sites for ions within the filter (each binding site is made up of two rings of four oxygen atoms). Because the K^+ ions are charged, adjacent binding sites cannot be occupied due to electrostatic repulsion between the two adjacent K^+ ions. As a consequence, the channel cycles between two semi-stables states when it is conducting ions (Figure 6). The difference between these two states is very subtle and does not involve significant rearrangements of the channel protein. As a consequence, cycling between the two states is very rapid and ions move through the channel very efficiently.

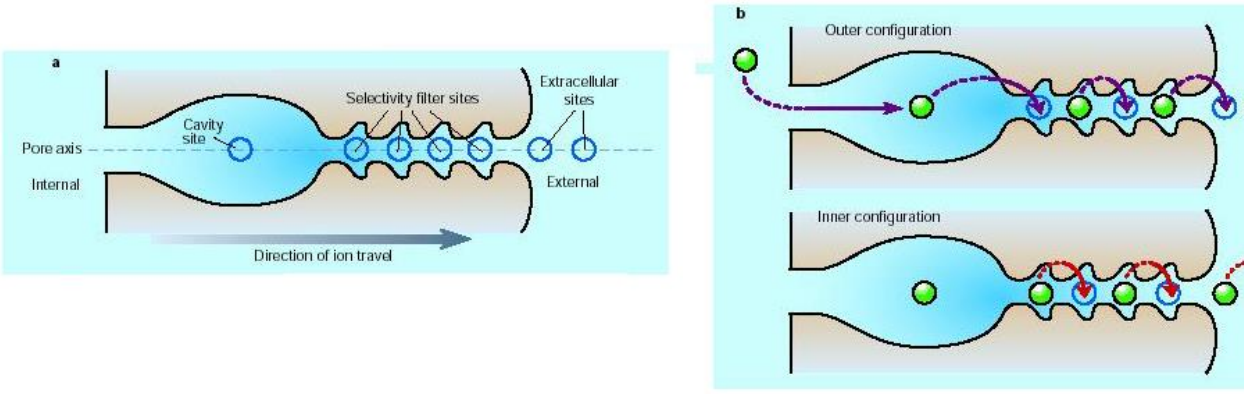

Figure 6 (A) Four binding sites for K^+ ions within the filter. (B) Two semi-stable states for ions in the filter. Ions move along the channel by jumping from one binding site to the next. Electrostatic repulsion by new ions entering the cavity pushes the chain of ions through the filter.

The constant arrival of new ions in the cavity acts to push ions out of the other end of the filter due to the electrostatic repulsion between the ions within the selectivity filter.

2. Ion Channel Gating

If all the channels in an electrically excitable cell were always open, the membrane would have a very large conductance. Ions would flow down their concentration gradients faster than the Na,K-ATPase pump could pump them back out again and the cell would die. In general, most of the ion channels in the cell membrane are in a non-conducting state most of the time. The transition between the non-conducting and conducting states is termed gating. This term refers to the idea that there is a physical "gate" that blocks access to the channel. Although this term was derived long before structures for ion channels were available, it still provides a reasonable description of the process.

Channels can be gated by several different stimuli including: changes in membrane voltage, changes in intracellular Ca^{2+} or H^+ ion concentrations, binding of G-proteins to the channel and covalent modification of the channel by phosphorylation. A given channel will only be gated by a subset of these different stimuli. In electrically excitable cells the most important gating mode is voltage-dependent gating in which the gate opens or closes in response to changes in membrane voltage.

3. Voltage-Dependent Ion Channels

Kinetic Properties of Voltage-Dependent Channels

Voltage-gated channels typically have three distinct states; open, closed and inactivated (Figure 7). Although the closed and inactivated states are functionally similar in that neither state allows the passage of ions through the channel, they are physically quite different states of the channel. The open state is the state during which ions can flow through the pore.

The rate of transition between these states depends on the membrane voltage. As a consequence, the rate constants that describe the transitions between these kinetic schemes are not really constant but change with membrane voltage and are known as voltage-dependent rate constants.

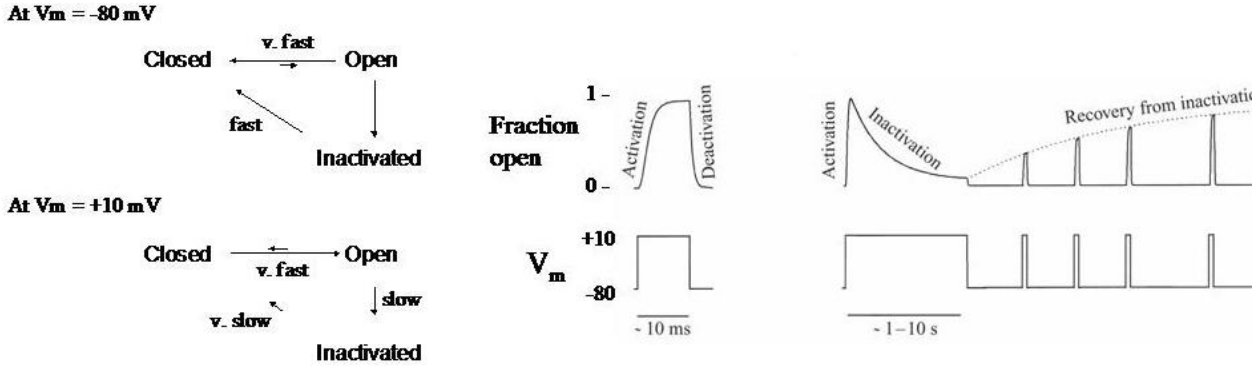

Figure 7 (left panel) Simple kinetic scheme for a typical voltage-gated ion channel with three channel states: closed, open and inactivated. (right panel) Time course of the fraction of channels that are open during step changes in membrane voltage.

For a typical voltage-gated ion channel at resting membrane potentials (V_m = -80 mV), almost all of the channels are closed, because the rate constants strongly favor the transition from the open and inactivated states back to the closed state. Following a step change in membrane potential to +10 mV, the rate constants rapidly change and the channels move from the closed state to the open state. This movement is known as **activation**. In most channels, the time course of activation is sigmoidal

(S-shaped) indicating a more complex kinetic scheme than that shown in Figure 7, with multiple closed states before the open state.

If the membrane potential is moved quickly back to rest, the channels move from the open state back to the closed state. This is known as **deactivation**.

If the voltage step to +10 mV is maintained for a prolonged period, the channels leave the open state and enter the inactivated state. This is known as **inactivation**. If, after most of the channels become inactivated, the membrane potential is returned to the resting value, the channels move from the inactivated state back to the closed state. This is known as **recovery from inactivation**.

It is important to recognize that the rate constants controlling the transitions between these different states vary dramatically among different voltage-gated channels. Unlike the pore properties, which are essentially invariant over large evolutionary distances, the kinetic properties of these channels have diversified significantly in eukaryotes. Some channels will activate and inactivate in a few milliseconds whereas other channels take minutes to inactivate and some do not inactivate at all. This will be discussed in more detail in Chapter 8.

Structure of Voltage-Dependent K^+ Channels

The minimal K^+ channel subunit described above has only two membrane spanning domains. This is sufficient for the channel to function as a pore for the selective movement of K^+ ions across the membrane. Typically, K^+ channels are more complex and have additional regions that are responsible for the channel gating and other functions or properties of the channel (Figure 8). Voltage-gated K^+ channels generally have six membrane spanning domains (S1-S6), the last two of which (S5 and S6) correspond to the two membrane spanning domains of the minimal K^+ channel. The amino- and carboxyl-terminals of the protein are intracellular.

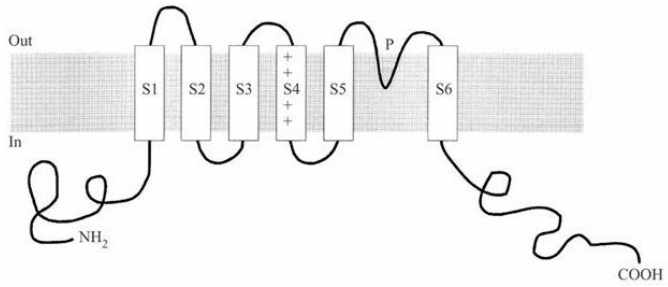

Figure 8 Six membrane spanning regions of a typical voltage-gated K^+ channel. A key features is the S4 domain, which has several positively charged residues and acts as the voltage sensor.

Activation

A voltage gated channel must have a **voltage sensor,** some part of the channel that can sense changes in membrane potential. The voltage sensor must contain charged residues since this is the only way that the protein can "see" a change in membrane voltage. The S4 helix of the channel acts as the voltage sensor in voltage-gated channels. The S4 region has a highly unusual structure for a membrane protein. Like a typical membrane spanning region, it is generally hydrophobic but, almost uniquely, it contains four or more positively charged lysine or arginine residues at every third position interspersed with the hydrophobic residues (Figure 8). It is these positive charges that sense the change in membrane potential and it is their movement within the membrane that triggers the conformational change that opens the gate.

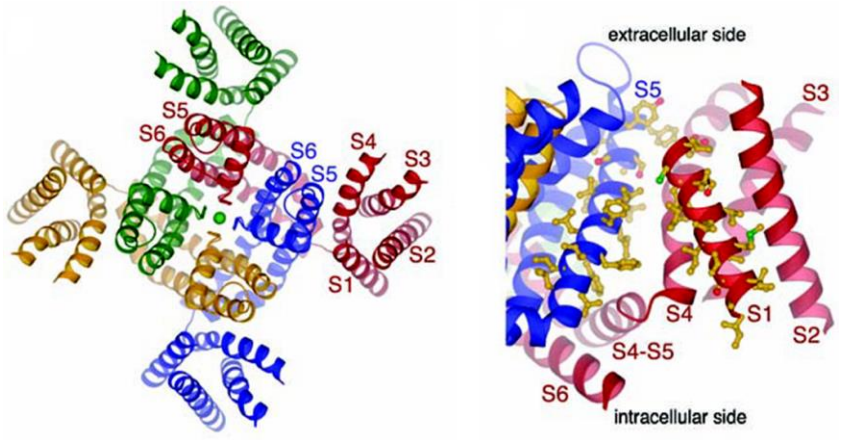

Figure 9 Structure of a voltage gated K^+ channel. The four subunits are each marked with a different color.

The channel has a core domain that is comprised of the S5 and S6 helices plus the selectivity filter (Figure 9). This region mediates ion permeation across the cell membrane. Attached to this core is the voltage sensor domain, which is comprised of the S1-S4 helices. This domain is linked to the gate of the core channel via the S4-S5 linker so that movement in the S4 domain is translated into movement in the gate of the channel.

In response to membrane depolarization the S4 helix twists and moves upwards (Figure 10). This movement opens the inner mouth of the pore allowing ions to flow through the selectivity filter. The gate itself is formed by the regions of the S6 helix located on the intracellular side of the channel.

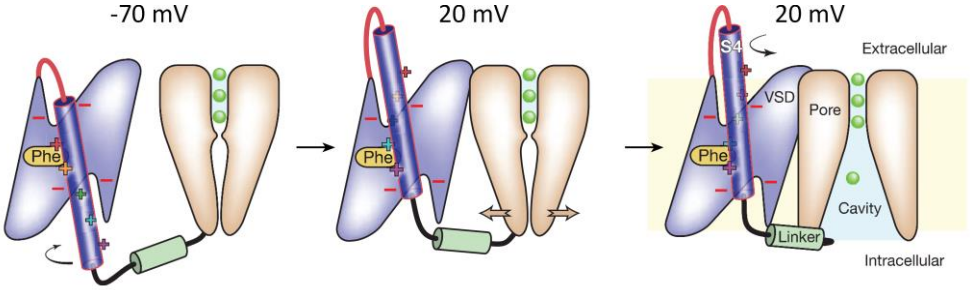

Figure 10 Cartoon showing the voltage sensor and gate of a voltage gated channel and how it may move as the channel activates in response to depolarization of the membrane potential.

The S4 domain moves through a hydrophobic 'gasket' formed by the other alpha helices in voltage sensor domain. Above and below this 'gasket' are water filled wells (Figure 10). During activation the S4 α helix twists clockwise and moves upward between 5-10Å. The structure of the S4 α helix remains largely unchanged during this movement.

Inactivation

There are two ways that a channel can inactivate, known as **N-type** and **C-type inactivation**. N-type inactivation is so-named because it involves the amino terminal (N terminal) of the channel and it is quite simple to understand.

There are two structural components required for N-type inactivation (Figure 11):

1. a tethered inactivation ball that can block conduction through the pore

2. a receptor site to which the inactivation ball can bind, thereby blocking conduction through the pore

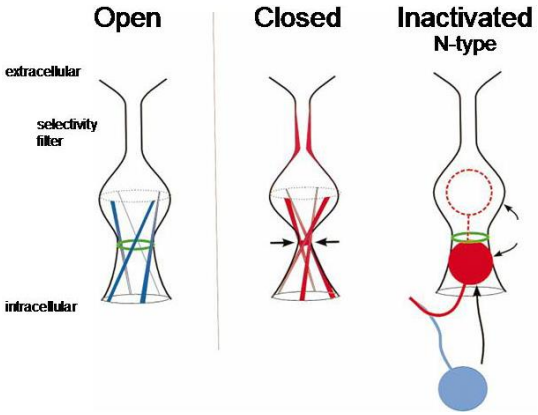

Figure 11 Cartoon showing the open, closed and inactivated states of the channel. Inactivation occurs when a region of the amino terminus known as the inactivation ball swings in to bind to the inner surface of the pore, physically blocking the channel and stopping ions from passing. Note that the closed and inactivated states are different, with different regions of the channel blocking or gating the pore.

The inactivation ball is located at the amino terminus of the protein. Using site-directed mutagenesis it is possible to delete the inactivation ball and show that this removes fast inactivation.

C-type inactivation is a more complex phenomenon, which may involve constriction of the pore near the selectivity filter.

3 Membrane Potential

Biological electricity is an electrochemical phenomenon that is underpinned by a complex web of biochemical processes. This chapter focuses on the most basic aspect of cellular electrical function, generation of the **membrane potential**. The membrane potential is an electrical potential across the cell membrane that is found, to a lesser or greater degree, in all cells.

1. Bioelectricity

Ions

In a household electrical circuit, the current carriers are the electrons in the copper wiring. The body contains only trace amounts of metals and the current carriers in the body are dissolved ions. These are charged atoms that move through aqueous solution by diffusion.

Conduction of Electricity in Biological Solutions

Conduction of electric current in a copper wire consists of the movement of electrons from the outer shell of one atom to another. In a salt solution, electric charge is carried by the physical movement of the ions. When a potential difference or voltage is applied to an electrolyte solution, the cations (Na^+ or K^+ ions) migrate toward the **cathode** (electrode with the negative potential) and the anions (Cl^-) migrate toward the **anode** (electrode with the positive potential) (Figure 1).

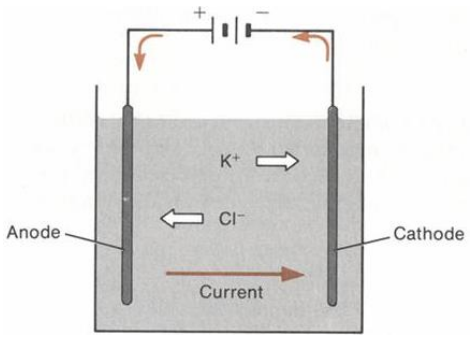

Figure 1 Movement of ions in an electric field.

Importantly, current flow in an ionic solution and across the cell membrane obeys Ohm's law for small currents and voltages.

2. Recording the Membrane Potential

If a small glass electrode is inserted into a typical mammalian cell an electrical potential can be recorded across the cell membrane (Figure 2). This electrical potential is known as the **resting membrane potential** and is typically in the range of -60 to -90 mV. All mammalian cells have a resting membrane potential, which is always negative with respect to the extracellular solution.

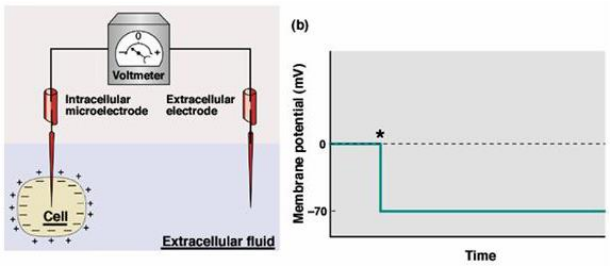

Figure 2 (left panel) Apparatus for recording the membrane potential. A voltmeter is used to record the difference in electrical potential between an electrode inside the cell and one in the extracellular solution. (right panel) Recording of the potential difference between two electrodes just before and just after one electrode has been advanced into a cell.

The electrodes that are used for intracellular recording are very fine glass capillaries that are filled with an electrolyte solution, typically 3 molar KCl (Figure 3). The tip diameters of the electrode that are used are very fine, approximately 0.5 μm in diameter, in order to limit the damage when they are pushed through the cell membrane. Because the electrical signals are small, an amplifier is used to amplify the membrane voltage signal, which is then recorded on a device that acts like a voltmeter. The potential inside the cell is recorded relative to a reference electrode in the bath solution surrounding the cell. This bath potential is arbitrarily defined to be 0 mV or ground.

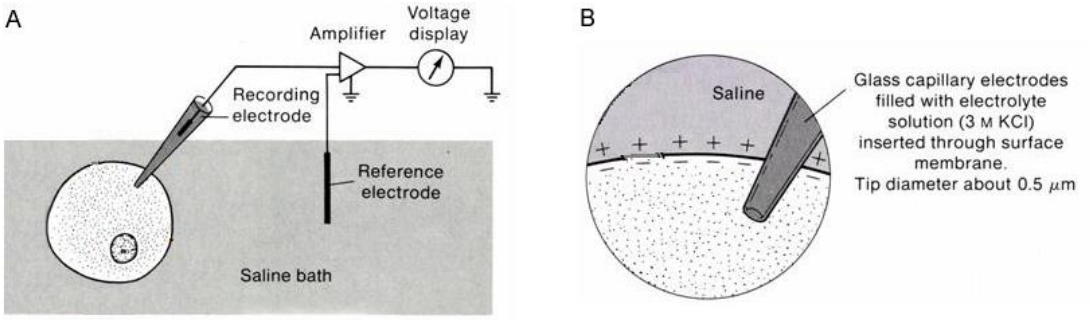

Figure 3 Experimental apparatus for recording of the membrane potential using an intracellular electrode. (A) Membrane potential is recorded as the difference in electrical potential between the recording electrode and the reference electrode. (B) The recording electrode is filled with a salt solution so that there is electrical continuity between the input to the amplifier and the interior of the cell.

3. Generation of the Resting Membrane Potential

The non-equilibrium distribution of ions produced by the pumps and transporters in the cell membrane provides a source of energy that can be converted into electrical potential energy. There are two structural components that are necessary for this conversion:

1. An ion-impermeant lipid bilayer, which can produce a separation of charge
2. Ion channels, which provide a pathway for ions to carry electric charge across the membrane

The **principle of electroneutrality** states that the sum of negative charges in solution must equal the sum of positive charges. In other words, in a normal solution the negative and positive charges must sum to zero so that the solution as a whole cannot have a net negative or positive

charge. This principle can be violated over very short distances. The thin lipid bilayer has the ability to separate electric charges, a property known as **capacitance**. In a typical cell, at rest, there is an excess of positive charges clustered on the outside of the cell membrane and of negative charges on the inside of the cell membrane (Figure 4). It is this **separation of charge** that generates the membrane potential. The inside of the cell is negative with respect to the outside of the cell.

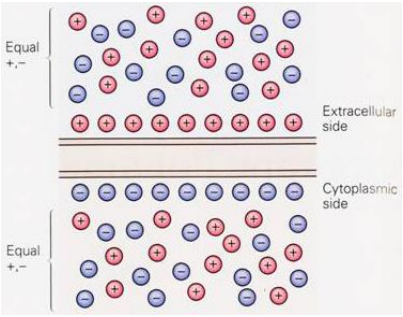

Figure 4 Separation of charge across the lipid bilayer.

The ion channels provide a circuit for movement of charge across the cell membrane to create the separation of charge. Since, K^+ ions can most easily flow out of the cell, because of the normally high membrane permeability to K^+ ions, there is an accumulation of an excess of positive charges on the outside surface of the membrane and of negative charges inside the membrane.

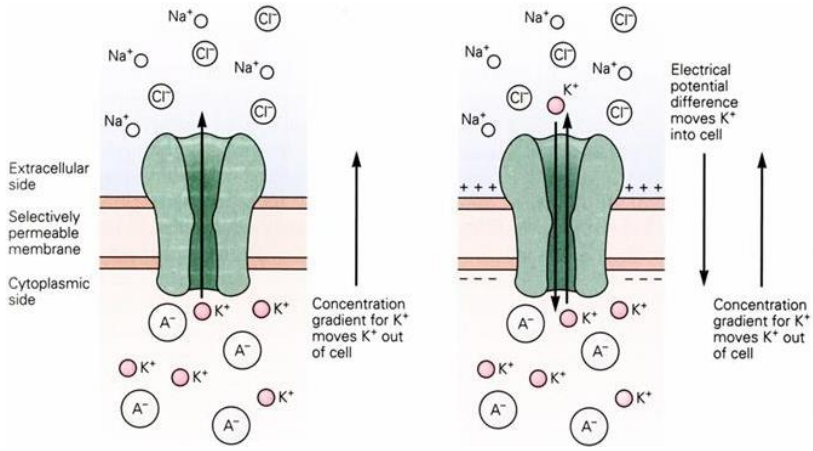

Figure 5 (left panel) Initially K^+ ions move out the cell, down their concentration gradient, through K^+ selective leak channels, creating a separation of charge across the lipid bilayer. (right panel) The membrane potential generated by the separation of charge creates an opposing electrical force favoring the movement of K^+ ions back into the cell limiting the size of the membrane potential.

Movement of relatively few K^+ ions across the membrane is required to generate the membrane potential. As the K^+ ions move across the membrane they create a negative potential inside the cell that attracts positively charged K^+ ions back into the cell limiting the net flux of K^+ ions out of the cell (Figure 5).

Typically, the K^+ ions in a cell are not in perfect equilibrium and the membrane potential will gradually dissipate as the K^+ ions leak out of the cell. The maintenance of the cell membrane potential requires the constant expenditure of cellular energy by the Na,K-ATPase pump to maintain the non-equilibrium distribution of ions.

Much of the early work on understanding membrane potentials was done by physicists who used one of two intellectual frameworks within which to work: either classical thermodynamics or electrical circuit theory.

4. Thermodynamic Models of the Membrane Potential

The typical approach taken by physicists when approaching biological problems has been to imagine a very simple situation, which is mathematically tractable, and devise a mathematical description for that simple case. Then, using reasonably valid assumptions, try to expand the application of the model to more complex situations in order to capture at least some of the complexity of the real biological situation. In the case of membrane potentials, this approach has been quite useful.

Equilibrium Potentials

Imagine a membrane that is permeable only to K^+ ions that separates two compartments (Figure 6). If the ion concentrations in both compartments are the same then there is no **net flux** of K^+ ions. The **one-way flux** of K^+ ions is the same in either direction. It is important to distinguish one-way fluxes, the flux of ions from one compartment to the other, from the net flux, the sum of the two one-way fluxes, remembering that the one-way fluxes will have opposite signs. The system is in equilibrium because there is no net movement of ions between the two compartments (Figure 6A).

If the K^+ ion concentration is higher in compartment I than in compartment II, initially the K^+ ions flow down their concentration gradient (Figure 6B). So, initially there will be a net flux of K^+ ions out of compartment I into compartment II. The separation of charge produced by the initial movement of K^+ ions out of compartment I produces an electrical potential across the membrane (Figure 6C). This electrical potential develops quickly and only a relatively small number of K^+ ions move across the membrane so that there is no significant change in the ion concentrations in the two compartments. Because K^+ ions are charged, there are two forces that can act on them in solution: a chemical potential difference, due to a concentration gradient, and an electrical potential difference, produced by the separation of charge. This electrical potential opposes the flow of K^+ ions out of compartment I because compartment I is negative with respect to compartment II. When there is a balance between the chemical and electrical forces that act on the K^+ ions there is electrochemical equilibrium, resulting in no net movement of ions between the two compartments.

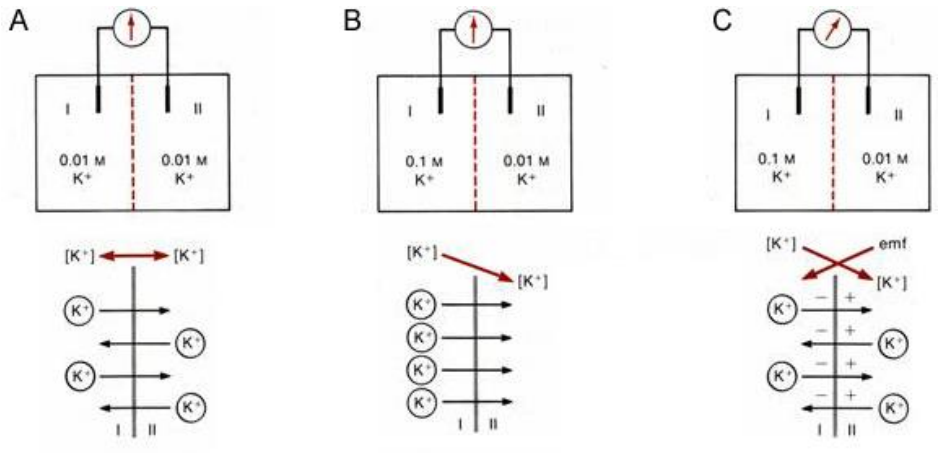

Figure 6 Simple model of a K^+ selective membrane separating two KCl solutions.

The simple situation shown in Figure 6 approximates a typical cell in that the cell membrane is predominantly permeable to K^+ ions and separates two solutions, one of which has a high K^+ ion

concentration relative to the other. There is a mathematical description of this simple system known as the **Nernst equation** that can be used to calculate the **equilibrium potential** (the membrane potential at which the electrical and chemical potentials for a given ion are equal and opposite).

The Nernst Equation

The Nernst equation at normal body temperature (37°) is:

$$E_i = \frac{61.5}{Z} \log \frac{[C]_0}{[C]_i} \quad \text{mV} \qquad 1$$

where:

E_i	equilibrium potential of ion i
Z	valence of the ion (+1 for Na^+ and K^+, -1 for Cl^-)
log	logarithm to the base 10
$[C]_o$	ion concentration outside the cell
$[C]_i$	ion concentration inside the cell.

For the model shown in Figure 6:

E_K = (61.5 /Z) log($[K^+]_o/[K^+]_i$)
= 61.5 log($[K^+]_o/[K^+]_i$)
= 61.5 log (.01 / 0.1)
= 61.5 × -1
= -61.5 mV

In this example, the equilibrium potential for K^+ ions is –61.5 mV. This is the potential at which the electrical and chemical potentials are equal and opposite and the efflux of ions from each compartment exactly matches the influx.

Equilibrium Potentials in a Real Cell

In a real cell none of the ions are in equilibrium. This can be easily demonstrated by calculating the equilibrium potential for each ion using realistic values for their internal and external ion concentrations and the membrane potential:

Table 1. Intracellular and Extracellular Ion Concentrations

	Intracellular	Extracellular
K^+	125	5
Na^+	12	120
Cl^-	5	125

E_K = 61.5 mV log ($[K^+]_o$ / $[K^+]_i$) = 61.5 log(5/125) = -86 mV

E_{Na} = 61.5 mV log ($[Na^+]_o$ / $[Na^+]_i$) = 61.5 log(120/12) = +61.5 mV

E_{Cl} = -61.5 mV log ($[Cl^-]_o$ / $[Cl^-]_i$) = -61.5 log(125/5) = -86 mV

Since the resting membrane in this cell would typically be equal to –70 mV, none of the ions are at equilibrium. This is because the cell membrane is not perfectly selective for K^+ ions. Other ions, particularly Na^+, can also cross the membrane.

Obviously the Nernst equation does not tell the whole story about the membrane potential in real cells but it remains a useful tool for describing the thermodynamic state of individual ions.

Nonequilibrium Membrane Potential

The Nernst equation deals only with the case when the ions are in equilibrium. For real cells we need a way to calculate the membrane potential when the ions are not in equilibrium and the membrane permeability to several ions contributes to setting the membrane potential. As a first approximation we can focus on the permeability to K^+ and Na^+ ions. Chloride ions do not contribute significantly to the determination of the resting membrane potential in many cells.

The permeability of a membrane to ions is determined by the types of ion channels found in the membrane. The total permeability of a membrane to a particular ion is governed by the total number of membrane channels that are open and their selectivity for a particular ion. As described previously, some ion channels are selective for K^+ ions and some ion channels, encoded by different genes, are selective for Na^+ ions. The relative permeabilities of the resting cell membrane for different ions depends on the channels that are normally open at rest, the so-called **leak channels**. In a typical cell these leak channels are predominantly K^+ ion selective but the membrane also has a small, but not negligible, Na^+ ion permeability.

The Goldman Equation

There are two factors that determine the resting membrane potential (Vm) in a real cell:

1. ion concentrations, which determine the equilibrium potentials
2. relative ion permeabilities, which determine the relative importance of a particular ion's contribution to the membrane potential

The Goldman equation describes the relationship between the Vm, ion concentrations and ion permeabilities for the permeant ions. For K^+ and Na^+ ions at normal body temperature (37°C):

$$V_m = 61.5 \log \frac{[\mathrm{K^+}]_o + b[\mathrm{Na^+}]_o}{[\mathrm{K^+}]_i + b[\mathrm{Na^+}]_i} \quad \text{mV} \qquad (2)$$

where:

V_m	resting membrane potential
$b = p_{Na}/p_K$	valence of the ion (+1 for Na^+ and K^+, -1 for Cl^-)
p_{Na}	permeability to Na^+ ions
p_K	permeability to K^+ ions.

In most nerve cells the ratio of sodium to potassium permeability (b) is approximately 0.02, i.e. the membrane is 50 times more permeable to K^+ ions than to Na^+ ions. Using the ion concentrations in Table 1 and $b = 0.2$:

$$V_m = 61.5 \log \frac{5 + 0.02 \times 120}{125 + 0.02 \times 12} \quad \text{mV}$$

$$V_m = -76 \text{ mV}$$

If the permeability to Na^+ ions was zero then the resting membrane potential would equal E_K. Even a small resting Na^+ permeability has a large effect on the membrane potential, moving the membrane potential significantly away from E_K = -86 mV. Similarly, if the permeability to K^+ ions was zero the membrane potential would equal E_{Na}.

Typically, the membrane potential will fall somewhere between the equilibrium potential for K^+ and Na^+ ions, depending upon the relative permeability to the two ions (Figure 7).

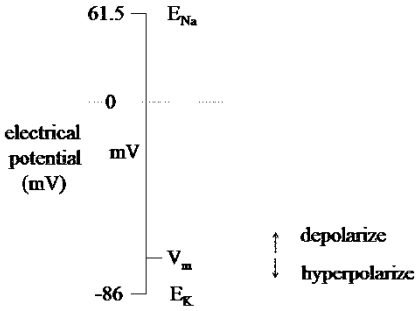

Figure 7 Relationship between E_K, E_{Na} and V_m in a typical cell at rest.

Forces that move the resting membrane potential to more positive potentials are said to **depolarize** the membrane and forces that make the membrane potential more negative are said to **hyperpolarize** the membrane.

Ionic Steady State

In a typical cell, neither K^+ nor Na^+ ions are at equilibrium because the membrane potential is not at either of their equilibrium potentials. Because of this there will be a constant net flux of ions in or out of the cell and the ionic gradients will eventually run down. To prevent this run down the Na,K-ATPase pump must work continuously, using chemical energy to maintain the ion gradients.

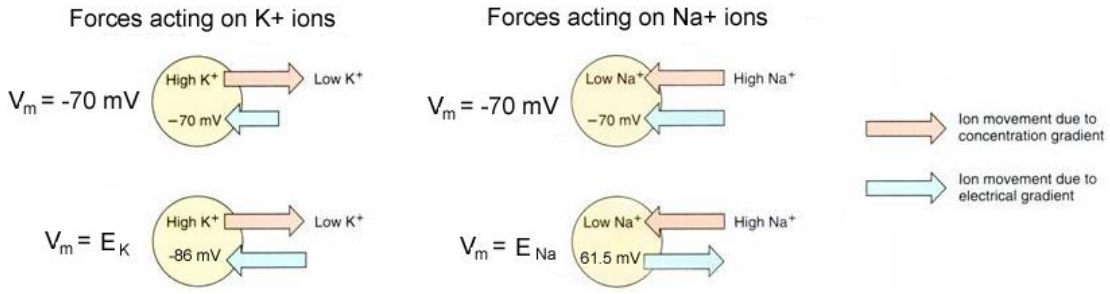

Figure 8 Forces acting on K^+ and Na^+ ions at the resting membrane potential and at their respective equilibrium potentials.

Error! Reference source not found. shows the balance of forces acting on K^+ ions when the membrane potential is at the resting potential or at the potassium equilibrium potential. At the resting membrane potential, there is a net efflux of K^+ ions out of the cell because the resting membrane potential is less negative than the potassium equilibrium potential. Only at the equilibrium potential are the two forces balanced. At rest, both the chemical and electrical forces favor an influx of Na^+ ions into the cell. The interior of the cell has to be very positive (+61.5 mV) for the electrical potential to equal the magnitude of the chemical potential resulting in no net flux of Na^+ ions.

5. Equivalent Circuit Models of the Membrane Potential

Simple electrical circuit theory has been used very successfully to model many aspects of the electrophysiological properties of cells. Only three electrical elements are required to provide an accurate description of the electrical behavior of a cell membrane at rest: conductors (or resistors), capacitors and batteries.

Equivalent Circuit Components

Membrane Conductance

Ion channels function like resistors and the conductance of a biological membrane is the sum of all the ion channels in the membrane that are open at the time of the measurement. Conductance is the reciprocal of resistance, which is the more commonly used to describe resistive elements in electrical circuits.

$$G = 1/R$$

where:

G	conductance (Siemens)
R	resistance (ohms)

Membrane Capacitance

Lipid bilayers are very thin nonconducting sheets that separate charge, exactly like capacitors in an electrical circuit. Within a limited voltage range, the lipid bilayer functions like a pure capacitive element and can be modeled exactly like its electrical circuit equivalent.

Membrane Battery

The non-equilibrium ion distribution acts like a battery providing electrical potential energy for the movement of ions (or charge) through the resistive elements (the ion channels) in the cell membrane.

Ohm's Law

Ohm's Law describes a linear relationship between current and voltage.

$$I = V/R$$

For biological circuits this is normally rewritten as:

$$I = GV \tag{3}$$

where:

I	current
V	voltage
G	conductance (Siemens)
R	resistance (ohms)

Ohm's Law assumes that there is a linear relationship between current and voltage i.e. that the resistance or conductance remains constant over a wide range of voltages. For many different types of channels this can be a close approximation. For cell membranes this assumption is usually only true over a limited range of voltages.

Driving Force

The electrical potential that acts on a given ion is known as the **driving force**. It is not simply the membrane potential, although it is dependent on the membrane potential. In addition, the driving force is dependent upon the equilibrium potential for each ion and, as a consequence, the driving force is different for each ion.

For K^+ ions

driving force = $(V_m - E_K)$

For Na^+ ions

driving force = $(V_m - E_{Na})$

Substituting into Ohm's law (equation 3),

$$I_K = g_K(V_m - E_K)$$
$$I_{Na} = g_{Na}(V_m - E_{Na})$$

Where:

V_m	membrane potential
E_K	equilibrium potential for K^+ ions
E_{Na}	equilibrium potential for Na^+ ions
g_K	conductance for K^+ ions
g_{Na}	conductance for Na^+ ions

Driving force can be a difficult concept. It is helpful to think about what happens when the driving force is zero for K^+ ions (when $V_m = E_K = -86$ mV, $I_K = 0$). At this membrane potential there is still a large electrical potential acting on the Na^+ ions. Unlike electrical circuits, in biological systems there are multiple current carriers each of which is independent and the currents carried by each ion species must be calculated independently.

An equivalent circuit for a membrane permeable to both Na^+ and K^+ ions is shown in Figure 9. There are two independent conductances and two independent driving forces that act in parallel across the membrane. By convention, a current flowing out of the cell is a positive current and an inward current is a negative current. Typically, the K^+ current will be positive and Na^+ current will be negative.

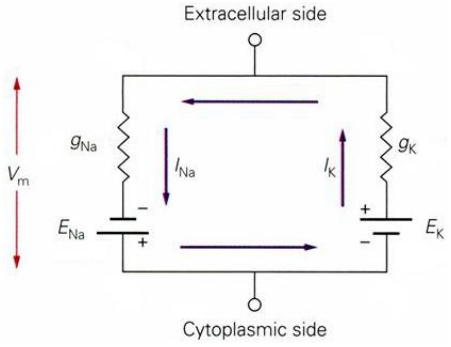

Figure 9 Equivalent circuit for a membrane permeable to both Na^+ and K^+ ions

At rest, the membrane potential of the cell is constant, implying that there is no net current flow across the cell membrane. This means that at steady state,

$$I_K + I_{Na} = 0 \qquad 4$$

The magnitudes of the two currents are equal, but I_K will have an opposite polarity to I_{Na}.

For, $E_K = -86$ mV
$E_{Na} = -61.5$ mV
$V_m = -76$ mV

$$I_K = g_K(V_m - E_K)$$

$$I_K = g_K(-76 - -86)$$

$$I_K = 10g_K \quad (5)$$

$$I_{Na} = g_{Na}(V_m - E_{Na})$$

$$I_{Na} = g_{Na}(-76 - 61.5)$$

$$I_{Na} = -137.5g_{Na} \quad (6)$$

Combining equations 4, 5 and 6,

$$10g_K = 137.5g_K$$

$$g_K \approx 14g_{Na}$$

In other words, at rest, for this particular combination of values, the K^+ ion conductance, g_K, is approximately fourteen times larger than the Na^+ ion conductance, g_{Na}.

4 Action Potentials

The defining feature of most electrically excitable cells is that they produce action potentials. An action potential is an electrical event during which the membrane potential rapidly depolarizes, typically to a positive potential, and then repolarizes back to the resting membrane potential. Action potentials have two functions; they provide the means by which electrical excitation can travel significant distances along specific neuronal structures known as **axons** and they can also trigger a rapid influx of Ca^{2+} ions into the cell for the purposes of triggering a cellular response such as neurotransmitter and hormone release or muscle contraction. The first of these functions will be described in this chapter.

1. Action Potentials

Action potentials are produced by changes in the state of the voltage-gated sodium and potassium channels found in the cell membrane.

Passive Electrical Properties of the Membrane

As described in Chapter 3, the electrical properties of the cell membrane can be modeled by equivalent electrical circuits. One equivalent circuit that is useful for understanding membrane electrical behavior is the RC circuit, so-named because it contains a resistor and a capacitor in parallel (Figure 1A).

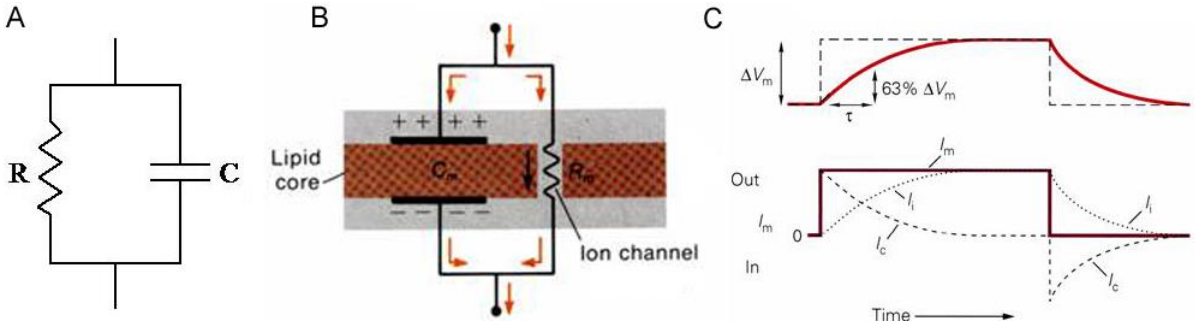

Figure 1 (A) Simple RC circuit. (B) The capacitor corresponds to the lipid bilayer and the resistor corresponds to the sum of all the open ion channels. (C) A current step is injected into an RC circuit and the change in voltage across the circuit is measured. Note that the change in voltage is not instantaneous but takes some time to "charge up" to the final voltage.

The capacitance of the lipid bilayer and the conductance of the ion channels in the membrane are in parallel and behave like an RC circuit (Figure 1B). If a square pulse of current is injected into an RC circuit the voltage does not change instantaneously (Figure 1C). The voltage changes slowly because of the capacitor. Initially the injected current flows preferentially onto the capacitor, this is known as the capacitive current (I_c). As charge accumulates on the capacitor an increasing amount of charge flows across the resistor and the voltage increases to reach a steady-state value that is determined by Ohm's Law. If there was no capacitor in the circuit, the change in voltage would be instantaneous because all of the current would flow across the resistor from the start of the current step.

The RC circuit can be used to model the behavior of spherical cells or cells that are electrically compact. The model assumes that the injected current "sees" all of the cell membrane capacitance and conductance simultaneously. This property is known as isopotentiality indicating that there are

no significant voltage gradients within the cell. Neurons can have quite complex architectures and this assumption is not usually valid in large neurons or in their axons, where more complex models are required.

The membrane capacitance acts to slow down the voltage response of the membrane to injected currents. This has a significant effect on the electrophysiology of cells, particularly their response to synaptic currents and local circuit currents (see later in this chapter).

Electrical Properties of an Active Membrane

If a current is injected into an axon of a neuron in increasing steps, the membrane initially behaves like a passive RC circuit. This is known as the **passive electrical response**. The voltage response to the injected current increases linearly with the amount of current that is injected, as expected from Ohm's law (Figure 2).

At a certain **threshold voltage**, however, the response changes dramatically. A regenerative response is elicited where the voltage rises rapidly towards +40 mV before rapidly repolarizing. This **all-or-nothing response** is nonlinear and is known as an action potential. Increasing the current stimulus above threshold does not induce a larger action potential.

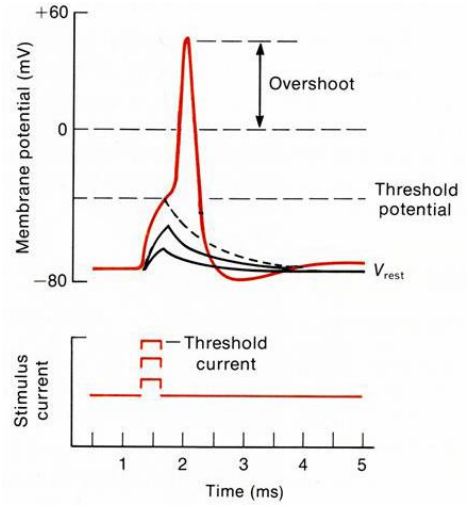

Figure 2 Response of an electrically excitable membrane to increasing depolarizing current steps.

Properties of the Action Potential

Action potentials in most excitable cells share several common characteristics (Table 1). As described above they are triggered by depolarization. In the example above the depolarizing current was artificially injected current into the cell. In a normal neuron the depolarizing stimulus will be excitatory synaptic input from a pre-synaptic cell.

Table 1. Characteristics of the Action Potential	
1.	triggered by depolarization
2.	threshold voltage level must be reached in order to trigger an action potential
3.	all-or-none event
4.	membrane potential at peak of action potential is positive (overshoot)
5.	absolute refractory period

A threshold level of depolarization must be reached in order to trigger an action potential. The threshold voltage is quite stable for a given cell and is typically in the range -50 to -30 mV for different cell types. In simple cells subthreshold currents produce linear membrane responses. Suprathreshold depolarizing currents initiate an action potential.

Action potentials are all-or-none events. This means that the height and duration of the action potential do not increase as the suprathreshold currents increase in size. A commonly used analogy is the firing of a pistol. The response is independent of how hard the trigger is pulled.

At the peak of the action potential, the membrane potential is positive. The height of the potential above zero is known as the **overshoot**. In many cells, following the action potential, the membrane potential becomes transiently more negative than the resting membrane potential. This is known as the **afterhyperpolarization**.

After a neuron fires an action potential there is a brief period during which it is impossible to fire another action potential. This is known as the **absolute refractory period**.

Changes in Sodium and Potassium Conductances During the Action Potential

An equivalent circuit for an excitable membrane is shown in Figure 3. In the resting membrane of a neuron there is a small leak conductance (g_L) that is predominantly a K^+ ion conductance, which sets the membrane potential close to but not quite at the equilibrium potential for K^+ ions. There are two other conductances, which correspond to the voltage gated sodium and potassium channels, g_{Na} and g_K respectively. These are variable conductances, meaning that their value can change over time. At rest the voltage gated Na^+ and K^+ channels are normally closed and g_{Na} and g_K are equal to zero. An action potential is initiated when sodium channels begin to open and the conductance to Na^+ ions begins to rise. During the upstroke of an action potential the Na^+ ion conductance increases rapidly. The sodium channels begin to inactivate quite rapidly after opening so that g_{Na} begins to decline soon after reaching a peak. Following a brief delay, the potassium channels also begin to open and g_K increases, although more slowly and to a lesser extent than g_{Na}.

The entire duration of the action potential is about 1 millisecond, although this is quite variable for different types of neurons. The rapid termination of the action potential is due to two factors:

1. Inactivation of the sodium conductance.
2. Activation of the delayed potassium conductance.

Immediately following the action potential, during the after-hyperpolarization phase, g_K is still elevated as the potassium channels slowly begin to deactivate. As a consequence, the membrane conductance for K^+ ions is elevated relative to rest during this period, and this pushes the membrane potential very close to E_K, the equilibrium potential for K ions. The membrane potential returns to the resting value as the potassium channels continue to deactivate.

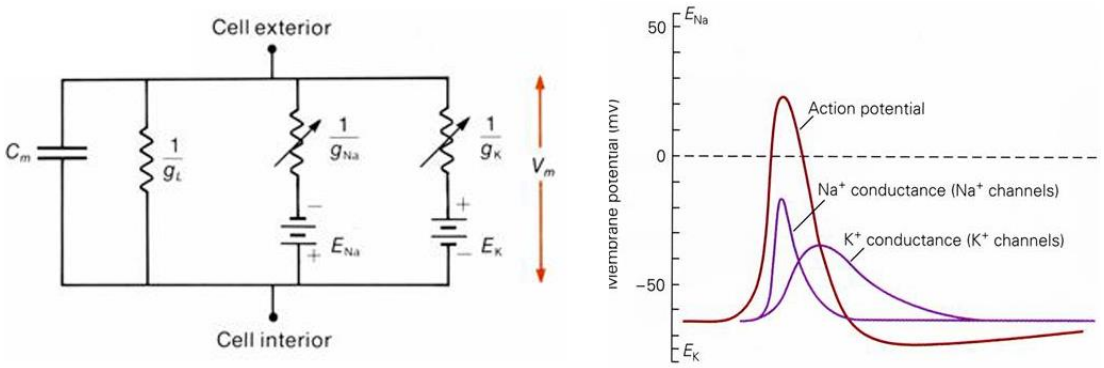

Figure 3 (Left panel) Equivalent circuit for an electrically excitable cell. The leak conductance (g_L) maintains the cell at the resting membrane potential. The two variable conductances (g_{Na} and g_K) are closed at rest but rapidly increase during an action potential. (right panel) Changes in Na^+ ion and K^+ ion conductance during the course of an action potential.

It is important to understand that the Na^+ and K^+ channels have very different kinetics, the rates at which they open, close and inactivate. The Na^+ channels activate quickly and then inactivate quickly. The K^+ channels activate more slowly than the Na^+ channels and this delay allows the Na channels to initiate the upstroke of the action potential. The K^+ channels have relatively slow deactivation kinetics and even slower inactivation kinetics. Inactivation is so slow that it is normally ignored when thinking about the action potential.

Changes in the Kinetic State of the Sodium and Potassium Channels During the Action Potential

As described in the previous chapter the sodium and potassium channels can cycle between three different states; closed, open and inactivated. These states predominate at different stages of the action potential (Figure 4).

1. At rest the activation gates of both channels are closed and the channels are not inactivated.
2. During the upstroke of the action potential, depolarization causes the activation gates of the Na^+ channel to open. This produces a large increase in the permeability to Na^+ ions. The K^+ channels also begin to open but much more slowly so that most are still closed during the upstroke.
3. During the repolarizing phase, the Na^+ channel inactivation gate closes and the activation gates of the K^+ channels are now fully open. This point corresponds to the absolute refractory period because the Na^+ channels are inactivated and are not ready to reopen and initiate another action potential.
4. During the afterhyperpolarization phase, the K^+ channels are still open and the Na^+ channels are beginning to recover from inactivation. This point corresponds to the relative refractory period.

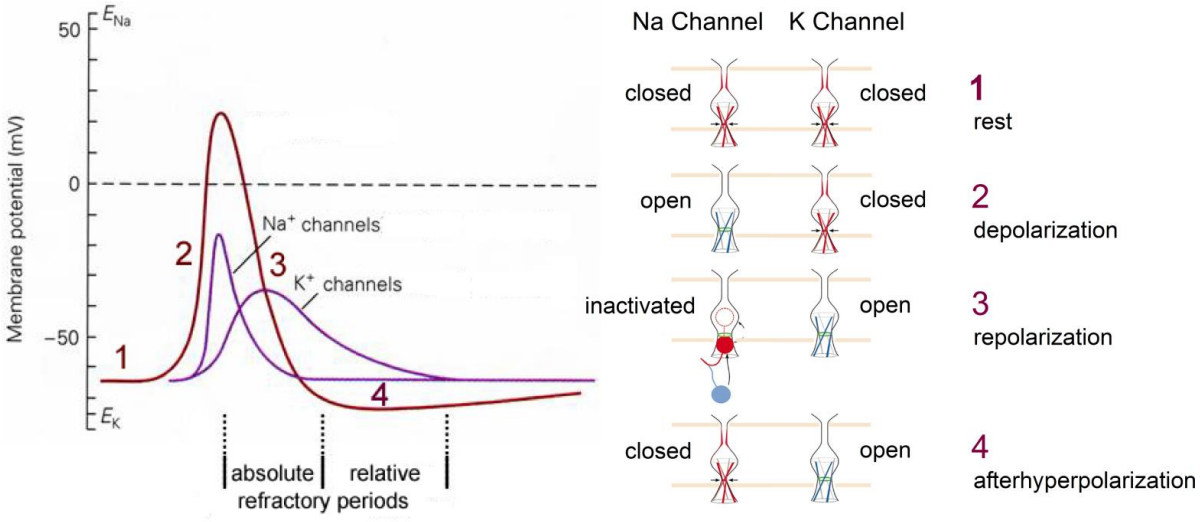

Figure 4 Cartoon showing the changing states of the Na^+ and K^+ channels during the course of an action potential.

You can think of the potassium channel activation gate as being on a stiffer hinge than the sodium channel gate. It responds to voltage but not as quickly as the sodium channel activation gate. This simple model is not too far removed from reality. The K^+ channel is more resistant to the conformational change that produces channel opening than is the Na^+ channel in response to the same change in membrane potential.

Refractory Period

An excitable membrane is said to be refractory when it either cannot support an action potential or when it can only do so if given a larger stimulus than normal. These two types of refractoriness are known as the **absolute refractory period** and the **relative refractory period**. The absolute refractory period corresponds to a period when most of the sodium channels are inactivated and there are insufficient closed channels ready to re-open to generate an action potential. During the relative refractory period there are enough sodium channels in the closed state available to produce an action potential but because there are still potassium channels open during the afterhyperpolarization phase a larger injected current is required in order to trigger an action potential.

Positive Feedback Cycle during the Upstroke of the Action Potential

The upshoot of the action potential is created by a positive feedback cycle (Figure 5). The opening of sodium channels produces an inward current that further depolarizes the membrane potential, which allows more sodium channels to open. This cycle repeats until most of the channels have opened.

This positive feedback cycle is the basis of the all-or-none behavior of the action potential. Once the membrane potential reaches threshold and the sodium channels begin to open, the cycle tends to run to completion, driving the membrane potential up towards the Na^+ ion equilibrium potential. The threshold potential is roughly equivalent to the potential at which the sodium channels begin to open.

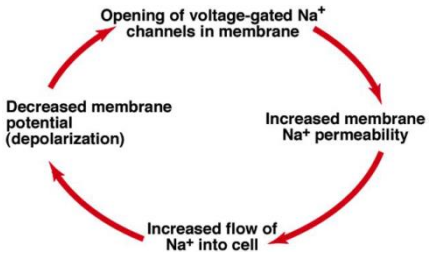

Figure 5 Positive feedback cycle during action potential upstroke.

2. Conduction of Action Potentials along Axons

Basic Neuron Anatomy

A typical neuron is comprised of several distinct subcellular compartments (Figure 6):

1. cell body (soma)
2. dendrites (dendritic tree)
3. initial segment (axon hillock)
4. axon
5. nerve terminal

The neuron is functionally polarized. Electrical information passes from the presynaptic nerve terminal to the dendrites or cell body of the postsynaptic neuron and then travels down the axon to the nerve terminal, where it is transmitted to the next neuron. In general, there is a one-way flow of electrical excitation from the presynaptic neuron to the postsynaptic neuron.

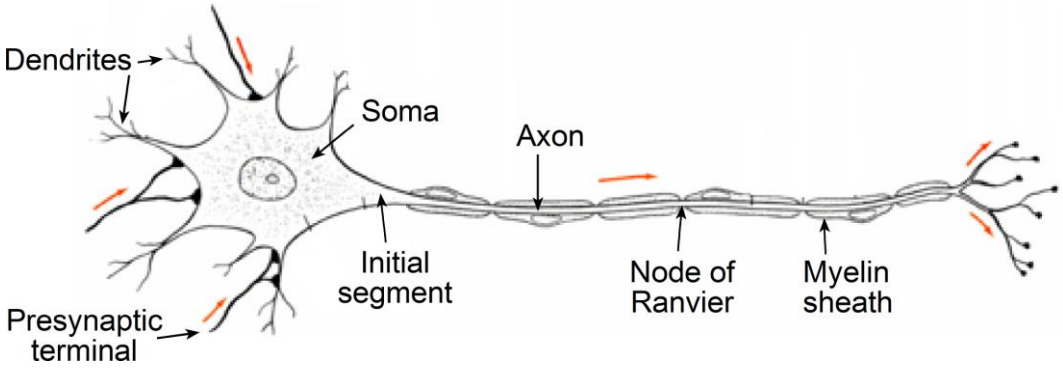

Figure 6 Structure of a typical neuron. Arrows indicate the normal direction of travel of electrical excitation.

The action potential typically initiates in the initial segment, since this is a region where there is a high concentration of Na^+ channels, and then propagates down the axon by depolarizing the neighboring axon membrane. This self-propagating wave of depolarization travels down the axon and ends in the nerve terminal.

Action Potential Propagation in an Axon

Cable Properties

The passive electrical properties of the axon membrane are more complicated than those of a simple spherical cell described previously. They can be described using a similar mathematical model

to that originally first used to analyze the electrical properties of transatlantic telegraph cables. As a consequence, the passive electrical properties of axons are known as its cable properties.

If a current is injected into the center of an axon at a single point the current can do one of two things (Figure 7). It can flow axially along the interior of the axon or it can flow back to ground across the membrane. The relative amount of current that crosses the membrane versus the amount of current that flows axially depends upon the resistance of the membrane relative to the resistance of the axial current path. With each increment in distance along the axon, the fraction of the injected current that flows down the axon again faces two paths and the amount of current flowing down the nerve fiber will gradually decrement as will the amount of current crossing the membrane resistance. As a consequence, the injected current will have a steadily decreasing influence on the membrane potential with increasing distance from the site of current injection.

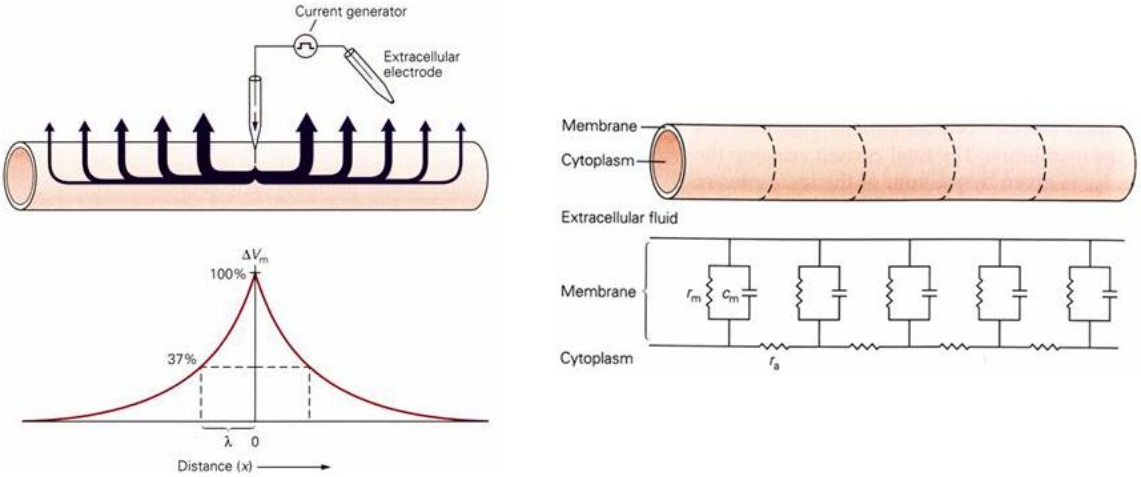

Figure 7 (left panel) (upper figure) Current flow in an axon following current injection at a single point in the axon. (lower figure) Change in membrane voltage as a function of distance from the point of current injection. (right panel) Electrical model of the axon as a series of RC circuits.

The axon cable can be mathematically modeled as a series of RC circuits connected together (Figure 7). The cable is imagined to be cut-up into small segments, with each segment corresponding to an RC circuit (with membrane resistance r_m) that is linked to its neighbors by an access resistance (r_a).

A measure of the electrical performance of a cable is known as the length constant (λ).

$$\lambda = \sqrt{\frac{r_m}{r_a}} \qquad 1$$

The length constant is the distance over which the steady-state membrane potential drops to 37% of the original amplitude. The conduction properties of the cable are best when r_a is relatively small and r_m is relatively large. In other words, decreasing the axial resistance increases the length constant and increasing the membrane resistance, increases the length constant.

Axons are not very good conductors by the standards of typical electrical components and length constants are relatively short. In a typical axon the voltage will decrement by about 95% within 1-2 mm of the site of current injection.

Local Circuit Currents

The key to understanding how an action potential propagates down an axon is to understand local circuit flow (Figure 8). The artificial injection of a current at one point in an axon causes currents to flow for some distance from the point of current injection. These are known as local circuit currents and the distance over which these currents flow is determined by the length constant. Local circuit current flow acts to depolarize the cell membrane for some distance from the site of current injection.

Current flow through the axon surrounding the peak of an action potential is directly analogous to the injected current model (Figure 8). At the peak of the action potential there is an inward flow of current carried by sodium ions. The membrane on either side of the action potential peak will be depolarized by local circuit flow, in the same way as for the artificially injected current. The region of membrane in front of the action potential wave front, whose membrane potential is pushed above the threshold potential by local circuit flow, will initiate an action potential, which is now some distance further down the axon from the original action potential. This cycle of local circuit flows initiating an action potential in front of the traveling action potential wave front repeats itself continuously as the action potential travels down the axon.

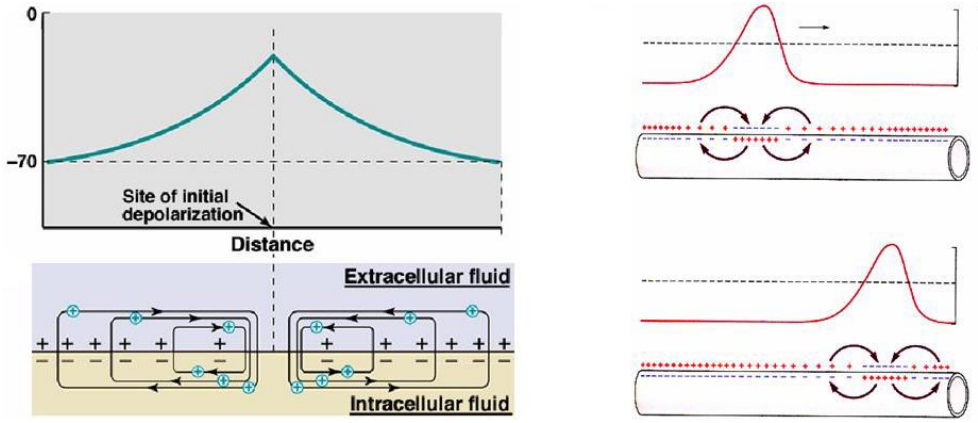

Figure 8 (left panel) Local circuit flow around the site of current injection in an axon. (right panel) Local circuit flow around a propagating action potential.

The action potential normally only moves in one direction down the axon because the membrane region behind the action potential wave front is in the refractory period and unable to support a new action potential. Normally the action potential travels from the cell body down the axon towards the nerve terminal. These are called **orthodromic** action potentials. The axon is functionally symmetric, however, and can conduct action potentials in either direction. Action potentials propagating in the opposite direction, from the nerve terminal to the cell body, are called **antidromic** action potentials. If an axon is artificially stimulated in the middle of its length then an action potential can travel in two directions away from the site of current injection.

Factors Affecting the Speed of Action Potential Propagation

The speed that electrical excitation travels down an axon is much slower than the speed of current flowing through a wire. Current flow in a wire is close to instantaneous at the dimensions of typical electrical circuits, because it travels at the speed of light (3×10^8 m/s). The rate of electrical conduction in an axon is vastly slower, varying over the range 0.1 to 100 m/s.

The two major factors that affect the rate of action potential propagation are the same as those that affect the length constant; axial resistance and membrane resistance. Either increasing membrane resistance or decreasing axial resistance will result in more current flowing inside the axon, as opposed to flowing across the cell membrane. As a consequence, local circuit flow will spread over a

greater length of the axon resulting in a greater spread of membrane voltage depolarization, which will initiate an action potential further down the axon and speed up the rate of conduction.

During the course of evolution two strategies have been used to increase the speed of action potential propagation:

1. Decrease the resistance of the axial path down the inside of the axon by increasing the diameter of the axon, which gives a greater cross-sectional area for current flow.
2. Increase the resistance of the cell membrane with a specialized sheathing, known as **myelin**.

Invertebrates only use the first approach and some invertebrates, such as squid, can have axons up to 1 mm in diameter. These giant axons are typically used to produce escape behavior from predators, the survival of individuals within the species being a significant factor in driving the evolutionary development of these axons. The problem with this strategy is that there is not enough space to do this with more than a handful of axons before the nervous system becoming inefficiently large. As a consequence, invertebrate nervous systems have some inherent limitations relative to vertebrates.

Vertebrates also use larger axons for the fastest conducting nerve fibers, but only up to 1 to 20 μm in diameter. The fastest vertebrate axons are faster than those of invertebrates, however, because vertebrates have developed specialized cells whose function is to increase the membrane resistance of the axon by producing a myelin sheath around the axon.

Myelination

Myelin forming cells are also known as glial cells. They form a sheath around the axon that acts somewhat analogously to the plastic insulation wrapped around the copper wire of household electrical circuits. There are periodic breaks in the myelin sheath known as **nodes of Ranvier**. Myelination alters the local current flow by reducing the capacitance and increasing the resistance of the internodal membrane, producing more efficient local circuit current flow. Most of the current flow across the membrane is limited to current flow through the internodal membrane.

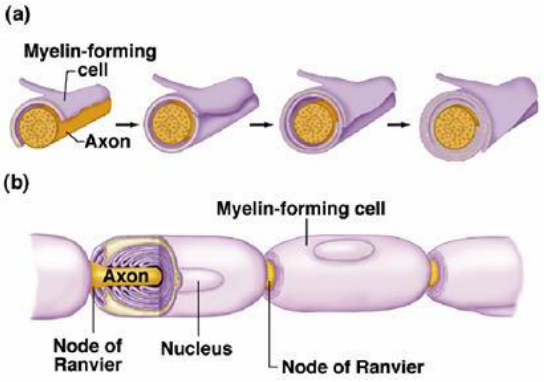

Figure 9 (a) During development myelin forming cells wrap around the axon. (b) The myelin sheath has periodic gaps known as the nodes of Ranvier.

Sodium channels are clustered at the nodes of Ranvier and are largely absent in the internodal membrane. As a consequence, a propagating action potential leaps from node to node. During action potential conduction the membrane potential in the internode region is depolarized by local circuit currents flowing from the previous node in which an action potential has fired. Conduction is fast

between nodes and then slows down in the node as a new action potential is triggered (Figure 10). In effect, the action potential jumps from node to node down the axon. This is known as **saltatory conduction** (from the Latin 'saltare' meaning to jump).

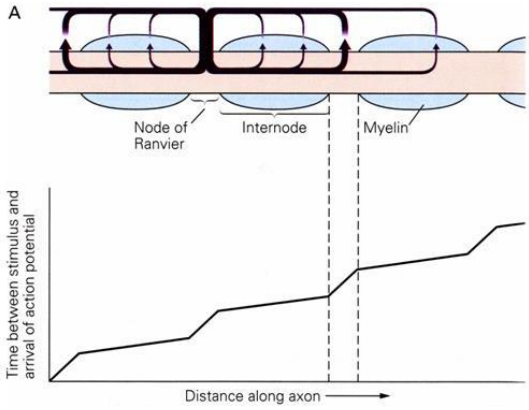

Figure 10 Excitation jumps rapidly between nodes of Ranvier.

In addition to streamlining electrical conduction, myelinated axons are also very efficient from a metabolic viewpoint. Less energy must be expended by the Na,K-ATPase in maintaining the Na^+ and K^+ ion concentration gradients because there are many fewer ion channels in the membrane. This is important because the axon is more susceptible to the run-down of ion gradients than the cell body, due to the much larger surface area to volume ratio of the axon.

6 Neurotransmitter Receptors

There are two broad classes of neurotransmitter receptors: those that contain an integral ion channel that is gated by **ligand** binding and those that are G protein-coupled (Table 1). The ligand-gated channels are also known as **inotropic receptors** and the G protein-coupled receptors are known as **metabotropic receptors**. Classic examples of a ligand-gated ion channel are the nicotinic acetylcholine receptor and the glutamate receptor. Classic examples of G protein-coupled receptors include the adrenergic receptors and the muscarinic acetylcholine receptors. Many neurotransmitters, acetylcholine, GABA, glutamate, serotonin, and ATP, have receptors of both types.

There is no homology between these two different families of receptors. This is true even for receptors that bind the same neurotransmitter, such as the nicotinic and muscarinic acetylcholine receptors. Within the ligand-gated ion channel family there are three distinct gene families (Table 2). These also share no homology with each other.

The G protein-coupled receptors belong to a single very large gene family, containing hundreds of members. The large size of this gene family reflects both the large number of different neurotransmitters that act through receptors of this type as well as the role of G protein-coupled receptors in many different non-neuronal signaling pathways.

The mechanism of action of these two types of receptors is fundamentally different (Figure 1). For the ligand-gated ion channels, the ion channel forms an integral part of the receptor. For the G protein-coupled receptors the linkage to the effector protein (channel or enzyme) is more convoluted, involving at least one intermediary protein, the G-protein. Not surprisingly then, the ligand-gated channels are much faster acting, they can open within microseconds of agonist binding whereas the G protein-coupled receptors generally act more slowly, typically acting in the hundred millisecond to second time frame.

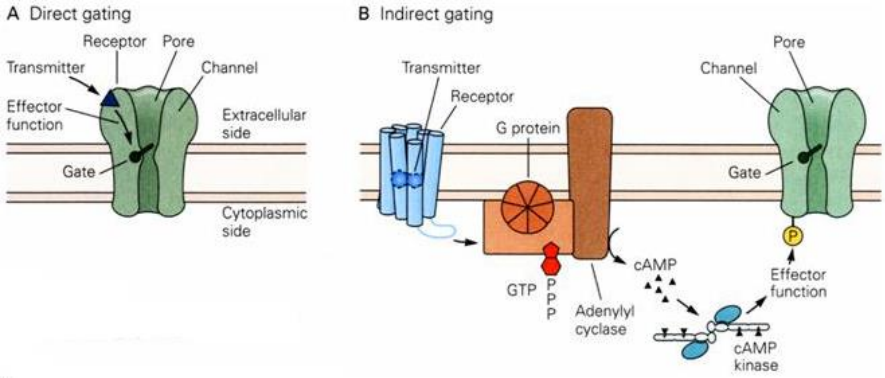

Figure 1 Comparison of ligand-gated ion channels and G protein-coupled receptors.

Receptors within the same gene family can have quite different physiological effects. The ligand-gated ion channels can be either excitatory or inhibitory. The excitatory channels (acetylcholine, glutamate) are cation selective. The inhibitory channels (GABA, glycine) are anion selective. The G protein-coupled receptors can have a myriad of different actions, dependent upon which effector proteins they activate.

Table 1. Classification of Neurotransmitter Receptors

A. Ligand-Gated Ion Channels

- integral ion channel, gated by ligand binding
- multiple subunits, either three, four or five subunits for complete receptor
- ≈ 80 genes in mammalian genome encode ligand-gated ion channel subunits
- underlie fast synaptic transmission

Neurotransmitter	Receptor	
Acetylcholine	nicotinic acetylcholine receptor	
GABA	$GABA_A$ receptor	
Glycine	glycine receptor	
Glutamate	glutamate receptor 3 subtypes	AMPA receptor NMDA receptor Kainate receptor
Serotonin	$5\text{-}HT_3$ receptor	
ATP	purinergic receptors	P2X receptor

B. G Protein-Coupled Receptors

- receptor is generally a single polypeptide
- ligand binding activates G-proteins, which are intermediary effector proteins
- receptor usually has seven membrane spanning domains
- ≈ 750 genes in genome encode G protein-coupled receptors

Neurotransmitter	Receptor	
Acetylcholine	muscarinic acetylcholine receptor	
GABA	$GABA_B$ receptor	
Glutamate	metabotropic glutamate receptor	
Norepinephrine (noradrenaline)	adrenergic receptor	
Serotonin	$5\text{-}HT_1$ receptor	
ATP	purinergic receptors	P2Y receptor
Dopamine	dopamine receptor	
Neuropeptides	includes: opioid, substance P, NPY and VIP receptors	

1. Ligand-Gated Ion Channels

The three main families of ligand-gated channels are the Cys-loop receptors, the glutamate receptors and the purinergic (P2X) receptors (Table 2). These three families share no homology or evolutionary history.

Table 2. Ligand-Gated Ion Channels
A. Cys-loop Receptors
• pentamers • monovalent cation (some have Ca^{2+} permeability) or anion channels • neurotransmitters: acetylcholine, GABA, glycine, serotonin
B. Glutamate Receptors
• tetramers • monovalent cation channels (some have Ca^{2+} permeability) • neurotransmitter: glutamate, three subtypes: AMPA, NMDA, Kainate
C. Purinergic (P2X) Receptors
• trimers • cation channels • neurotransmitter: ATP

2. Cys-loop Receptors

The Cys-loop receptor family encompasses a broad range of receptors, including the nicotinic acetylcholine, $GABA_A$, glycine and 5-HT3 receptors (Table 3). The name of this class derives from a shared structural feature, a loop formed by a disulfide bond between two cysteine residues found in the N terminal extracellular domain of the receptor.

There are two main subfamilies, cation selective and anion selective channels. This is a key distinction physiologically, since the cation channels are excitatory in function, they depolarize the membrane potential, whereas the anion channels are generally inhibitory in function.

Table 3. Cys-loop Receptors	
A. Cation Channels	
• nicotinic acetylcholine receptors	16 genes
• serotonin 5-HT3 receptors	5 genes
B. Anion Channels	
• $GABA_A$ receptors	19 genes
• glycine receptors	5 genes

Cys-loop Receptor Structure

The prototypical Cys-loop receptor is the acetylcholine receptor expressed in skeletal muscle. It is a **pentamer** comprised of four different subunits: α, β, γ, δ, with the stoichiometry: $\alpha_2\beta\gamma\delta$. Each of these subunits has four membrane spanning domains. The five subunits assemble in the receptor to form a pseudo-fivefold symmetry, with each subunit contributing to the formation of the pore (Figure 2).

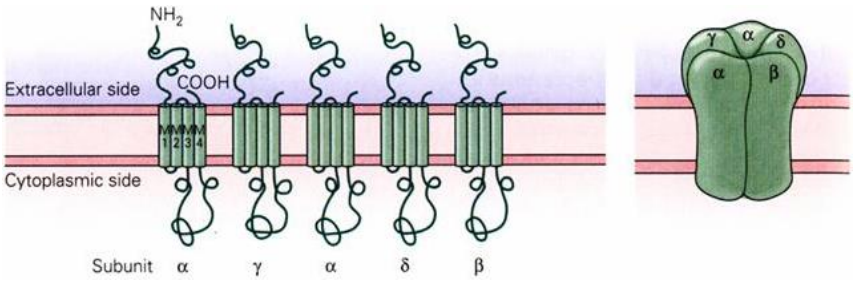

Figure 2 Structure of the neuromuscular nicotinic acetylcholine receptor

The subunits have three main functional domains: the ligand binding (LBD), transmembrane (TMD) and intracellular domains (IND) (Figure 3). The receptor has two agonist binding sites that reside primarily in the α-subunits and are found at the interface between each of the two α-subunits and the neighboring γ and δ subunits. The two binding sites have different affinities for acetylcholine. A striking feature of the receptor is how much of it projects out of the plane of the cell membrane (Figure 3A). The extracellular region of the receptor projects more than 65Å into the extracellular space. The agonist binding site is located a considerable distance (50Å) from the gate of the channel, which is located in the middle of the membrane spanning domain. The intracellular surface projects 20Å into the intracellular space. The large blob that hangs from the base of the receptor is comprised partly of receptor protein but also contains a clustering protein (rapsyn). There are large tunnels between the blob and the main part of the receptor that allow ion movement into the channel.

The Cys-loop receptors are evolutionary ancient. A simpler form of the receptor can be found in prokaryotes (Figure 3C), where it appears to function as a chemoreceptor.

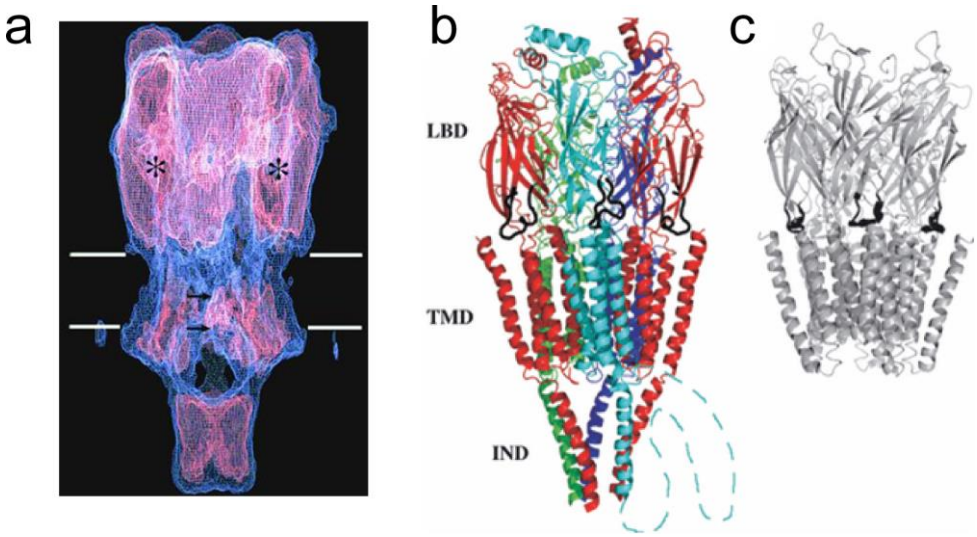

Figure 3 A. Low resolution structure of the nicotinic acetylcholine receptor. The two white lines indicate the boundaries of the cell membrane. The ACh binding pockets (asterisks), gate of the channel (upper arrow) and selectivity filter of the open channel (lower arrow) are marked. The subunits are slightly tilted around the axis of the receptor. The ion conduction pathway goes through tunnels between the large intracellular domain at the base of the receptor and the main part of the receptor. B. High resolution structure of the nicotinic acetylcholine receptor. Each of

the five different subunits has a different color. The ligand binding (LBD), trans-membrane (TMD) and intracellular domains (IND) are marked. C. High resolution structure of the prokaryotic Cys-loop receptor. The Cys-loops of the receptors are marked in black in (b) and (c). Only the three front loops can be seen.

The four subunits are similar in size and folding pattern (Figure 4). The ligand binding domain is a β-sandwich comprised of two β-sheets made from six (inner) and four (outer) strands joined through the Cys-loop disulphide bridge. The transmembrane domain is comprised of four hydrophobic α-helices. The pore-lining helix M2, in the closed channel, is bent slightly inward towards the lumen of the pore. The intracellular domain has one α-helix and other less ordered regions that are not resolved in the structure shown in Figure 4.

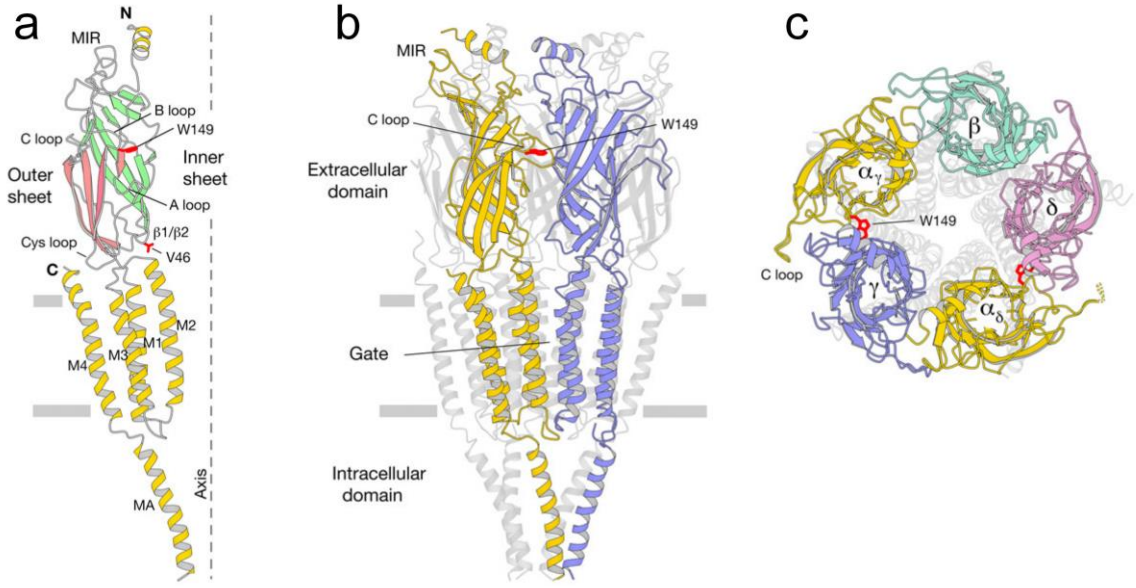

Figure 4 A. Alpha subunit. B. Side view of receptor. C. Top view. Marked in red are the side-chains of the ACh-binding residues αW149 on the B loop and αV46 on the β1/β2 loop.

Ion Permeation through the Acetylcholine Receptor

The four membrane spanning domains of each subunit are named M1 through M4 (Figure 5). The M2 domain lines the inner surface of the channel and the other helices are arranged between this helix and the lipid bilayer. The M2 helix is the primary determinant of the ion permeation properties of the channel.

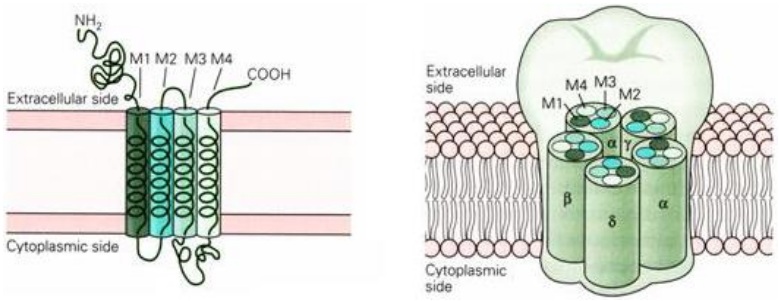

Figure 5 Location of M2 membrane spanning region within the acetylcholine receptor.

The skeletal muscle acetylcholine receptor has similar permeability to Na^+ ions as it has to K^+ ions, but does not allow Cl^- ions to pass. The structure of the pore is less specialized than that of the K^+ ion selective channels described previously because it only has to distinguish between positively and negatively charged ions, not between ions with the same charge but of different size.

Charged residues within the channel pore play a major role in determining the ion selectivity of the pore. There are three rings of negatively charged amino acid side chains within the pore (Figure 6). These rings contain three or four negative charges. The external and inner rings act to decrease the local concentration of anions around the entrance to the pore. The selectivity filter is most directly associated with the intermediate ring of negative charges on the cytoplasmic surface of the channel.

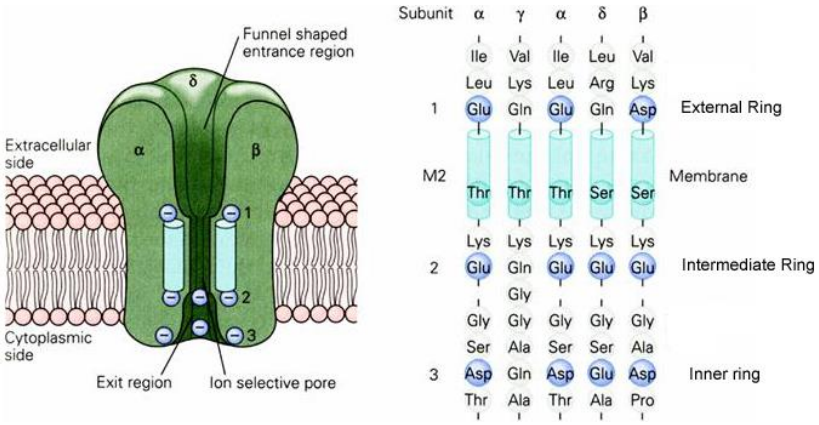

Figure 6 Location of three rings of negatively charged side chains within the channel pore. Notice that immediately before the selectivity filter (intermediate ring) is a positively charged lysine residue. This positive charge is normally turned away from the pore.

The intermediate ring is the region where the pore is at its narrowest in the open state. The pore is physically quite a bit larger than the K^+ channel pore and the ions do not completely lose their hydration shell during their passage through the channel. Selectivity is produced by electrostatic interactions between the ions and charged side chains.

The central role of the intermediate ring in determining ion selectivity is shown by experimental manipulation of the charges in these side chains. Although something of a simplification, a cation selective channel can be converted to an anion selective channel by changing the intermediate ring from a negatively charged ring to a positively charged ring.

The structure of the cation selective AChR and the anion selective Glycine receptor are quite similar. A key difference lies within the pore sequences of the two receptors (Figure 7). Just two mutations can convert the cation channel to an anion channel and vice versa; the conversion of the intermediate negative ring to uncharged alanine and the addition of a proline residue, which twists the positively charged arginine to face into the pore. All GABA and Glycine receptors have this proline residue. This experiment shows that the ion selectivity of the channel largely depends upon electrostatic interactions between the ions and the charged residues in this intermediate ring.

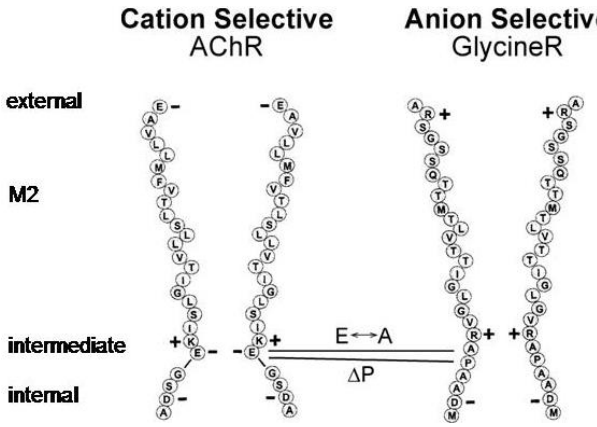

Figure 7 Comparison of the M2 pore lining regions of the acetylcholine receptor and the glycine receptor.

Although mutations in the intermediate ring largely determine whether or not the channel is an anion or a cation channel this does not mean that other regions of the pore are unimportant. Negative charges in the other rings act to increase the local concentration of cations, which increases the single channel conductance of the channel.

Gating of the Acetylcholine Receptor

Acetylcholine binds to two pockets that are relatively deep and provide multiple contact sites between the ligand (ACh) and the receptor ensuring a high degree of binding specificity (Fig. 8).

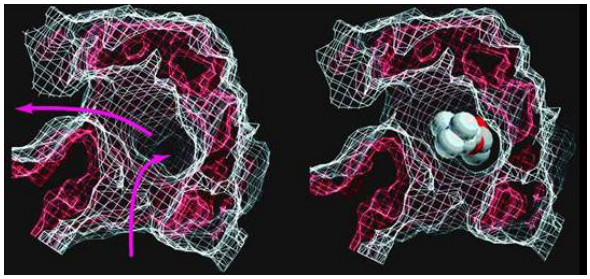

Figure 8 High resolution image of the ACh binding pocket in the alpha subunit. Figure shows the pocket with (right) and without ACh.

It is the binding of ACh to the receptor that induces a conformational change in the receptor which leads to channel opening. Acetylcholine binding produces rearrangements in the regions of the protein surrounding the agonist binding site (Figure 9). Gating of the channel is dependent on the

energy associated with ACh binding. This is in contrast to voltage-gated ion channels where changes in the membrane potential provide the energy for the conformational change that produces gating.

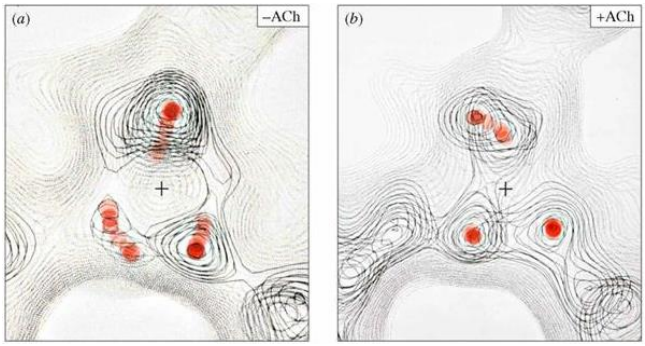

Figure 9 Changes in the local structure of the receptor following ACh binding. Note that the rearrangement of the protein around the binding site (marked with red dots) following ACh binding.

The gate in the closed channel is formed by the hydrophobic region of the M2 helix (Figure 10). The leucine and valine side-chains form a hydrophobic ring that closes the channel by making an energy barrier that hydrated ions cannot cross.

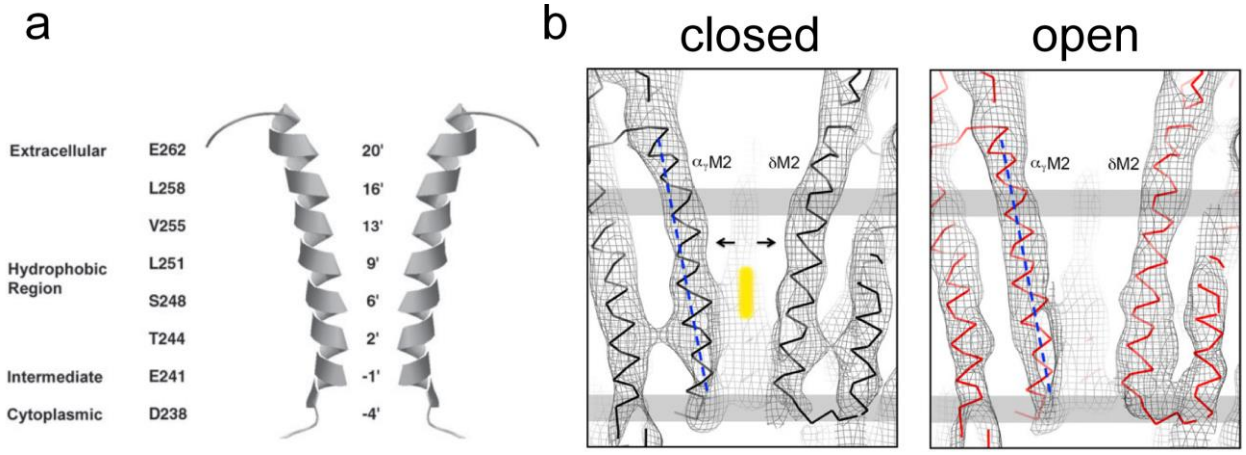

Figure 10 A. M2 channel lining residues. B. Structure of the pore in the closed and open conformations. The vertical yellow bar in identifies the location of the gate, near the middle of the membrane (grey bars).

Opening of the channel by ACh binding is a result of widening of the hydrophobic region of the pore (Figure 10B). At this point the channel becomes a water-filled pore allowing movement of ions across the membrane. The structural changes are relatively subtle but produce a significant change in the energy landscape for ion permeation through the channel.

3. Glutamate Receptors

There are three main types of glutamate receptors that are distinguished on the basis of their different pharmacology (Table 4). They all respond to the neurotransmitter glutamate in the brain but have different responses to artificial agonists or antagonists.

Table 4. Glutamate Receptors			
Receptor	**Agonist**	**Antagonist**	**Number of Genes**
AMPA Receptors	AMPA	CNQX	4
NMDA Receptors	NMDA	APV	9
Kainate Receptors	Kainic acid		5

The two main subtypes, the AMPA receptors and NMDA receptors, have quite distinct functional properties (Table 4).

Table 5. Comparison of AMPA and NMDA Receptors
AMPA Receptors
• fast kinetics • fast onset, offset and desensitization in response to glutamate • small single channel conductance • kainate activates non-desensitizing currents • main form of GluR at most central excitatory synapses • most native receptors contain the GluA2 subunit which limits Ca^{2+} permeability
B. Anion Channels
• slow kinetics • large single channel conductance • high Ca^{2+} permeability • blocked by Mg^{2+} ions • glycine is a co-agonist

Structure of Glutamate Receptors

The mammalian glutamate receptors share a similar topology and quaternary structure. The individual subunits have three membrane spanning domains and the channel is a tetramer, assembled from four subunits (Figure 11). There is no homology between the amino acid sequence of glutamate receptors (GluRs) and Cys-loop receptors.

A protein homologous to the mammalian glutamate receptor is found in prokaryotes where it is involved in chemoreception. The evolution of this protein provides some insight into the glutamate receptor structure (Figure 11). The prokaryotic receptor appears to have arisen from the fusion of a periplasmic binding protein (PBP) and a two membrane spanning domain K^+ channel. Periplasmic binding proteins are involved in high affinity active transport of amino acids and other nutrients in bacteria. The topology of the membrane spanning domain in the fused protein is inverted in comparison to K^+ channels. This receptor retains its K^+ ion selectivity and is activated by amino acids. The receptor assembles as a tetramer, which further supports the idea that it is derived from a K^+ channel. The bacterial periplasmic binding proteins have a clamshell-like structure that clamps around the ligand when it enters the binding site, a function that is retained in the mammalian receptor.

A second fusion event involving the leucine–isoleucine–valine binding protein (LIVBP), another bacterial periplasmic binding protein, and the proto-receptor appears to have added the amino terminal domain (ATD) found in eukaryote glutamate receptors. A third membrane spanning domain was added in the eukaryote receptor and the K^+ selectivity of the pore was lost.

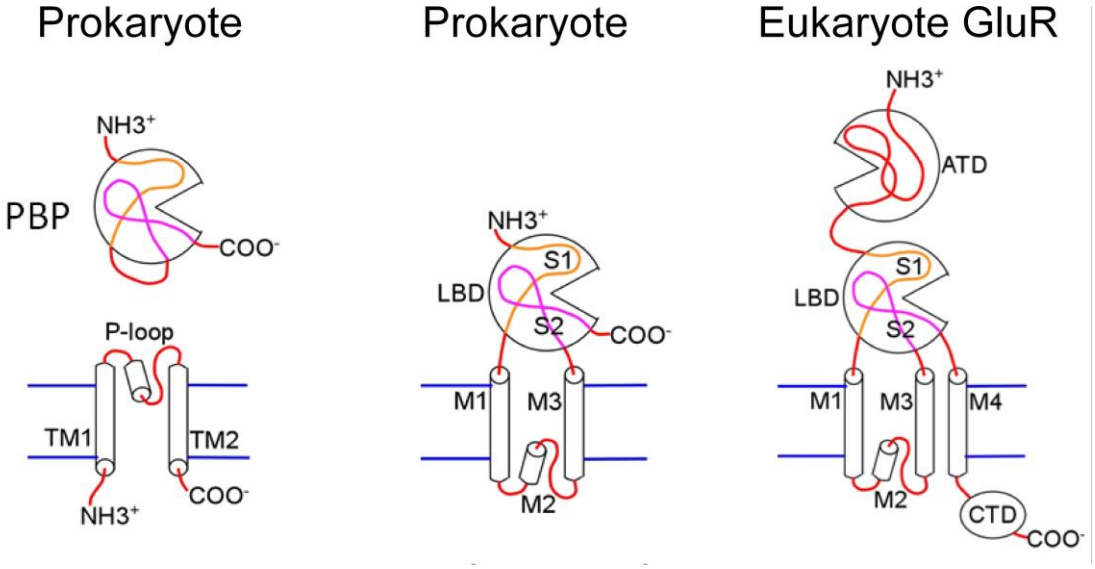

Figure 11 Bacterial periplasmic binding protein (PBP) and K+ channel proteins appear to be the precursors of the prokaryote receptor. Abbreviations: ligand binding domain (LBD), amino terminal domain (ATD).

The GluR is a good example of the modular nature of protein design. Evolution has used a cut-and paste process to create a new protein, combining protein domains from several different sources to generate a protein with unique functional properties.

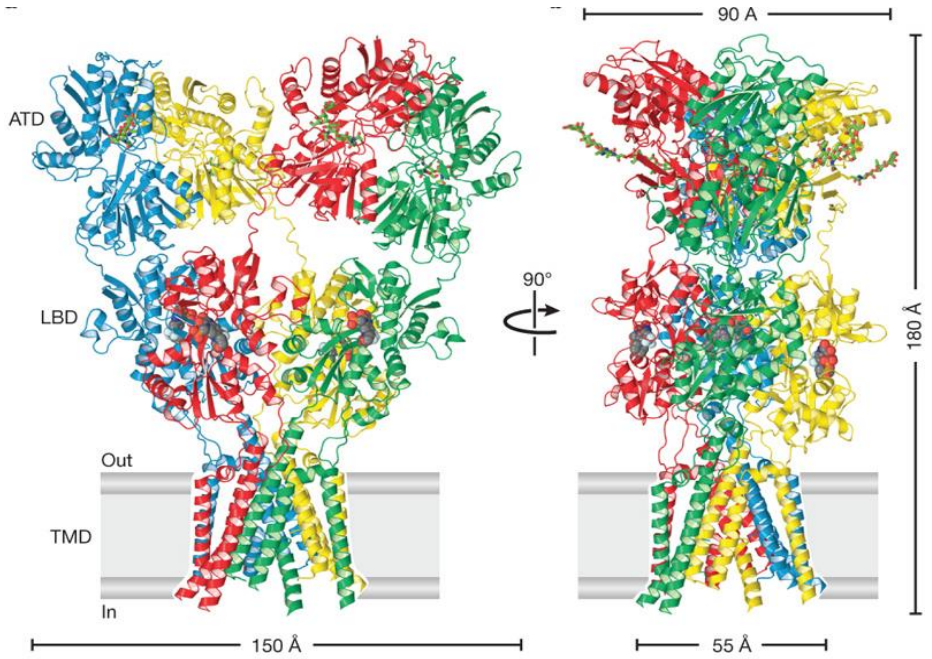

Figure 12 Structure of the AMPA receptor. Competitive antagonist molecules lodged within each LBD clamshell are shown in space-filling representation. Abbreviations: ligand binding do-main (LBD), amino terminal domain (ATD), transmembrane domain (TMD).

The ATD and LBD have 2-fold symmetry whereas the transmembrane domain (TMD) retains the 4-fold symmetry of the original K^+ channel.

4. G Protein-Coupled Receptors

The G protein-coupled receptors generally share a common structure; they have seven membrane spanning regions and the agonist binding site lies in a pocket between the membrane spanning domains (Figure 13). These receptors do not contain an integral ion channel. Instead they act indirectly, generally via intermediary proteins, on effector proteins that can be, but are not necessarily, ion channels.

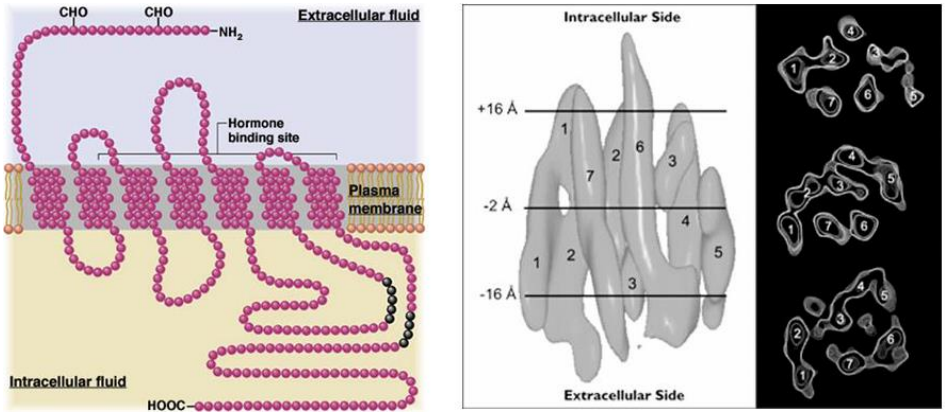

Figure 13 Membrane topology of G protein-coupled receptors, with the amino and carboxy ter-mini located extracellularly and intracellularly respectively and the seven mem-brane spanning domains (left panel). Low resolution structure showing the membrane spanning regions within

the membrane (right panel). The ligand binding site is typically in a pocket within the structure. Note the relatively small size of the receptor compared to the ligand-gated ion channels.

Most of the actions of G protein-coupled receptors are mediated via intermediary proteins known as G-proteins. The G-proteins are peripheral membrane proteins located on the intracellular surface of the membrane. The G-proteins are heteromultimers, comprised of three different subunits: α, β, γ. The α-subunit binds the nucleotide GTP (hence the name G-protein). The three subunits are encoded by more than 100 different genes and the different combinations of subunits that this allows provides for the specificity of effect following receptor activation i.e. different G-proteins bind to different receptors and target different effector molecules.

The basic mechanism by which G protein-coupled receptors work is shown in Figure 14. At the core of this mechanism is the fact that the α-subunit is a GTPase, albeit a rather inefficient one. In each passage of the cycle one GTP molecule is converted to GDP. When ligand binds to the receptor, the α-subunit of the G-protein releases GDP and binds GTP. Binding of GTP induces a conformational change and the trimeric G-protein separates into two parts, the α-subunit and the β/γ subunits. These two components can then activate or inhibit effector proteins independently. The cycle ends when the α-subunit hydrolyzes GTP to GDP and the α-subunit rebinds to the β/γ subunits, thereby inactivating both components of the G-protein. The efficiency of the GTPase determines how long the system is turned on. Typical values are of the order of one minute, a relatively long-lasting effect.

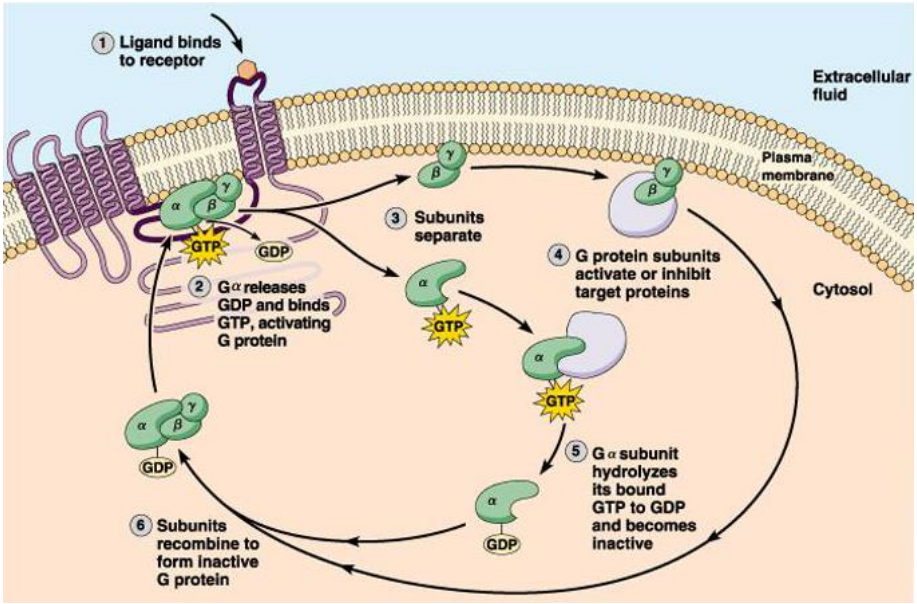

Figure 14 Cycle of G protein activation following receptor stimulation.

The effector proteins that can be stimulated or inhibited by the G-protein subunits are a remarkably diverse set of proteins. Typically, a subunit of the G-protein can directly activate or inhibit an ion channel or it can activate an enzyme that produces a second messenger that activates a second effector protein, such as a kinase, that can then modify the function of an ion channel. Channels are not the only targets of G-proteins however, and activation of G-protein receptors can modulate almost any cellular function.

7 Synaptic Transmission

Synapses are the single most characteristic feature of neurons. Neurons in the mammalian central nervous system typically have from 100 to 100,000 synapses per cell. In a human brain there are a total of approximately 10^{14} synapses. From one perspective, neurons are simply the cellular scaffolding that allows the expression of synapses.

The **synapse** is a highly specialized cellular structure that facilitates rapid communication between two electrically excitable cells. The transfer of electrical excitation is usually a one-way process; from the **presynaptic** nerve terminal to the **postsynaptic** cell.

Most synapses are **chemical synapses**, which means that the presynaptic cell releases a signaling molecule known as a **neurotransmitter**. This neurotransmitter molecule then diffuses towards the second cell where it binds to a **neurotransmitter receptor**. Binding of the neurotransmitter then triggers a response in the second cell via activation of the neurotransmitter receptor.

The unique geometry of the synapse has two functions: it **reduces diffusion times** and **increases the specificity of signaling**. The time taken for molecules to diffuse through solutions is a common problem for biological organisms. Much of the architecture of different organ systems can be explained by the necessity to reduce diffusion times. Diffusion times increase in proportion to the square of the distance over which the molecules diffuse. As a consequence, reducing the distance for diffusion has a dramatic effect on the time taken for diffusion. The synapse brings the membrane of the pre- and post-synaptic cells into very close apposition to minimize diffusion times. Typically, there is a gap of 10 to 40 nm between the pre- and post-synaptic membranes resulting in a diffusion time of significantly less than 1 millisecond. Bringing the presynaptic terminal so close to the postsynaptic cell also increases signaling specificity, so that at most synapses only the two cells making the synapse are in communication. This is very different to how signaling molecules, such as hormones or cytokines, are used. Hormones for example are released into the blood stream and can affect a broad number of cells due to their diffuse distribution pattern.

1. Basic Features of Synaptic Transmission

Synaptic Structure

The synapse is an unusual subcellular structure because it is made by two cells. During formation both cells have to communicate with each other in order to successfully form a synapse. They each have to contribute several different structural components to the synapse to make it work. Typically, several signaling systems in addition to normal synaptic transmission are involved in the back and forth communication between the two cells in order to correctly assemble the synapse.

The locations of the main structural elements found at a typical synapse are shown in Figure 1. The nerve terminal is filled with small spherical structures known as **synaptic vesicles**. These are membrane-bound spheres that are filled with neurotransmitter. The nerve terminal also has specializations on the surface facing the post-synaptic cell known as **vesicle docking sites** or **active zones**. These are the points where the vesicles bind and then fuse with the cell membrane to release neurotransmitter into the synaptic cleft. Also in the presynaptic membrane are **voltage-gated calcium channels**. On the post-synaptic side are located the neurotransmitter receptors and associated molecules that are collectively known as the postsynaptic density.

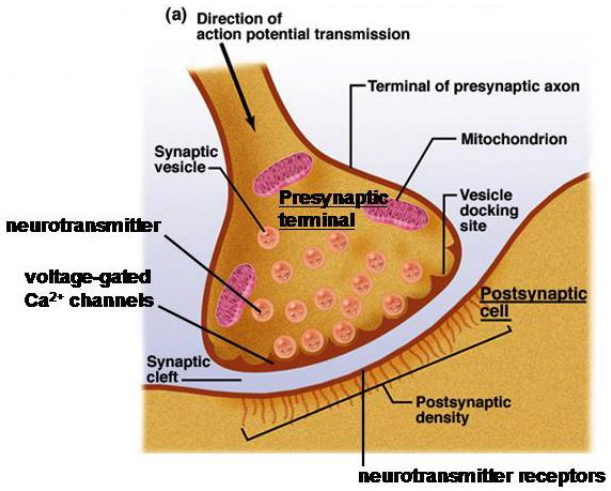

Figure 1 Features of a typical synapse.

Synaptic Transmission

The following sequence of events occurs during synaptic transmission at a typical synapse:

1. Action potential travels down axon.
2. Action potential invades the nerve terminal causing a depolarization.
3. Depolarization opens voltage-gated Ca^{2+} channels.
4. Influx of Ca^{2+} ions through the Ca^{2+} channels raises the Ca^{2+} concentration inside the nerve terminal.
5. Increase in internal Ca^{2+} concentration triggers the fusion of synaptic vesicles with the cell membrane.
6. Fusion of synaptic vesicles releases neurotransmitter into synaptic cleft.
7. Neurotransmitter binds to neurotransmitter receptors in cell membrane of post-synaptic cell.
8. Binding of neurotransmitter to the receptor induces a conformational change in the receptor that opens an ion channel.
9. Opening of ion channels produces a synaptic current in the postsynaptic cell.
10. The synaptic current produces a change in the membrane potential of the postsynaptic cell, possibly triggering an action potential.
11. Neurotransmitter is removed from the synaptic cleft.
12. Components of the synaptic vesicles are recycled.

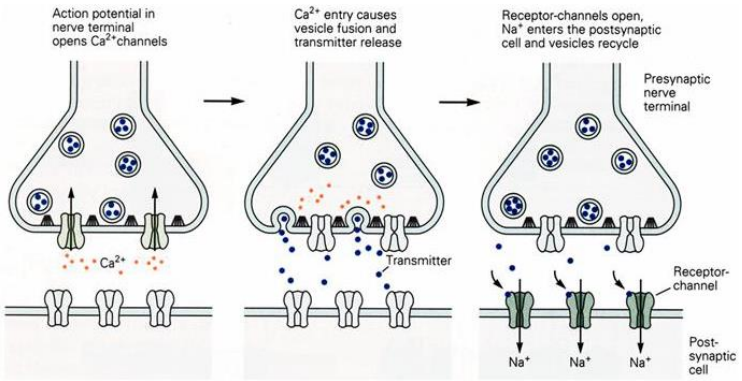

Figure 2 Sequence of events during synaptic transmission.

An action potential arriving at the terminal of a presynaptic axon causes voltage-gated Ca^{2+} channels at the active zone to open (Figure 2). The influx of Ca^{2+} ions through these channels produces a high concentration of Ca^{2+} ions near the active zone, which causes the vesicles containing neurotransmitter to fuse with the presynaptic cell membrane and release their contents into the synaptic cleft (**exocytosis**), the neurotransmitter molecules then diffuse across the synaptic cleft and bind to specific receptors on the post-synaptic membrane. These receptors cause ion channels to open, thereby changing the membrane conductance and membrane potential of the postsynaptic cell.

There are several different types of synapses. The nature of the synapses is determined by the kind of the neurotransmitter that the synapse releases and the type of neurotransmitter receptor found on the postsynaptic membrane. It is usually most useful to categorize synapses on the basis of the kind of neurotransmitter receptor that it expresses.

Ligand-gated ion channels can be either excitatory or inhibitory. Excitatory receptors allow cations to pass (typically Na^+ and K^+, and sometimes Ca^{2+}) through their integral ion channels. Opening of these channels depolarizes the cell membrane potential bringing the membrane potential closer to the threshold for action potential firing (Figure 3). This is known as an **excitatory postsynaptic potential** (**epsp**). The integral ion channel of inhibitory receptors is typically permeable to Cl^- ions, the major extracellular anion. Activation of these inhibitory receptors moves the membrane potential away from the threshold potential. This is known as an **inhibitory postsynaptic potential** (**ipsp**).

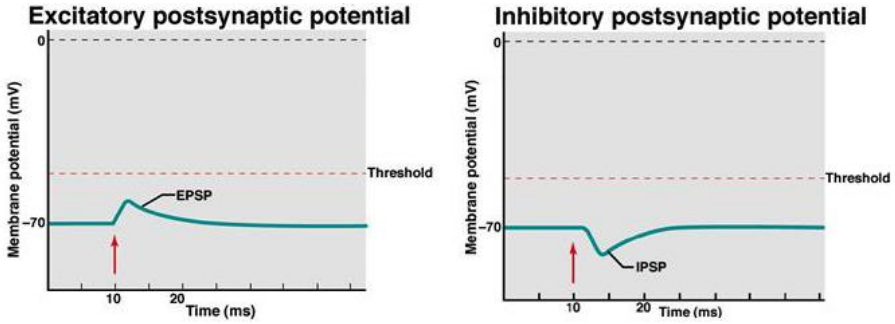

Figure 3 Effect of opening excitatory, cation channels or inhibitory, cation channels on membrane potential.

2. The Neuromuscular Junction and the Legacy of Bernard Katz

For many years the most intensively studied synapse was the **neuromuscular junction** (**NMJ**). This is a synapse between a motor neuron and a skeletal muscle fiber that is large and relatively easy to study (Figure 4). The person who is most closely associated with these studies is Bernard Katz. It is rare in science for someone to so completely dominate a field as important as synaptic physiology in the way that Katz did for two decades between 1950 and 1970. A large part of everything that we know about synaptic transmission was first discovered or suggested by Katz. He received the Nobel prize in 1970.

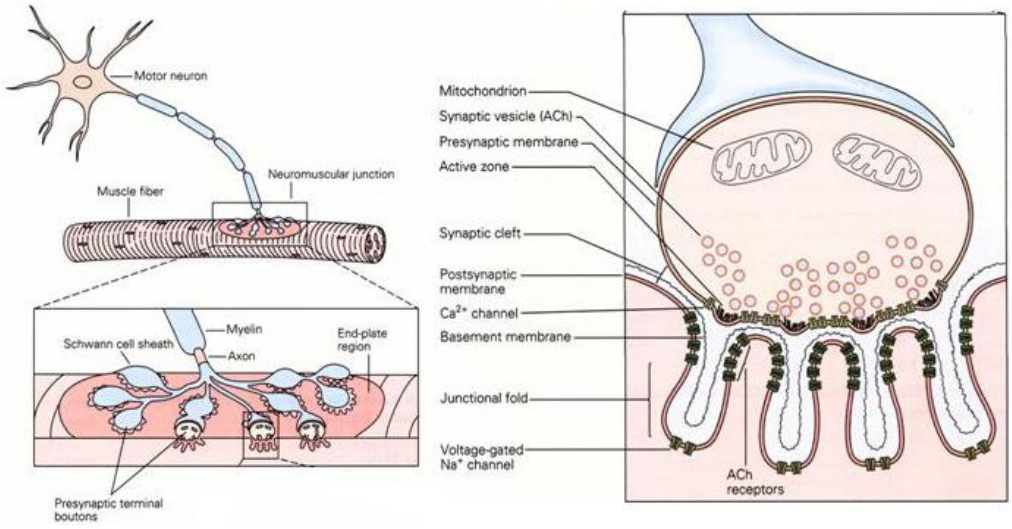

Figure 4 Structure of the neuromuscular junction

The neurotransmitter at the neuromuscular junction is **acetylcholine** (**ACh)**. At this synapse, ACh is an excitatory neurotransmitter, meaning that it depolarizes the cell membrane. The neuromuscular junction is made up of multiple synaptic boutons, making it an unusually large synapse (Figure 4). There are large, junctional folds in the postsynaptic membrane positioned opposite to the active zones in the presynaptic membrane. At the crest of each fold AChRs are clustered in a very high concentration (~10,000 receptors per square micrometer). The active zone contains voltage-gated Ca^{2+} channels.

In his studies on the neuromuscular junction Katz made numerous important contributions including:

1. The vesicle hypothesis
2. The Ca^{2+} hypothesis
3. The two-step kinetic model of AChR activation
4. A kinetic model of AChR desensitization
5. Measurements of single channel conductance and open time using noise analysis

A typical experiment performed by Katz and his colleagues involved stimulating the axon of the presynaptic nerve and then recording the voltage change in the postsynaptic cell (). One of his most important experiments involved nothing more than turning up the gain on the recording amplifier.

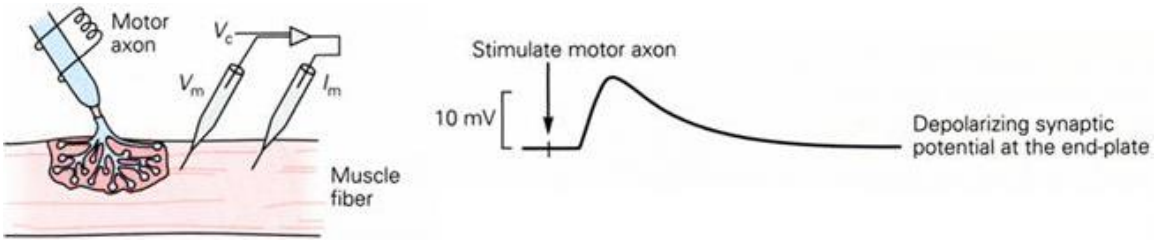

Figure 5 Experimental set-up for recording from the neuromuscular junction (left panel). Excitatory postsynaptic potential recorded following nerve stimulation (right panel).

Original recordings from an experiment by Katz are shown in Figure 6. In the bottom trace is a recording of an epsp and subsequent action potential in the muscle fiber. In the upper traces the amplifier gain is set much higher and the small blips in the traces are spontaneous epsps. They tend to be all much the same size and occur spontaneously and randomly without any electrical excitation.

At the same time as Katz was recording his miniature epsps other scientists were starting to use electron microscopes to study biological samples. When they looked at the neuromuscular junction they saw that the nerve terminal was filled with hundreds of small spherical structures (Figure 6).

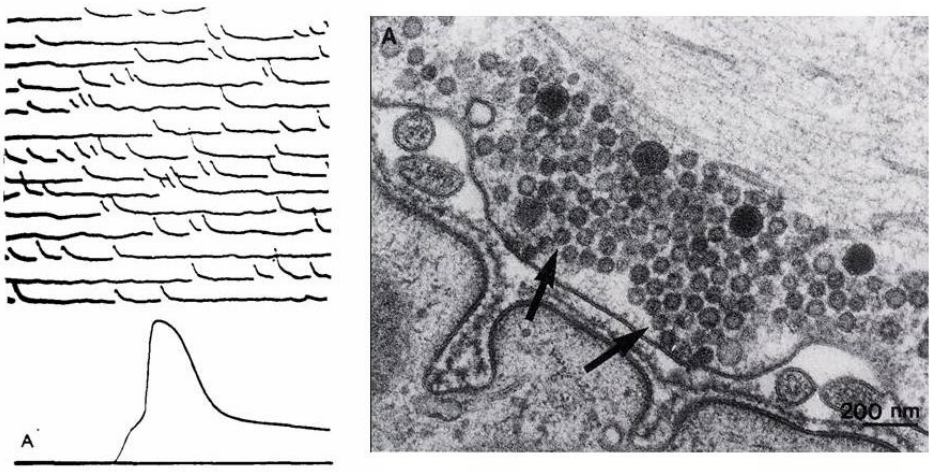

Figure 6 Spontaneous miniature end-plate potentials (left panel). Electron micrograph of vesicles in the nerve terminal (right panel).

In 1955 Katz put these two observations together and surmised that the vesicles seen in the electron micrographs were filled with neurotransmitter and that the miniature epsps were due to the spontaneous fusion of these vesicles with the membrane. In his vesicle hypothesis, a normal epsp occurred when an action potential invaded the nerve terminal and caused a large number of vesicles to be released. He also anticipated that there would be a specialized docking site where the vesicles attached to the nerve terminal membrane prior to release.

The second major contribution Katz made was to begin to understand how the electrical signal in the nerve terminal induced the release of neurotransmitter. In 1965 he again performed a critical experiment that was both conceptually and technically quite simple. Katz removed all the extracellular Ca^{2+} ions from the external media. Under these conditions synaptic transmission completely fails. He then brought a pipette up close to the synapse and allowed a small amount of calcium to leak out of the pipette. Under these conditions synaptic transmission is partially restored. More external Ca^{2+} produced more neurotransmitter release (Figure 7).

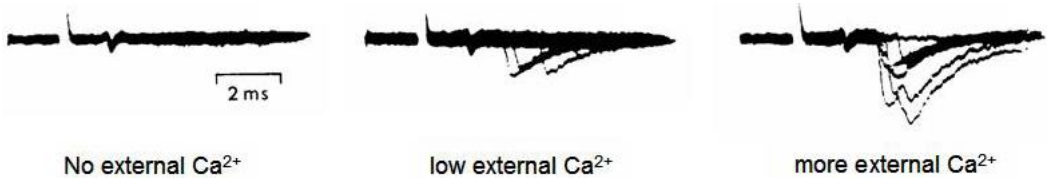

Figure 7 Effect of increasing external Ca^{2+} concentration on neurotransmitter release.

These two basic concepts, the vesicle hypothesis and the observation that calcium ions are the link between excitation and secretion are the central to our understanding of synaptic transmission.

3. Sequence of Events During Synaptic Transmission

1. Action potential travels down axon.

The action potential travels down the axon and invades the nerve terminal as described in Chapter 4.

2. Action potential invades the nerve terminal causing a depolarization.

Voltage gated Na^+ and K^+ channels are also found in the nerve terminal so that when the action potential reaches the nerve terminal the membrane potential in the terminal is rapidly depolarized.

3. Depolarization opens voltage-gated Ca^{2+} channels.

There are also voltage-gated Ca^{2+} channels in the nerve terminal, which are not present in the axon. The voltage-gated Ca^{2+}channels are activated during an action potential by depolarization, much like voltage gated Na^+ and K^+ channels, but do not contribute greatly to current flow during the action potential because they are significantly less abundant than the other channels. They are critically important because they mediate the influx of Ca^{2+} ions into the nerve terminal.

4. Influx of Ca^{2+} ions through the Ca^{2+} channels increases the Ca^{2+} concentration inside the nerve terminal.

The coupling between nerve terminal depolarization and neurotransmitter release is not direct. Calcium ions act as second messengers triggering the release of neurotransmitter. As Bernard Katz showed, if Ca^{2+} ions are removed from the extracellular fluid then the action potential can no longer elicit the release of neurotransmitter. Neurotransmitter release is absolutely dependent upon the influx of Ca^{2+} ions into the presynaptic cell.

Calcium ions can act as a second messenger because they are the exception to the general rule, that ion fluxes across the cell membrane induced by electrical activity do not have a significant effect on intracellular ion concentrations. This difference is due to the fact that intracellular Ca^{2+} ion concentrations are extremely low inside the cell ($[Ca^{2+}]_i$ = 100 nM) relative to external Ca^{2+} ion concentrations ($[Ca^{2+}]_o$ = 2 mM), so that the influx of relatively few Ca^{2+} ions can produce a significant, if transient, increase in Ca^{2+} ion concentration close to channels in the cell membrane.

The influx of Ca^{2+} ions converts an electrical signal into a biochemical signal, which triggers all the subsequent events inside the nerve terminal.

5. Increase in internal Ca^{2+} concentration promotes the fusion of synaptic vesicles with the cell membrane.

The rise in internal Ca^{2+} levels triggers neurotransmitter release by promoting the fusion of synaptic vesicles with the plasma membrane. It is possible to visualize the vesicles, using electron microsopy. A subset of the vesicles are docked or tethered to a structure known as the **release site** or **active zone**. It is the vesicles located at the active zone that are the ones released following an influx of Ca^{2+} ions.

Also clustered at these release sites are the voltage-gated Ca^{2+} channels. Influx of Ca^{2+} produces a large increase in Ca^{2+} concentrations immediately beneath the cell membrane at the release

sites. The increase in Ca^{2+} concentration is much larger near these channels than in the bulk of the cytoplasm.

6. Fusion of synaptic vesicles releases neurotransmitter into synaptic cleft.

The regulation of vesicular fusion and its responsiveness to changes in Ca^{2+} ion concentration is complex and requires the coordinated action of a large number of different proteins. The process of vesicle fusion is known as **exocytosis.** Exocytosis is evolutionary ancient, dating back at least to stem eukaryotes. It is necessary in eukaryotes to move material between different membrane delimited compartments within the cell. This process is known as **constitutive exocytosis**. Synaptic vesicle release is an example of **regulated exocytosis**, where exocytosis will only proceed in response to a specific signal, calcium ions.

The main protein components necessary for synaptic vesicle fusion are shown in Figure 8.

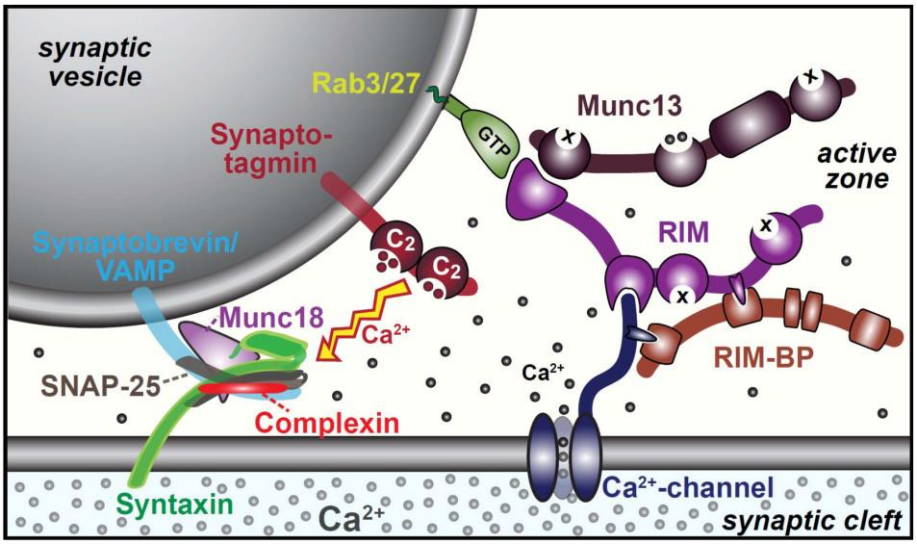

Figure 8 Main protein components that mediate synaptic vesicle release.

There are three basic functions that these proteins perform in order to facilitate rapid and regulated synaptic vesicle release.

1. Vesicle tethering
2. Calcium triggering of fusion
3. Vesicle fusion

Each of these processes is mediated by a different set of proteins.

Table 1. Proteins Involved in Synaptic Vesicle Fusion		
Vesicle tethering	Rab3/27 Munc13 RIM RIMBP Ca^{2+} channel	
Calcium triggering of fusion	Synaptotagmin	
Vesicle Fusion	Synaptobrevin/VAMP Syntaxin SNAP-25	SNARE proteins

	Munc18 Complexin	regulate the SNARE proteins

The vesicle tethering proteins create a **nanodomain** by bringing the calcium channel into very close proximity with the calcium sensing protein synaptotagmin and the vesicle fusion proteins. This organization dramatically increases both the speed and specificity of calcium signaling. Large changes in free calcium ion concentration occur only in the immediate vicinity of the channel if it only opens briefly and the short diffusion distances reduce the time taken to complete the signaling reaction.

Synaptotagmin is the protein that binds Ca^{2+} ions and then triggers the vesicle fusion process. This second step requires cooperation with the protein complexin.

Vesicle fusion requires the generation of force to overcome the electrostatic repulsion between the vesicle and cell membranes. This force is generated by the zippering of the three SNARE proteins synaptobrevin, syntaxin and SNAP-25.

Subsequent recycling of the entangled SNARE proteins requires the NSF protein.

7. Neurotransmitter binds to neurotransmitter receptors in cell membrane of post-synaptic cell.

When the vesicle fuses, the neurotransmitter molecules inside the vesicle are released into the synaptic cleft and begin to diffuse across the cleft to the post-synaptic cell where a fraction of the molecules bind to neurotransmitter receptors.

8. Binding of neurotransmitter to the receptor induces a conformational change in the receptor that opens an ion channel.

The neurotransmitter receptor combines two functions, it has a binding site for neurotransmitter and it functions as an ion channel. Binding of neurotransmitter opens a gate in the channel, which then allows ions to flow through the pore of the channel.

9. Opening of ion channels produces a synaptic current in the postsynaptic cell.

The opening of individual agonist-activated channels occurs almost simultaneously (Fig. 9) because the neurotransmitter is released from the nerve terminal within a relatively brief time window. The channels remain open for random time intervals. Since processes with random lifetimes decay exponentially, the sum of the individual currents has an exponential decay (Figure 9). This current is known as the **excitatory postsynaptic current (epsc)**.

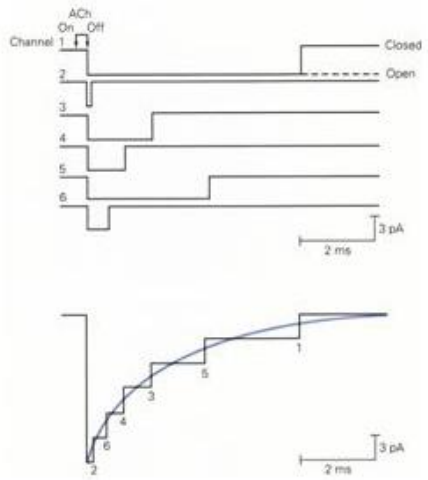

Figure 9 Individual agonist-activated channels open simultaneously following neurotransmitter release and then close at random intervals (top panel). The sum of individual currents results in a postsynaptic current that decays exponentially (bottom panel).

10. The synaptic current produces a change in the membrane potential of the postsynaptic cell, possibly triggering an action potential.

An excitatory postsynaptic current produces a depolarization in the post-synaptic cell. This depolarization is known as an **excitatory post-synaptic potential** (**epsp**). The epsp is called excitatory because it tends to drive the membrane potential towards the threshold for action potential generation. The membrane potential change (epsp) has a slower time course than the underlying current (epsc) because the membrane capacitance takes a certain amount of time to charge up and then discharge (Figure 10).

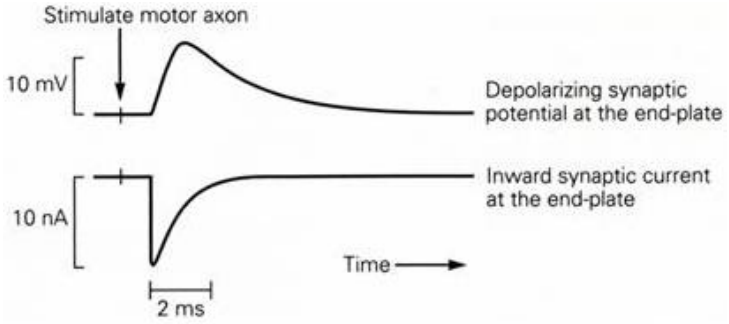

Figure 10 Time course of an epsp and epsc. Note that the epsc is significantly faster than the epsp due to the capacitance of the membrane in the postsynaptic cell .

If the epsp is large enough to reach threshold, Na^+ channels begin to open and an action potential is generated by a positive feed-back cycle rapidly opening more Na^+ channels.

11. Neurotransmitter is removed from the synaptic cleft.

Once the neurotransmitter is released, it is important to remove it quickly in order to reset the system ready for the next action potential. Typically, neurotransmitter is removed by enzyme action, reuptake, diffusion, or some combination of these mechanisms.

As an example, ACh at the NMJ is quickly inactivated by the enzyme **acetylcholinesterase**. This enzyme is located in the synaptic cleft. It splits ACh into acetate and choline, neither of which can activate the AChR by themselves. Because of the rapid action of the acetylcholinesterase enzyme, the pulse of ACh in the synaptic cleft following a presynaptic action potential is quite brief.

12. Components of the synaptic vesicles are recycled.

The nerve terminal is quite small and it is a relatively long way from the cell body. As a consequence, its resources can be easily depleted. To minimize this problem a considerable amount of recycling occurs at the nerve terminal.

For example, at the NMJ following the enzymatic degradation of ACh most of the choline is then taken back up into the synaptic terminal by active transport. The choline is then converted into ACh by the intracellular enzyme choline acetyltransferase and then pumped back into the vesicle. In the central nervous system neurotransmitters such as glutamate and GABA are transported back into the nerve terminal by specific transporters.

Similarly, the membrane in the synaptic vesicles is recycled by a process known as **endocytosis**. After fusing with the plasma membrane to release neurotransmitter the membrane of the vesicle is reabsorbed into clathrin coated pits and ultimately recycled to make new vesicles. These vesicles are refilled with ACh and then transported to the active zone ready for release again. The SNARE proteins are also recycled.

4. Synaptic Delay

The time taken between an action potential arriving in the presynaptic nerve and the initiation of the post-synaptic action potential is known as **synaptic delay** (Figure 11). There are multiple sources for this delay. There is a delay associated with the activation of the Ca^{2+} channels, which have slower kinetics than the Na^{+} channels. Other processes, including exocytosis, diffusion, and activation of neurotransmitter receptors take time, as does charging of membrane capacitance until the voltage reaches threshold to activate Na^{+} channels. Typical values for synaptic delay are 1-2 ms. Synaptic transmission is significantly longer than if the two cells were electrically connected so that electrical excitation passed directly from one cell to the other.

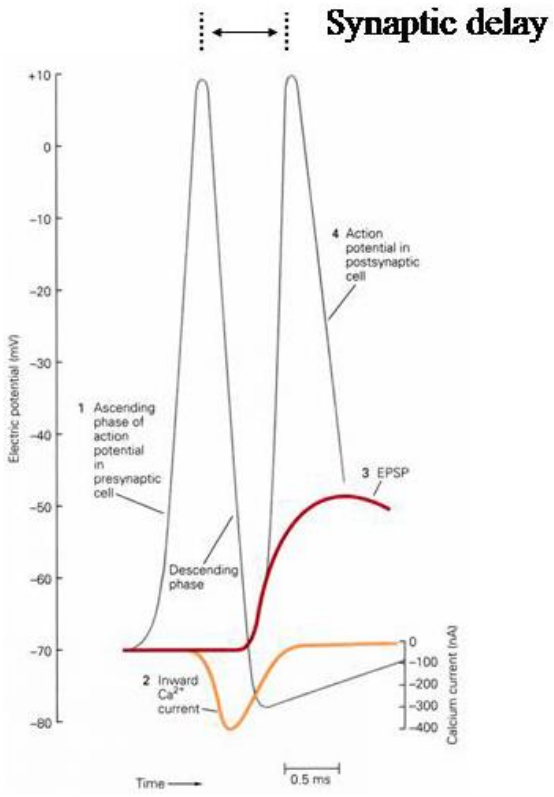

Figure 11 Synaptic delay. Note the delay before the activation of the Ca2+ channels, which turn on during the falling phase of the action potential .

5. Synaptic Transmission at the Neuromuscular Junction

The NMJ is an unusual synapse in that synaptic transmission is 'fail-safe', it always works except under extreme conditions. This is because the synapse is so large. A large amount of neurotransmitter is released by a single action potential invading the presynaptic terminal and there are a very large number of receptors available to bind the neurotransmitter and then open. The resultant epsp is of the order of 70 mV in size (Figure 12).

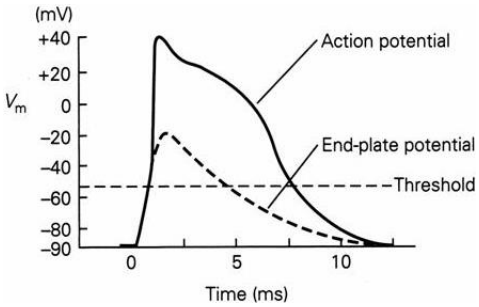

Figure 12 Excitatory postsynaptic potential (also known as end-plate potential) at the neuromuscular junction.

The epsc underlying the epsp at the neuromuscular junction is approximately three times larger than needed to cross threshold. (There is a non-linear relationship between epsc size and epsp size so the epsp does not look this large in Figure 12). This excess epsc size is known as the **safety margin** and provides a measure of security at neuromuscular synapses during stress or disease. A failure of synaptic transmission at these synapses is fatal. This is particularly true for the diaphragm muscle of the lung, where synaptic failure results in a cessation of breathing and rapid death. Neuromuscular junction toxins are used in the natural world to stun or kill prey e.g. the snake venom toxin α-bungarotoxin.

6. Synaptic Transmission in the Central Nervous System

The number of synapses on a neuron ranges between 100 and 100,000 with a typical value being 10,000. For a given connection between two cells, however, the number of synaptic connections is relatively low, of the order of 1-25 synaptic contacts (Figure 13).

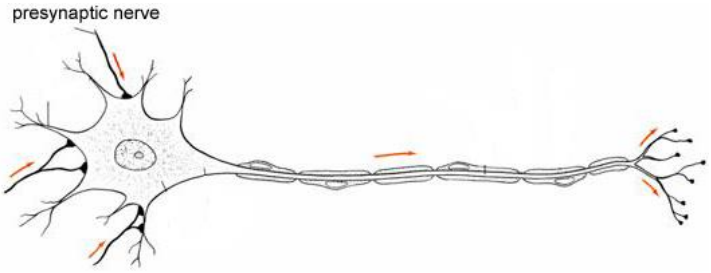

Figure 13 Neuron showing three different presynaptic nerves synapsing on its dendritic tree. For clarity, most synaptic connections are not shown .

The connections between a given presynaptic nerve and the postsynaptic cell in the CNS are generally quite small; epsps are only of the order of 1 mV in size, much smaller than seen at the NMJ. As a consequence, when a single pre-synaptic axon fires the post-synaptic cell will generally not fire. Synaptic transmission in the CNS generally requires the coordinated actions of a number of cells acting on the post-synaptic neuron rather than the relatively simple 1:1 mapping between pre- and post-synaptic firing that occurs at the NMJ. This co-ordination is known as **summation**. There can be both **temporal summation** and **spatial summation** between synaptic inputs to bring the membrane potential to threshold (Fig. 14).

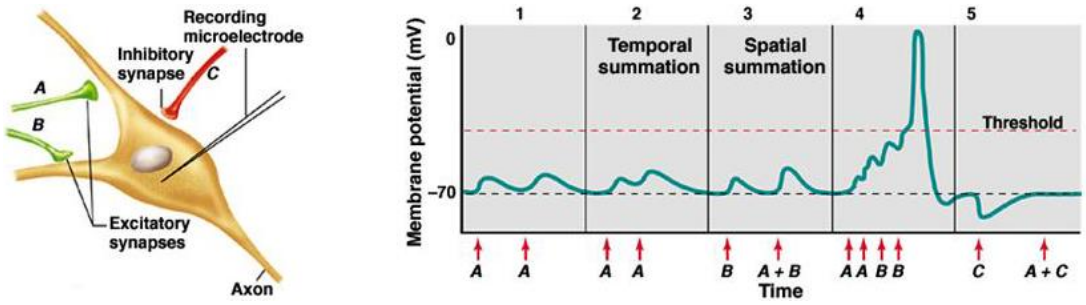

Figure 14 Synaptic transmission in the CNS.

Temporal summation means summation over time. Repetitive firing of the same synapse causes the membrane potential to become more depolarized than if the synapse fired more slowly. This phenomenon is due in part to the membrane capacitance, which slows down the voltage response to a synaptic current, spreading the response over time and allowing summation with subsequent epscs. Spatial summation simply means the summation of more than one synaptic input firing simultaneously.

7. Excitatory Synapses in the CNS

The receptors at most excitatory receptors in the CNS are glutamate receptors. There are two types of glutamate receptors that are of particular importance: the **AMPA receptors** and the **NMDA receptors** (Table 2).

Table 2. Glutamate Receptor Genes

	Genes	Properties
AMPA Receptors	GluA1	main form of GluR
	GluA2	fast kinetics
	GluA3	fast opening, closing and desensitization
	GluA4	most native receptors in principal neurons contain the GluA2 subunit
		GluA2 containing receptors
		- low Ca2+ permeability
		- small conductance
NMDA Receptors	NR-1	all receptors contain the NR-1 subunit, which has the agonist binding sites
	NR-2A	slow kinetics
	NR-2B	large single channel conductance
	NR- 2C	high Ca^{2+} permeability
	NR-2D	channel blocked by Mg^{2+} ions
		glycine is a co-agonist

Pharmacology of Glutamate Receptors

Initial progress in understanding the function of excitatory synapses in the CNS depended on work by Jeff Watkins, an Australian, who spent 20 years developing specific synthetic agonists and antagonists to the glutamate receptor. There are two main types of glutamate receptors the AMPA receptor and NMDA receptors. The AMPA receptors are activated by a specific agonist known as AMPA (hence the name) and blocked by the specific antagonist CNQX (Table 3). The NMDA receptors

are activated by NMDA, which does not activate the AMPA receptors. NMDA receptors can be pharmacologically blocked with APV.

Table 3. Glutamate Receptor Pharmacology		
	Agonist	**Antagonist**
AMPA Receptors	AMPA	CNQX
NMDA Receptors	NMDA	APV

AMPA Receptors

The AMPA receptors function similarly to the AChRs of the NMJ. They are cation channels with relatively fast kinetics. They are responsible for mediating most of the synaptic current at glutaminergic synapses at membrane potentials below threshold.

In principal neurons most AMPA receptors contain the GluA2 subunit. These receptors are impermeable to calcium ions and have a linear current-voltage curve with a reversal potential close to 0 mV. These properties are dependent on RNA editing of the GluA2 subunit, conversion of a glutamine to an arginine residue in the pore loop, which is known as Q/R editing. In contrast, in local circuit neurons, a large fraction of the receptors lacks the GluA2 subunit. This form of the AMPA receptor is calcium permeable, have a non-linear I-V relationship and higher single-channel conductances.

NMDA Receptors

The NMDA receptors are permeable to Ca^{2+} ions. Calcium flux through the NMDA receptors is very important in modulating the strength of synaptic connections.

The function of the NMDA receptor is considerably more complicated than the AMPA receptor. A key property is that the receptor is gated by both voltage and agonist. The current-voltage curve for the NMDA receptor is non-linear. In the depolarized region, at normal Mg^{2+} concentrations (0.5 mM), the current-voltage curve has a negative slope (Figure 15). At positive potentials it is close to linear. The reason for this is that external Mg^{2+} ions block the channel by binding in the pore of the channel. If the external Mg^{2+} ions are removed the current-voltage curve becomes linear over most of the voltage range.

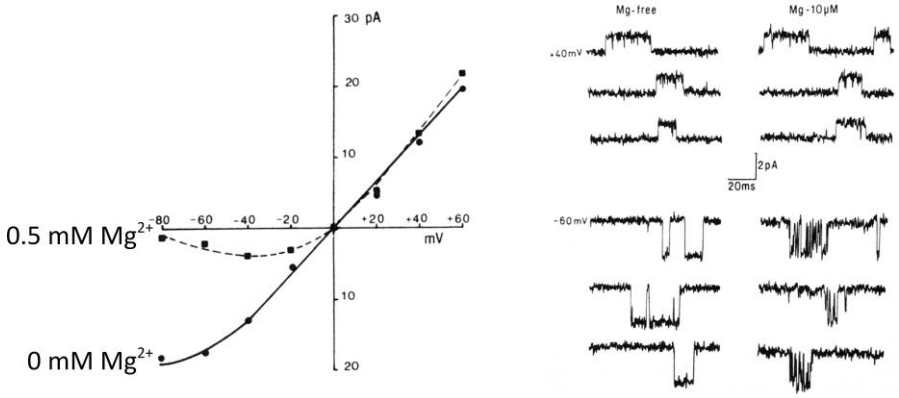

Figure 15 Current-voltage curve for the NMDA receptor in the presence and absence of external Mg^{2+} (left panel). Mg^{2+} block of single channel currents (right panel).

At the single channel level, in the absence of Mg^{2+} ions the channel openings are relatively simple (Figure 15). In the presence of Mg^{2+} ions however the channels openings are very short and spiky and occur in bursts, which is characteristic of channel blocking by ions.

Synaptic Transmission at Glutaminergic Synapses

AMPA and NMDA receptors are often both found at the same excitatory synapse. At synapses where both are present when glutamate is released from the presynaptic terminal both classes of receptors can be activated simultaneously.

Under normal conditions, at negative membrane potentials, it is primarily the AMPA receptors that open and contribute significantly to the synaptic current because the NMDA receptors are largely blocked by Mg^{2+}. At positive potentials the NMDA receptors are no longer blocked and they make a much larger contribution to the synaptic current resulting in much slower decay of the synaptic current, reflecting the slower kinetics of the NMDA receptor (Figure 16).

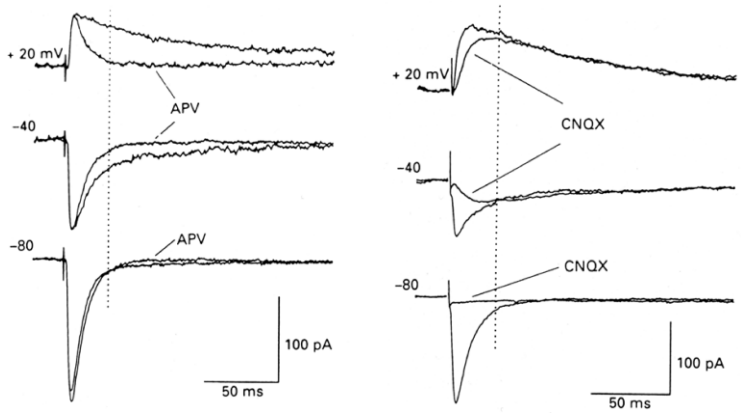

Figure 16 APV blocks the NMDA receptors leaving only the AMPA receptors (left panel). CNQX blocks the AMPA receptors leaving only the NMDA receptors (right panel). Note that at typical resting membrane potentials (-80 mV) there is almost no NMDA receptor mediated current.

APV has very little effect on synaptic transmission at -80 mV but has a large effect at +20 mV when the NMDA receptors are making a significant contribution to the synaptic current. CNQX eliminate the AMPA receptor current leaving the NMDA receptor current intact, illustrating the slow activation as well as the slow inactivation of the NMDA receptor, even though both receptors see the same changes in glutamate in the synaptic cleft. The AMPA receptor current decays much faster (≈6 ms) than the NMDA receptor (≈100 ms). Neither decay time is dependent on voltage.

The relative ratio of NMDA receptors to AMPA receptors at different glutaminergic synapses is quite variable. Typically, this is due to a wide variation in the number of AMPA receptors at the synapses due to the ongoing regulation of AMPA receptor expression by electrical activity.

Long term potentiation

The strength of synaptic connections in the CNS are strongly dependent on the prior level of electrical activity at the synapse. This general phenomenon is known as **synaptic plasticity**. **Long-term potentiation (LTP)** is a form of synaptic plasticity that occurs at glutaminergic synapses.

If the nerve fibers innervating a neurons are stimulated at a low frequency, there is a baseline level of synaptic input that is essentially unchanging (Figure 17C). If a series of rapid stimulation of the nerve is applied, known as tetanic stimulation (100 Hz for 1s), two changes in synaptic transmission occur. Following the tetanus there is a transient increase in synaptic strength known as post-

tetanic potentiation (PTP). PTP is found at most synapses and its duration is typically a few minutes. PTP is due to a transient increase in the concentration of calcium in the nerve terminal that enhances transmitter release following the tetanus. After the tetanus the calcium concentration in the nerve terminal gradually falls and transmission returns to normal levels at many synapses. LTP is a maintained enhancement of synaptic transmission that can last for up to a week in intact animals depending on the duration of tetanic stimulation.

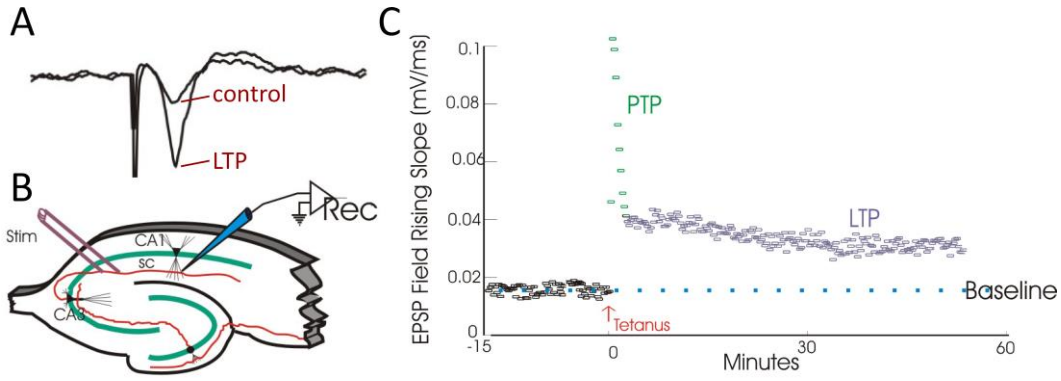

Figure 17 A. Field potential recordings of excitatory synaptic transmission before (control) and after tetanic stimulation (LTP). B. Recording setup in hippocampal slice. Schaffer collaterals (SC) were stimulated and recordings were made in CA1. C. Following tetanus there is a short period of enhanced synaptic transmission known as post-tetanic potentiation (PTP) followed by a long sustained enhancement known as long-term potentiation (LTP) (right panel).

The recordings shown in Figure 17A measure LTP in a population of cells. The recording electrode is placed amongst a group of cells and it records what is known as a field potential, which reflects the current flow produced by epscs occurring at a large number of synapses. This way of recording, because it averages across many synapses, tends to be a more reliable way to examine LTP than recording single synaptic inputs.

Properties of LTP

LTP has three key properties (Figure 18):

1. Specificity - When a strong input (a relatively large number of fibers) is stimulated it will display LTP but synapses in other regions of the neuron will not. Inputs that are not active at the time of the tetanus of the strong input do not show potentiation.

2. Cooperativity - If only a weak input (relatively few fibers) is stimulated, LTP does not develop. It is only when a relatively large number of inputs are stimulated that there is induction of LTP. There is a threshold for induction of LTP.

3. Associativity - If a strong input is paired with a weak input, then the weak input will display LTP, even though the weak input by itself cannot induce LTP.

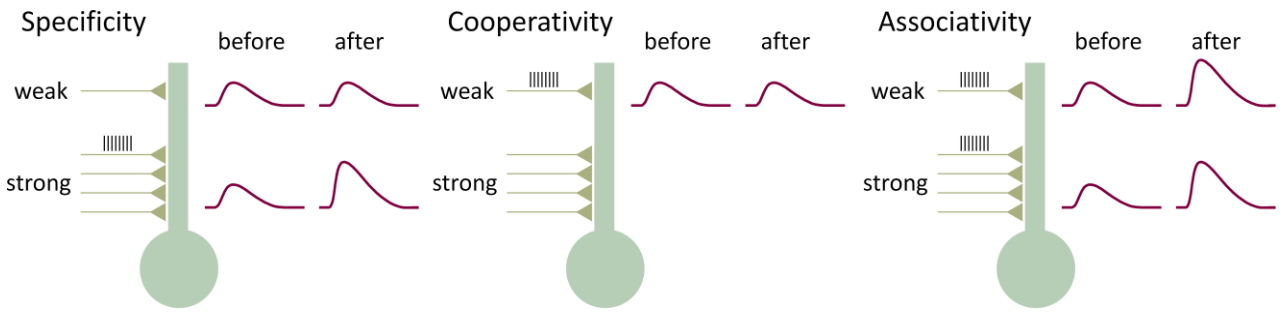

Figure 18 Properties of LTP. The figure illustrates the effect of stimulating both a strong input and/or a weak input to the neuron.

The properties of LTP can be explained by the fact that depolarization of the postsynaptic cell is required for the induction of LTP. If depolarization of the postsynaptic cell by synaptic input is blocked by voltage-clamping the cell, then LTP does not occur. Conversely, if a weak input is paired with an experimentally induced depolarization, using current injection into the cell, then the weak stimulus will elicit LTP, even though it would not do so in the absence of the depolarizing current. The depolarizing current is sufficient to replace the strong paired synaptic stimulus, which is required in associativity. These synapses are known as **Hebbian** synapses because of the requirement of post-synaptic activity in conjunction with presynaptic activity in order to evoke strengthening of the synapse. This requirement was originally proposed by Canadian psychologist Donald Hebb as a mechanism for synaptic learning. Modulation of the strength of synaptic connections is also important during development in establishing the correct synaptic connections.

Calcium Influx is Required for LTP

At normal resting membrane potential, the NMDA receptor is blocked by magnesium ions, which sit in the channel (Figure 19). To open the NMDA receptor two things must happen. First the neurotransmitter glutamate must bind to the receptor. Second, the cell membrane must be depolarized in order to relieve the magnesium block.

The NMDA receptor is doubly gated both by the agonist glutamate and by voltage, which acts to relieve the magnesium block. The receptor acts as a coincidence detector. It only opens when there is a coincidence of synaptic input and postsynaptic depolarization. When the NMDA receptor channel is both activated by glutamate and depolarized, relieved of Mg^{2+} block, then Ca^{2+} ions can flow into the cell, which is the essential first step for the induction of LTP.

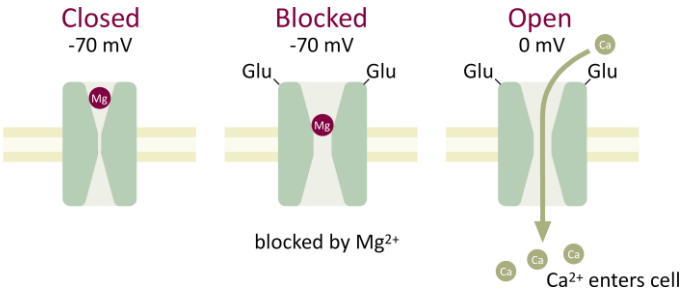

Figure 19 Double gating of the NMDA receptor by glutamate (Glu) and depolarization.

The key role of Ca^{2+} influx is demonstrated by injecting the Ca^{2+} chelating agent BAPTA into the neuron. In the presence of BAPTA the Ca^{2+} concentration does not rise significantly because all the Ca^{2+} influx is mopped up by the buffer. Under these conditions LTP is no induced, even during a

strong synaptic input. Similarly, APV can also block the formation of LTP and this effect appears to be due to blocking Ca^{2+} influx through the NMDA receptor.

The property of specificity (Figure 18) is explained by the fact that only the strong inputs depolarize the cell sufficiently to relieve the Mg^{2+} block of the NMDA receptor and allow a Ca^{2+} influx. Cooperativity occurs because a strong synaptic input is required in order to depolarize the cell to produce a Ca^{2+} influx. Associativity occurs because the strong input can depolarize the cell sufficiently to allow Ca^{2+} influx at the synapses innervated by the weak input.

Regulation of AMPA Receptor Expression

The level of AMPA receptor expression at individual synapses is tightly regulated. Associative LTP works predominantly via the upregulation of AMPA receptor expression at specific synapses. Calcium influx via calmodulin activates the kinase CaMKII located at the synapse. This, in turn, triggers transport of AMPA receptors to the post-synaptic density.

Other Forms of LTP

Associative, or Hebbian, LTP described above is not the only form of LTP found in the brain. Hebbian LTP is NMDA receptor dependent. It is called associative because a strong input can result in the enhancement of a weak input thereby creating an association between the two inputs if they occur together in time. This form of LTP provides a mechanism for encoding associations between temporally correlated events. In addition

Other forms of LTP that are not associative and do not require NMDA receptors have also been described. Non-Hebbian LTP was first well characterized at the synapses between the mossy fibers and the CA3 neurons. These synapses have few or no NMDA receptors. Formation of LTP is not dependent on post-synaptic depolarization and appears to be primarily a presynaptic event. Because depolarization of the post-synaptic cell is unimportant, strong inputs cannot enhance weak inputs.

Long-Term Depression (LTD)

In addition to being strengthened synapses can also be weakened. These balancing effects are important to maintaining a stable level of synaptic input to a given neuron. One mechanism by which weakening of synaptic contacts occurs is Long-Term Depression (LTD). LTD can be triggered in CA1 neurons of the hippocampus by persistent weak synaptic stimulation and it involves a reduction of AMPA receptor expression

Excitotoxicity

Calcium influx through NMDA receptors can also have very negative consequences. During strokes, when the blood flow is blocked to parts of the brain, the nerve terminals can depolarize releasing glutamate. The glutamate activates NMDA receptors allowing Ca^{2+} ions to flow into the postsynaptic neuron. The resulting rise in internal Ca^{2+} concentrations can kill the postsynaptic cell. This phenomenon is known as **excitotoxicity**, because cell toxicity is produced by excitatory neurotransmitters.

8. Inhibitory Synapses

The primary inhibitory neurotransmitter in the CNS is **gamma-aminobutyric acid (GABA).** These receptors function much like the AChR with one crucial difference. Instead of the channel being permeable to cations the channel is permeable to chloride ions. This means that when the receptor is activated it tends to either hyperpolarize the membrane potential or at least stabilize it close to the resting membrane potential.

In many neurons active chloride transport maintains the chloride equilibrium potential, E_{Cl}, more negative than the resting membrane potential. When the GABAR channels open in these cells the membrane is hyperpolarized. This is known as an inhibitory postsynaptic potential, ipsp. If an excitatory and an inhibitory input occur close together in time they tend to cancel each other out (Figure 14).

In a typical neuron, whether or not the cell fires an action potential will depend upon the balance of excitatory and inhibitory synaptic inputs that the cell is receiving at any particular point in time. Normally the neuron is receiving a constant barrage of glutaminergic and GABAergic inputs, influencing its excitability millisecond by millisecond. A recording from a neuron in the nervous system looks a lot like random noise (Figure 20). The membrane potential is continuously changing as both excitatory and inhibitory synapses are banging away on the cell and sometimes the cell reaches threshold firing an action potential.

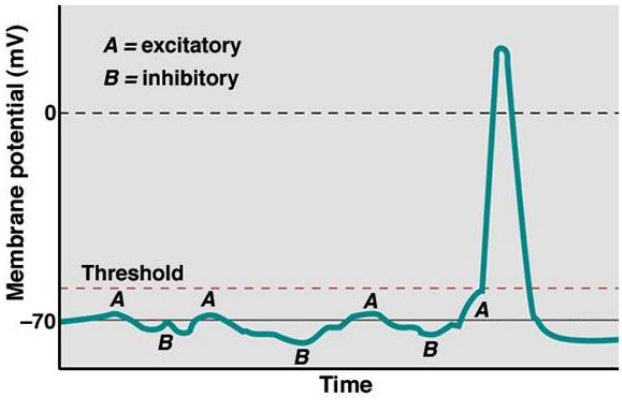

Figure 20 Intracellular recording from a single CNS neuron.

The behavior of single neurons appears anarchic and probabilistic. Individual neurons typically function as part of an ensemble. In general, a single neuron is not solely responsible for anything in particular since there is considerable overlap in function. Rather, the averaged responses of multiple neurons are required to make a decision or produce an action.

9. Slow Synaptic Transmission

In addition to fast synaptic inputs there are slow synaptic inputs. These slow synaptic inputs are mediated by G-protein linked receptors. For a long time, it was not understood how these slow synaptic inputs worked.

One key to understanding slow synaptic transmission was the recognition that these receptors modify the function of voltage-gated ion channels. This was first shown in neurons by Paul Adams, a Professor at Stony Brook. He discovered that one key target for the muscarinic receptor was a voltage-gated potassium channel called the **M-channel** (M for muscarine sensitive).

In the experiment shown in Figure 21 a neuron's response to increasing amounts of injected current is shown. In the control case, with no drug, only a single action potential is elicited by the injected current. After addition of muscarine, which mimics the effect of acetylcholine on these neurons, the neuron is much more excitable.

Figure 21 Effect of muscarine on neuronal firing properties .

Muscarine activates muscarinic acetylcholine receptors that act through G-proteins to inhibit the M-channel. In general, inhibiting K^+ channels will make a neuron more excitable and activating them will make the cell less excitable. In this way slow synaptic inputs can modulate the excitability of a given neuron over time.

There is an interplay between the slow and fast synaptic inputs. The fast excitatory synaptic inputs will have a larger effect on a neuron after it has received an excitatory neuromodulatory input than before, similar to that shown in Figure 21. The response of the neurons is dependent both on the nature of the fast synaptic inputs that it receives and how the excitability has been modulated by prior slow synaptic inputs.

12 Models of Electrical Excitability

One of the earliest and most enduring successes in the mathematical modeling of biological systems is the model devised by Hodgkin Huxley (1952) to describe the propagation of the action potential along the squid axon. The success of this model derives in part from the fact that it is grounded in two well understood physical concepts, electric circuit theory and thermodynamics (the Nernst equation). The complete mathematical description of the action potential, however, required the introduction of arbitrary mathematical equations to describe voltage-gated channel function that were based on curve fitting to experimental data rather than being derived from physical principles. These equations and the underlying model were well thought out and have become a standard method to describe the function of voltage-gated channels at the cellular electrophysiology level.

This chapter will build from the passive electrical behavior of a simple spherical cell to action potential conduction in an axon. The mathematical model requires a modest understanding of differential equations (Appendix 1), numerical methods (Appendix 2) and linear algebra (Appendix 3).

1. Equivalent Circuit of a Small Cell

The equivalent electrical circuit of a small cell is a resistor and capacitor in parallel (an RC circuit). It is assumed that the intracellular fluid is a perfect conductor and, hence, the electrical potential within the cell is the same at every point. This is known as the **isopotential** assumption. This assumption applies reasonably well to most small cells, irrespective of their shape, because the resistance between different regions within the cell is small relative to the resistance across the membrane. However, this assumption does not apply for most neurons, which have complex dendritic trees and long axons.

Another key assumption is that the lipid membrane behaves like a perfect capacitor and has essentially zero conductance for ions (see section 3.5.1.2). For small voltages this assumption holds surprisingly well. At large voltages the membrane begins to fail resulting in a significant increase in conductance to ions.

Membrane capacitance is normally expressed per unit area of membrane, known as the specific capacitance. A small cell, having a smaller membrane area, will have a smaller cell capacitance than a larger cell, even though they have similar specific capacitances. The typical value for the specific capacitance of a cell membrane is $C_m = 1\ \mu\text{F/cm}^2$.

It is also generally assumed that the ion channels in the cell membrane behave as ideal resistors. For sodium and potassium channels and normal membrane voltages this assumption generally holds up well. As described in Chapter 2, the permeation properties of ion channels are usually close to symmetrical, which is a key requirement for this assumption to be valid. At higher voltages the single channel conductance tends to deviate from linearity in part because of a lack of sufficient ions in solution to maintain the required higher current flows. This is a particular problem for the calcium channel because of the very low internal calcium ion concentration and linearity is not generally assumed for this channel. Channel blocking by ions can also modify the channels electrical conduction properties, even when the channel can behave linearly in the absence of channel block. An extreme case is the inward rectifier potassium channel but milder ion blocking is seen for many channels.

The cell membrane resistance is most commonly expressed as a conductance.

membrane conductance (G_m) = 1/ membrane resistance = $1/R_m$

Individual ion channel conductances sum to give the total membrane conductance,

$$G_m = n \times g$$

where n is the number of open channels in the cell membrane and g is the single channel conductance of those channels.

Membrane conductance is also normally given as a specific conductance, conductance per unit membrane area. In the original Hodgkin Huxley model the resting membrane conductance was 0.3 mS/cm^2. Unlike membrane capacitance, which is relatively constant for all cells, due to the similar chemical makeup of the lipid bilayer, specific membrane conductance varies widely between different cell types due to large variations in ion channel protein expression.

The equivalent circuit of a small cell is shown in Figure 1. It is known as an RC circuit, a resistor (conductor) and capacitor in parallel.

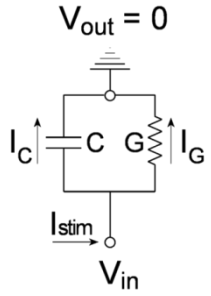

Figure 1. Equivalent circuit of a small cell. The extracellular potential is assumed to be at ground or zero potential and the internal potential (V_{in}) is expressed relative to this value. An injected current (I_{stim}) has two pathways to ground, either through the membrane ion channels modeled as a resistor with conductance (G) or across the membrane capacitance (C).

Current flow across the capacitor is proportional to the rate of change of the voltage across the capacitor, where the voltage $V = V_{in} - V_{out}$.

$$I_C = C\frac{dV}{dt} \qquad 1$$

Current flow through the conductance, G, is given by Ohm's Law.

$$I_G = GV \qquad 2$$

A stimulus current can be applied to the center of the cell using an intracellular electrode. From Kirchhoff's current law, the sum of inward and outward currents at a given node in the circuit should equal zero. At the internal node, with the direction of current flow defined by the arrows in Figure 1 Kirchhoff's law gives.

$$I_{stim} - I_C - I_G = 0 \qquad 3$$

Substitute 1 and 2 into 3,

$$I_{stim} = C\frac{dV}{dt} + GV \quad 4$$

which can be rearranged to give the differential equation.

$$\frac{dV}{dt} = (I_{stim} - GV)/C \quad 5$$

It is possible to derive an analytical solution for equation 5 only if it is assumed that the stimulus current (I_{stim}) is constant over time. If current flow is allowed to vary with time then a solution generally requires numerical methods.

Assuming constant current flow, at infinite time there will be no current flow through the capacitor ($dV/dt = 0$) and the final voltage (V_∞) is given by Ohm's Law.

$$V_\infty = I_{stim}/G \quad 6$$

The time constant of the membrane, τ, is defined as

$$\tau = C/G \quad 7$$

The inverse time constant $1/\tau$ describes the rate at which the membrane voltage approaches steady state following a step change in the stimulus current. The membrane time constant can be determined experimentally by examining the response of the cell to a small injected current step. It corresponds to the time taken for the membrane potential to reach 63% of the steady state voltage (Fig. 2). Together with a measure of the membrane resistance (conductance) the membrane capacitance can be calculated using equation 7, which also gives an indirect measure of membrane area, assuming $C_m = 1\mu F/cm^2$.

To obtain the analytical solution of equation 5, rearrange,

$$\frac{dV}{dt} = \frac{I_{stim}/G - V}{C/G} \quad 8$$

substitute equations 6 and 7 into 8,

$$\frac{dV}{dt} = (V_\infty - V)/\tau \quad 9$$

which can then be integrated to give,

$$V(t) = V_\infty + (V_0 - V_\infty)\exp(-(t - t_0)/\tau) \quad 10$$

where, V_0 is the voltage at time t_0.

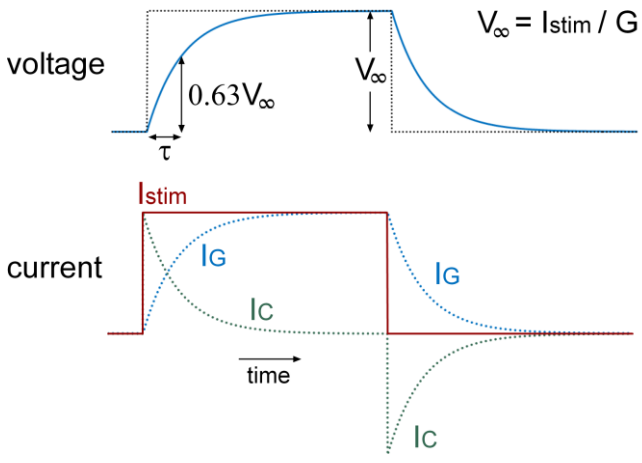

Figure 2. Plot of voltage and current flow through the capacitor and conductor produced by a step change in the stimulus current (I_{stim}) for the equivalent circuit shown in Figure 1. The traces were obtained using equation 9 with discontinuities where the value of I_{stim} was changed. The

dotted trace in the voltage panel corresponds to the step change in voltage that would occur in the absence of any capacitance. At the initiation of a current step, current initially flows onto the capacitor. As the capacitor becomes charged there is a steady increase in current flow through the conductance. The change in current flow through the conductance parallels the changes in voltage. The membrane time constant (τ) corresponds to the time taken for the membrane voltage to reach 63% of V_∞.

An RC circuit (Fig. 1) functions as a low-pass filter, meaning that it filters out the high frequency components of any injected current. This filtering effect can be seen in the voltage response to a current step (Figure 2), where the voltage response of the RC circuit (blue line) is slower than the time course of the injected current (red line). RC filtering will also filter the high frequency components of natural inputs such as synaptic currents.

For most purposes it is not reasonable to assume that current flow through the circuit is constant and it is necessary to use numerical methods to solve equation 5.

Using the forward Euler method (Appendix 2).

$$y_{n+1} = y_n + \Delta t \cdot f(t_n, y_n) \qquad 11$$

Substitute 5 into 11.

$$V_{n+1} = V_n + \Delta t \cdot (I_{stim} - GV)/C \qquad 12$$

This equation can be used to calculate the membrane voltage for any time variant current. An example Matlab program is provided, *ForEulerRC.m*.

2. Leak Conductance and Resting Membrane Potential

Unlike the RC circuit described above, the voltage (V_{in}) inside a cell relative to ground will be in the range -60 to -90 mV, depending on the cell type. This value is known as the membrane voltage (V_m) or membrane potential. The conductance of the cell membrane at the normal resting membrane potential is known as the leak conductance (G_L). This conductance is almost always relatively small, since this minimizes the rate at which ions leak in or out of the cell, thereby minimizing the metabolic cost of maintaining the ion gradients in the cell.

This conductance is typically modeled in one of two ways. All the channels in the cell that are open at rest can be lumped together into a single conductance. The voltage determining current flow through these channels is then given by the driving force for the leak ions ($Vm - V_L$), where V_L is the leak potential and is the membrane voltage at which net current flow through G_L is zero. In a typical model this value is adjusted to give the desired resting membrane potential (V_m) for the cell.

Alternatively, and analogously to the Goldman equation, two conductances for potassium and sodium ions ($G_{L,K}$ and $G_{L,Na}$), with their respective equilibrium potentials (E_K and E_{Na}) can be used to describe current flow. The ratio between the two conductances is then adjusted to give the desired resting membrane potential.

The equivalent circuits for both methods are shown in Figure 3.

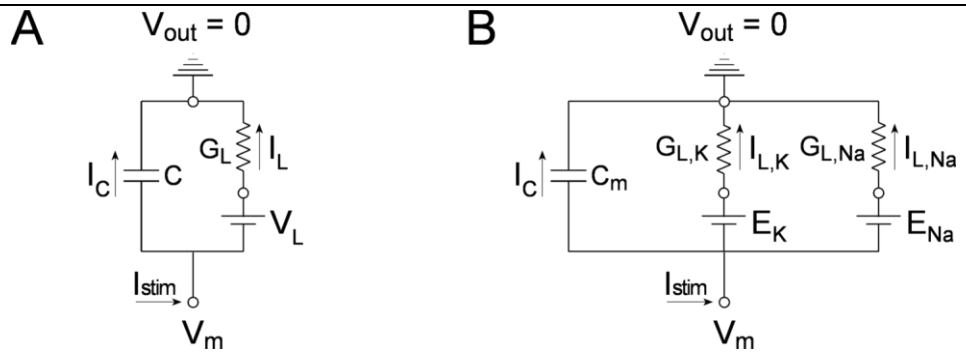

Figure 3. Equivalent circuits of a small cell with a resting leak conductance. The extracellular potential is assumed to be zero. The voltage difference across the membrane is the membrane potential (V_m). A. The leak potential (V_L) is modeled as a battery in series with the leak conductance (G_L). B. Two leak conductances, $G_{L,K}$ and $G_{L,Na}$, each of which has a battery in series, the voltage of which is given by the equilibrium potential for potassium (E_K) or sodium ions (E_{Na}). The direction of current flow is defined as shown by the arrows. The sodium leak current ($I_{L,Na}$) will normally flow into the cell and is defined as a negative current. The potassium leak current ($I_{L,K}$) will normally flow out of the cell and is defined as a positive current.

A key difference between these biological electrical circuits and a typical electrical circuit is that there can be multiple current carriers (the various ions to which the membrane is permeable) and as such the potential acting on each ion species is usually different. The convention for describing the direction of current flows is shown by the arrows in Figure 3. Ion currents flowing out of the cell are positive and currents flowing into the cell are negative.

2.1 Units

The units used to describe the cell membrane capacitance and conductance are critical to interpreting any results. For a cell with a diameter of 40 μm, assuming that it is perfectly spherical, the surface area of the cell membrane is $4\pi r^2$ = 5,027 um² or 5.03×10⁻⁵ cm². The specific capacitance of the membrane (C_m) is 1 uF/cm² giving a cell capacitance of C = 50.3 pF. For a specific resting leak conductance (G_L) of 0.3 mS/cm², the cell's leak conductance is G = 15.1 nS. A typical single channel conductance value is 10 pS, so for this cell approximately 1,500 leak channels will be open at any one time. The membrane time constant is, $\tau = C/G = (50.3 \times 10^{-12}) / (15.1 \times 10^{-9}) = 3.33$ ms. The time constant can also be computed directly from the specific capacitance and conductance values, τ = (1 uF/cm²)/ (0.3 mS/cm²). The steady state voltage change in response to a 200 pA stimulus current injection is given by Ohms law, ΔV_∞ = 13.3 mV.

It is necessary to scale the specific membrane conductance (G_L) and capacitance (C_m) using the membrane area of the cell (A). It is also necessary to use the driving force ($V-V_L$) to describe current flow through the leak conductance. Both these changes can be incorporated into equations 4 and 5.

$$I_{stim} = AC_m \frac{dV}{dt} + AG_L(V - V_L) \qquad 13$$

$$\frac{dV}{dt} = (I_{stim}/A - G_L(V - V_L))/C_m \qquad 14$$

The response of a cell to hyperpolarizing and depolarizing current pulses can be modeled using equation 14. This model gives a reasonable approximation of the voltage response of a typical cell to small injected currents. For small currents the steady state voltage response is approximately linear. With larger current injections the non-linear behavior of the cell's membrane conductance systems will become increasingly apparent. This will require a more complex model incorporating voltage-gated channels.

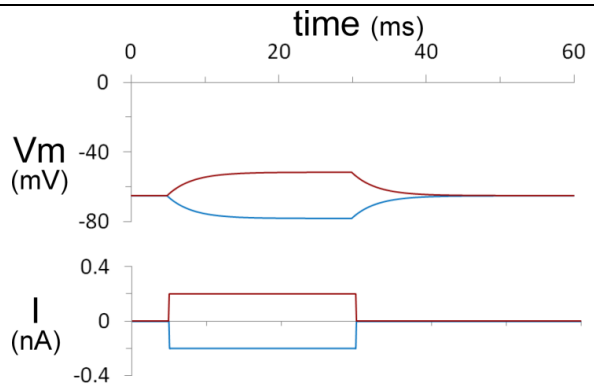

Figure 4. Response of a 40 µm diameter spherical cell with a resting membrane potential of -65 mV to 0.2 nA (red) and -0.2 nA (blue) current injections. The cell membrane has a specific capacitance of 1 uF/cm^2 and a specific leak conductance of 0.3 mS/cm^2. Matlab file *ForEuler-Leak.m* was used for the simulation.

3. Voltage-Gated Channels

In their study of action potential generation Hodgkin and Huxley introduced multiple innovations. The most important technical innovation was the use of a voltage clamp to control the membrane potential and directly measure the currents during steps to different membrane potentials. Using voltage-clamp it was possible to examine the kinetic behavior of the voltage-gated sodium and potassium channels at different potentials (Figure 5).

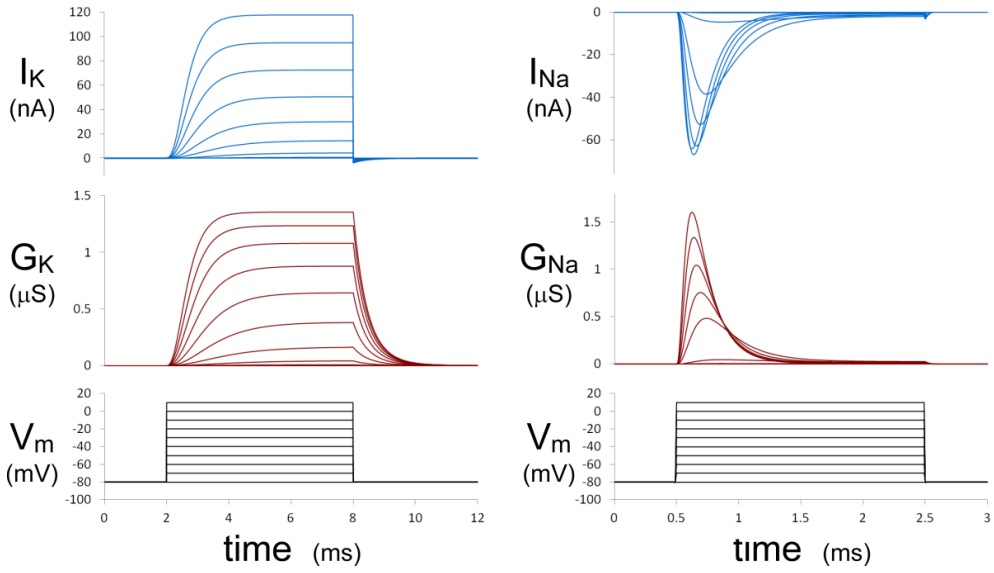

Figure 5. Simulated voltage clamp of a 40 µm diameter spherical cell from a holding potential of -80 mV with voltage-gated potassium and sodium channels in the cell membrane. A. Potassium current and conductance. B. Sodium current and conductance. The cell membrane has a specific voltage-gated sodium conductance of 120 mS/cm^2 and a specific potassium conductance of 36 mS/cm^2. Equations 14, 15 and 18 were used to generate simulated current and conductance traces (Matlab program *VoltageClamp.m*).

They interpreted their results in terms of the equivalent circuit shown in Figure 6. The key feature of this circuit is the addition of two time and voltage variable conductances corresponding to the voltage-gated sodium and potassium channels in the cell membrane. They assumed that current flow through the voltage-gated sodium and potassium channels obeyed Ohm's law,

$$G_{Na} = I_{Na}/(V - E_{Na}) \quad 15$$

$$G_K = I_K/(V - E_K) \quad 16$$

With this assumption the voltage and time dependence of the two variable conductances could then be determined directly from the experimental data (second row Figure 5). The changes in the sodium and potassium conductances reflect the summed behavior of the individual voltage gated ion channels in the membrane.

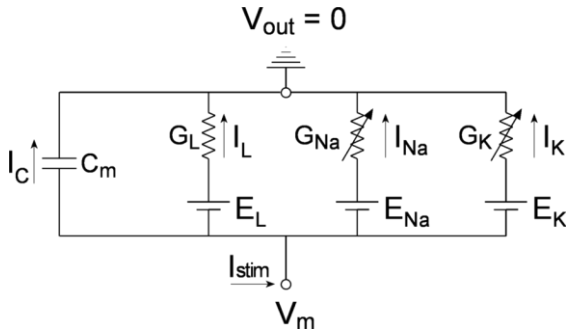

Figure 6. Equivalent circuit of an excitable cell. The arrows though the GNa and GK resistors indicate that these are variable conductances, varying with both voltage and time.

3.1 Gating Probabilities and Voltage-dependent rate equations

A description of the voltage and time dependent conductances was then required in order to fully describe the behavior of the electrically active cell membrane. The mathematical model designed by Hodgkin and Huxley to describe the voltage-gated sodium and potassium conductances has proven surprisingly resilient, especially given how little was known about the function of the channel proteins at the time. The underlying idea was that there were gating particles in the membrane, the movement of which opened or closed gates that controlled ion flow through the channel. The model builds from the simple kinetic scheme shown in Figure 7. In the model *1-n* and *n* are dimensionless probabilities that describe the probability of a hypothetical gating particle being in either the closed (1-n) or open (n) states.

$$\text{1-n} \underset{\beta(V)}{\overset{\alpha(V)}{\rightleftharpoons}} \text{n}$$

Figure 7. Kinetic scheme for a channel gating particle with voltage dependent rate constants α(V) and β(V).

A key innovation was the use of voltage dependent rate constants to describe the transition between these two states. The behavior of this model is described by the following differential equation,

$$\frac{dn}{dt} = \alpha(V)(1 - n) - \beta(V)n \quad 17$$

If it is assumed that the voltage (V) remains constant, equation 13 has the following exact solution,

$$n(t) = n_0 + (n_\infty - n_0)(1 - e^{-t/\tau})$$

where $\tau = 1/(\alpha + \beta)$ and $n_\infty = \alpha/(\alpha + \beta)$ for a given fixed voltage and $n = n_0$ when $t = 0$.

For a continuously changing voltage, which is required to simulate the action potential, equation 17 can be solved using numerical methods. While any of the numerical methods described in Appendix 2 can be used to solve this equation the use of an implicit method has advantages that become more apparent

in the later sections of this chapter when simulating action potential generation in the axon. A common way to solve this equation is the implicit trapezoid method, which is an implicit second order method (equation A2.8).

$$n_{j+1} = n_j + \frac{\Delta t}{2}\Big(f(t_j, y_j) + f(t_{j+1}, y_{j+1})\Big) \qquad 18$$

Substituting equation 17 into 18 and rearranging gives an explicit solution for time dependent changes in the gating particle *n*.

$$n_{j+1} = \frac{(1/\Delta t - (\alpha(V) + \beta(V))/2)n_j + \alpha(V)}{1/\Delta t + (\alpha(V) + \beta(V))/2} \qquad 19$$

The next step in model construction was to fit the mathematical description of the gating to the experimental data showing how conductance changes with voltage (Figure 5).

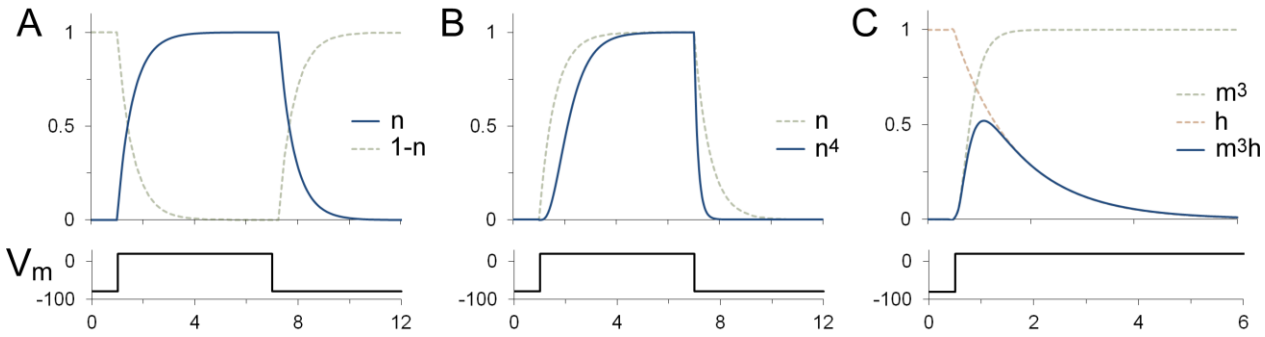

Figure 8. A. Behavior of the kinetic model shown in 7 and described by equation 17, assuming that at time zero all the particles are in the *1-n* state and following a step change in voltage they all transition to the *n* state at infinite time. B. For the potassium channel the *n* probability was raised to the fourth power to mimic the sigmoidal activation of the channel. C. Activation of the sodium channel was handled similarly only the sodium activation probability, *m*, was raised to the third power. Inactivation of the sodium channel was modeled by assuming that there was second gating particle, *h*, that controlled the rate of inactivation. The voltage dependency of this particle was opposite to that of the two activation particles. The sodium conductance was described as the product of these two probabilities, m^3h.

The time dependent behavior of the simple kinetic model (Figure 7 and equation 17) in response to a voltage step is shown in Figure 8A. Immediately following a voltage step the probability *n* increases from a low resting value towards a steady state value. The shape of this transition does not perfectly match the activation of G_K (Figure 5). The gating particle has an exponential transition (channel opening or activation) whereas the potassium conductance activates sigmoidally (most easily seen for smaller voltage steps). To more closely match the behavior of the potassium conductance the activation probability term *n* was raised to the fourth power. The probability n^4 gives a close approximation to the shape of the potassium conductance change (Figure 8B). This gating probability was incorporated into a description of potassium current flow as follows

$$I_K = G_K n^4 (V - E_K) \qquad 20$$

where, G_K is the peak potassium conductance that is scaled by the activation probability n^4.

The final step in the modeling of the voltage-dependent channels required a mathematical description of the voltage-dependence of the rate constants (α_n and β_n). Equation 20 was used to fit the voltage-clamp data in order to obtain a description of the voltage and time dependent behavior of *n*.

Both the form of the equations describing the voltage-dependent rates and their parameter values were determined empirically. For a resting membrane potential of -65 mV these equations are as follows.

K^+ Channel

$$\alpha_n(V) = 0.01(V + 55)/(1 - \exp(-(V + 55)/10)$$ - activation rate

$$\beta_n(V) = 0.125 \exp(-(V + 65)/80)$$ - deactivation rate

These equations are plotted in Figure 9A.

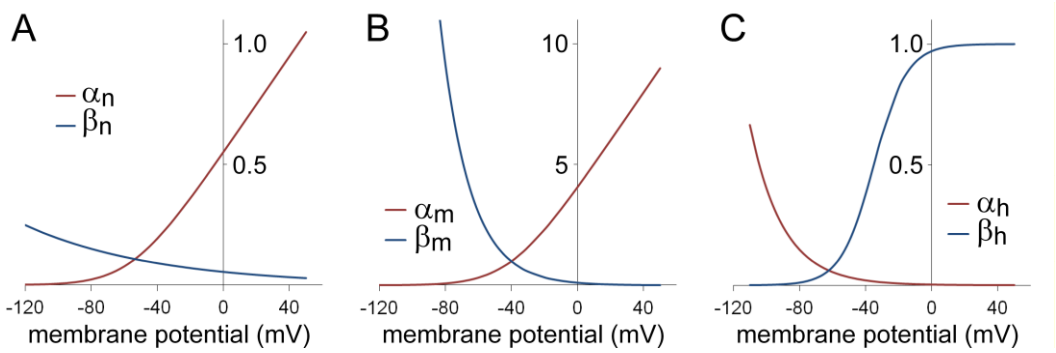

Figure 9. Voltage-dependent rate constants. A. Potassium channel activation and deactivation rates. B. Sodium channel activation and deactivation rates. C. Sodium channel recovery from inactivation and inactivation rates. The y-axis scale is ms^{-1}. The rate constants are temperature dependent and are calculated for T = 6°C.

For the sodium channel the activation probability was called m . The sodium current also activated with a sigmoidal time course and the activation probability was raised to the third power, m^3, in order to model this behavior (Figure 8C). The sodium channel also inactivates. Inactivation had an approximately exponential time course. This was modeled using a single inactivation particle, h. These gating probabilities were incorporated into a description of sodium current flow as follows,

$$I_{Na} = G_{Na} m^3 h (V - E_{Na}) \qquad 21$$

where G_{Na} is the peak sodium conductance that is scaled by the activation and inactivation probabilities m and h.

The equations describing the voltage-dependent rate constants were obtained by curve fitting to the sodium current traces using equation 21.

Na^+ Channel

$$\alpha_m(V) = 0.1(V + 40)/(1 - \exp(-(V + 40)/10)$$ - activation rate

$$\beta_m(V) = 4 \exp(-(V + 65)/18)$$ - deactivation rate

$$\alpha_h(V) = 0.07 \exp(-(V + 65)/20)$$ - recovery from inactivation rate

$$\beta_h(V) = 1.0 \,/\, (1 + \exp(-(V + 35)/10))$$ - inactivation rate

The activation rates (α_n and α_m) for both channels become much faster as the membrane potential is depolarized (Figure 9). The sodium channel activation rate (α_m) is approximately 10 times faster than the potassium channel activation rate (α_n), which is important for determining the sequence of activation of the two channels during the action potential. The sodium channel inactivation rate (β_h) also increases with depolarization but is approximately ten times slower than the activation rate, allowing the channel to

first activate and remain open for some time before then inactivating. The rate of recovery from inactivation of the sodium channel (α_h) is a primary determinant of the duration of the refractory period for action potential generation.

4. Action Potential in a Small Cell

Using these equations it is now possible to create a model of an electrically active cell by combining the equivalent circuit model of the passive electrical properties of a small cell with the models of the voltage-gated channels. Combining equations 13, 20 and 21 gives,

$$I_{stim} = AC_m \frac{dV}{dt} + AG_L(V - V_L) + AG_K n^4 (V - E_K) + AG_{Na} m^3 h (V - E_{Na}) \qquad 22$$

and rearranging gives the differential equation.

$$\frac{dV}{dt} = (I_{stim}/A - \ G_L(V - V_L) - G_K n^4 (V - E_K) - G_{Na} m^3 h (V - E_{Na}))/C_m \qquad 23$$

This equation can be solved numerically in combination with the three differential equations describing the behavior of the gating probabilities.

$$\frac{dn}{dt} = \alpha_n(V)(1 - n) - \beta_n(V)n \qquad 24$$

$$\frac{dm}{dt} = \alpha_m(V)(1 - m) - \beta_m(V)m \qquad 25$$

$$\frac{dh}{dt} = \alpha_h(V)(1 - h) - \beta_h(V)h \qquad 26$$

One way to solve this set of equations is to solve the three rate equations (24-26) first after each time step using the implicit Trapezoid method described above. To maintain second order accuracy, equation 23 is then solved at the midpoint of the time step Δt using the backward Euler method with a half time step, i.e. at time $t_j + \Delta t/2$.

Applying the backward Euler method (equation A2.7) to equation 23 at time step $t_j + \Delta t/2$ gives,

$$V_{j+1/2} = V_j + \Delta t/2 \cdot (I_{stim}/A - \ G_L(V_{j+1/2} - V_L) - G_K n^4 \left(V_{j+1/2} - E_K\right) - G_{Na} m^3 h (V_{j+1/2} - E_{Na}))/C_m$$

which can be rearranged to give an explicit solution for V at time, $(t_j + \Delta t/2)$.

$$V_{j+1/2} = \frac{(2C_{\mathrm{m}}/\Delta t)V_{\mathrm{j}} + I_{\mathrm{stim}}/\mathrm{A} + \ G_L V_L + G_K n^4 E_K + G_{Na} m^3 h E_{Na}}{2C_{\mathrm{m}}/dt + G_L + G_K n^4 + G_{Na} m^3 h} \qquad 23$$

The voltage is then linearly advanced an additional half-step to complete the cycle for each Δt.

$$V_{j+1} = 2V_{j+1/2} - V_{\mathrm{j}}$$

This method is second order accurate for V. Although the system of equations 23-26 is not stiff for a single compartment and can be solved using any of the methods outlined in Appendix 2, the system becomes increasingly stiff as more membrane compartments are added, as will be seen for the axon described below, and this method can be shown to reliably converge under these more stringent conditions when the explicit methods will only be conditionally stable.

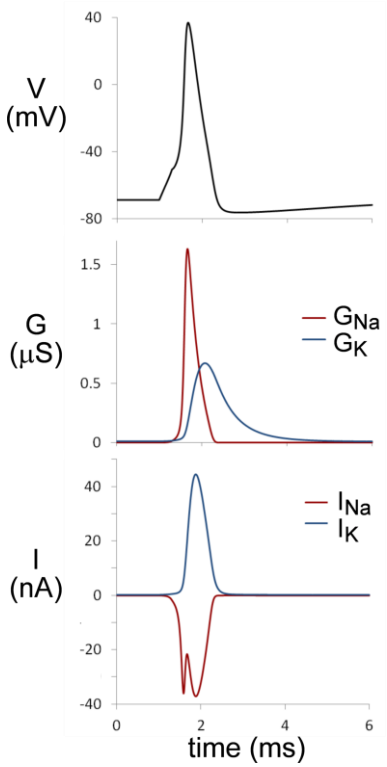

Figure 10. Simulation of an action potential in a 40 μm diameter spherical cell. A. Membrane potential B. Voltage-gated potassium (red) and sodium (blue) conductance. C. Voltage-gated potassium (red) and sodium (blue) current. The cell membrane has a specific voltage-gated sodium conductance of 120 mS/cm^2 and a specific potassium conductance of 36 mS/cm^2. Equations 23-26 were used to generate the voltage, current and conductance traces (Matlab program *HHcell.m*).

Simulation of an action potential is shown in Figure 10. The sodium conductance (G_{Na}) activates much more rapidly than the potassium conductance (G_K). This is due to the difference in the voltage-dependent rates of activation, both channels see the same changes in membrane potential but the voltage dependent rate constants controlling sodium channel activation are much faster (Figure 9), producing the faster activation of the sodium conductance. This is an essential feature of the system because it is the initial inrush of sodium ions that generates the rising phase of the action potential.

5. Passive Electrical Properties of the Axon

The passive electrical properties of most neurons cannot be well approximated by the single compartment model shown in Figure 3. Neurons usually have large dendritic trees and long axons, which will not be isopotential with the cell body when there is significant current flow, as will occur during an action potential. As a consequence, more complex passive electrical models are required. The simplest of these is the uniform cable, which is often used to describe the passive electrical properties of axons.

5.1 Discrete Passive Cable Equation

Models of the passive electrical properties of a cable have to incorporate both spatial and temporal dimensions. A common way to approach this problem is to discretize the spatial dimension as shown in Figure 11. This particular spatial discretization method is second order, meaning that the local truncation error will be $O(\Delta x^2)$.

A cable of length l is divided into N compartments, each of length $\Delta x = l/N$. It is assumed that the voltage within each compartment is isopotential but that voltage can vary between the nodes associated with each compartment (V_1, V_2, etc.). For a cable of radius, r, each compartment will have a surface area = $2\pi r \Delta x$ and a cross-sectional area = πr^2.

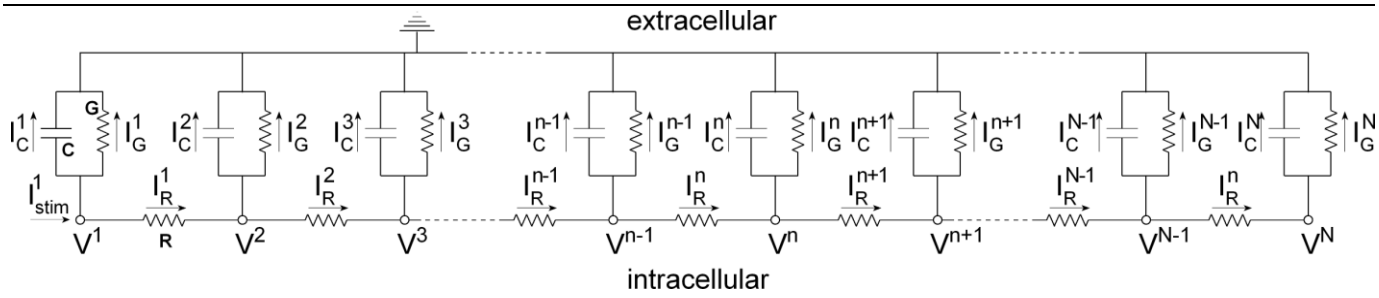

Figure 11. Equivalent electrical circuit model of a uniform cable. The direction of positive current flow through the capacitors and conductances in each compartment is defined by the arrows. Stimulus current injection into the cell interior is defined as positive. In this figure the stimulus current is applied only at the first node but stimulus currents can be applied to the nodes associated with any and all compartments.

For a uniform cable, the three different circuit elements associated with each compartment are assumed to be invariant throughout the cable. They can be described in terms of the specific membrane capacitance and resistance and the specific resistivity of the cytoplasm (R_a).

compartment capacitance	$C = 2\pi r\Delta x\, C_m$	$= AC_m$
compartment conductance	$G = 2\pi r\Delta x\, G_L$	$= AG_L$
coupling resistance	$R = \Delta x R_a / \pi r^2$	

where, A is the membrane area (cm^2), C_m is the specific membrane capacitance ($\mu F/cm^2$), G_L is the specific membrane leak conductance (mS/cm^2) and R_a is the specific resistivity of the cytoplasm ($k\Omega cm$).

Current balance at the first node gives:

$$I_{1,stim} - I_{1,C} - I_{1,G} - I_{1,R} = 0$$

$$I_{1,stim} - C\frac{dV_1}{dt} - GV_1 - (V_1 - V_2)/R = 0$$

$$C\frac{dV_1}{dt} = I_{1,stim} - GV_1 + (V_2 - V_1)/R \qquad 24$$

At the second node:

$$I_{2,stim} - I_{2,C} - I_{2,G} - I_{2,R} + I_{1,R} = 0$$

$$I_{2,stim} - C\frac{dV_2}{dt} - GV_2 - (V_2 - V_3)/R + (V_1 - V_2)/R = 0$$

$$C\frac{dV_2}{dt} = I_{2,stim} - GV_2 + (V_1 - 2V_2 + V_3)/R \qquad 25$$

At the *n*th node:

$$C\frac{dV_n}{dt} = I_{n,stim} - GV_n + (V_{n-1} - 2V_n + V_{n+1})/R \qquad 26$$

At the last node:

$$\mathrm{C}\frac{dV_N}{dt} = \mathrm{I}_{N,stim} - \mathrm{G}V_N + (V_{N-1} - V_N)/\mathrm{R} \qquad 27$$

The voltage and stimulus currents in each compartment at time, *t,* can be collected into column vectors.

$$\mathbf{v}(\mathrm{t}) = (\mathrm{V}_1, \mathrm{V}_2, \mathrm{V}_3, \ldots \mathrm{V}_{\mathrm{N}-1}, \mathrm{V}_{\mathrm{N}})^{\mathrm{T}}$$

$$\mathbf{i}(\mathrm{t}) = \left(\mathrm{I}_{1,\mathrm{stim}}, \mathrm{I}_{2,\mathrm{stim}}, \mathrm{I}_{3,\mathrm{stim}}, \ldots \mathrm{I}_{\mathrm{N}-1,\mathrm{stim}}, \mathrm{I}_{\mathrm{N,stim}}\right)^{\mathrm{T}}$$

Combining equations 24, 26 and 27 gives:

$$\mathrm{C}\frac{d\mathbf{v}}{dt} = \mathbf{i}(t) - \mathrm{G}\mathbf{v}(t) + \mathbf{M}\mathbf{v}(t)/\mathrm{R} \qquad 28$$

with a matrix multiplication using a tridiagonal matrix (**M)**, known as the second difference matrix:

$$\mathbf{M} = \begin{bmatrix} -1 & 1 & 0 & \ldots & 0 \\ 1 & -2 & 1 & \ldots & 0 \\ \vdots & \vdots & \vdots & \vdots & \vdots \\ 0 & \ldots & 1 & -2 & 1 \\ 0 & \ldots & 0 & 1 & -1 \end{bmatrix}$$

To model an axon of a specific radius it is necessary to rewrite equation 28 in terms of specific capacitance, conductance and resistance values.

$$(2\pi r\Delta x)C_m \frac{d\mathbf{v}}{dt} = \mathbf{i}(t) - (2\pi r\Delta x)\mathrm{G_L}\mathbf{v}(t) + \frac{\pi r^2}{\Delta x \mathrm{R}_a}\mathbf{M}\mathbf{v}(t)$$

$$C_m \frac{d\mathbf{v}}{dt} = \mathbf{i}(t)/A - G_L\mathbf{v}(t) + \frac{r}{2R_a}\frac{1}{\Delta x^2}\mathbf{M}\mathbf{v}(t)$$

where, the membrane area of each compartment is given by, $\mathrm{A} = 2\pi r\Delta x$

Substituting in the matrix $\mathbf{S} = 1/\Delta x^2\mathbf{M}$ gives:

$$C_m \frac{d\mathbf{v}}{dt} = \mathbf{i}(t)/A - G_L\mathbf{v}(\mathrm{t}) + \frac{r}{2R_a}\mathbf{S}\mathbf{v}(t) \qquad 29$$

Divide equation 29 by G_L and substitute in the time constant τ and the length constant λ.

$$\tau = C_m/G_L \qquad\qquad \lambda = \sqrt{\frac{r}{2\,R_a\,G_L}}$$

$$C_m/G_L \frac{d\mathbf{v}}{dt} = \mathbf{i}(t)/AG_L - \mathbf{v}(t) + \frac{r}{2R_aG_L}\mathbf{S}\mathbf{v}(t)$$

$$\frac{d\mathbf{v}}{dt} = \mathbf{i}(t)/AC_m + (\lambda^2\mathbf{S}\mathbf{v}(t) - \mathbf{v}(t))/\tau$$

Substitute in

$$\mathbf{B} = (\lambda^2\mathbf{S} - \mathbf{I})/\tau \quad \text{and} \quad \boldsymbol{f}(t) = \mathbf{i}(t)/AC_m$$

where **I** is the identity matrix, giving

$$\frac{d\mathbf{v}}{dt} = \mathbf{B}\mathbf{v}(t) + \boldsymbol{f}(t) \qquad 30$$

5.2 Numerical Solutions for the Discrete Passive Cable Equation

To solve the discrete cable equation it is necessary to also discretize with respect to time. Because the spatial discretization method is second order, it will generally be most optimal to also use a second order time discretization method so that the local truncation errors are $O(\Delta t^2)$ and $O(\Delta x^2)$ and the global errors are not dominated by either discretization method. Because local truncation errors in the spatial dimension are second order there is generally very little to be gained by using time discretization methods higher than second order.

The methods commonly used to solve this equation are the first order forward and backward Euler methods and the second order backward Trapezoid method.

The forward Euler method is only conditionally stable, with stability being dependent on the ratio $\Delta x/\ \Delta t^2$. As the spatial resolution increases the time resolution must increase much more rapidly in order to maintain stability. This is very inefficient from a computational standpoint and effectively limits the number of spatial compartments that can be used with this method. The forward Euler method has the advantage of being very simple to implement (*ForEulerCable.m*) since it only requires a matrix multiplication for solution.

$$\mathbf{v}_{n+1} = \mathbf{v}_n + \Delta t(\mathbf{B}\mathbf{v}_n + \boldsymbol{f}_{\mathrm{n}})$$

The limited stability of this explicit method highlights the distinct advantages of implicit methods. The backward Euler method is unconditionally stable for any combination of Δt and Δx.

$$\mathbf{v}_{n+1} = \mathbf{v}_n + \Delta t(\mathbf{B}\mathbf{v}_{n+1} + \boldsymbol{f}_{\mathrm{n+1}})$$

$$(\mathbf{I} - \Delta t\mathbf{B})\mathbf{v}_{n+1} = \mathbf{v}_n + \Delta t\boldsymbol{f}_{\mathrm{n+1}} \qquad 32$$

Equation 28 is a system of linear equations that must be solved at each time step,

$$\mathbf{v}_{n+1} = \mathbf{A}^{-1}(\mathbf{v}_n + \Delta t\boldsymbol{f}_{\mathrm{n+1}})$$

where $\mathbf{A} = (\mathbf{I} - \Delta t\mathbf{B})$. This problem can be handled very efficiently in Matlab (*BackEulerCable.m*).

Because the backward Euler method is only first order with respect to time, for small step sizes, errors associated with the time discretization will dominate, assuming $\Delta t \approx \Delta x$.

The backward trapezoid method can also be used for time discretization. This is also known as the Crank-Nicolson method. It is second order accurate in both space and time.

$$\mathbf{v}_{n+1} = \mathbf{v}_n + \frac{\Delta t}{2}\left(\mathbf{B}\mathbf{v}_n + \boldsymbol{f}_{\mathrm{n}} + \ \mathbf{B}\mathbf{v}_{n+1} + \boldsymbol{f}_{\mathrm{n+1}}\right)$$

$$(\mathbf{I} - \frac{\Delta t}{2}\mathbf{B})\mathbf{v}_{n+1} = (\mathbf{I} + \frac{\Delta t}{2}\mathbf{B})\mathbf{v}_n + \frac{\Delta t}{2}(\boldsymbol{f}_{\mathrm{n}} + \boldsymbol{f}_{\mathrm{n+1}}) \qquad 33$$

Equation 3 can also be expressed as a system of linear equations

$$\mathbf{v}_{n+1} = \mathbf{A}^{-1}(\mathbf{C}\mathbf{v}_n + \frac{\Delta t}{2}(\boldsymbol{f}_{\mathrm{n}} + \boldsymbol{f}_{\mathrm{n+1}}))$$

where, $\mathbf{A} = (\mathbf{I} - \Delta t\mathbf{B})$ and $\mathbf{C} = (\mathbf{I} + \Delta t\mathbf{B})$.

This method is more accurate than the backward Euler but for large Δt or small Δx it can produce oscillations, making the less accurate backward Euler method preferable under these conditions. It is implemented in *ImplicitTrapCable.m*.

5.3 Response to Current Injection in a Passive Cable

Figure 12 shows the effect of injecting a brief current pulse into a single membrane compartment at the center of the squid axon model. This is an unusually large axon so the current injection is correspondingly large. For brief current injections the voltage change is localized to a relatively small region of the cable and quickly declines as the current passes to ground.

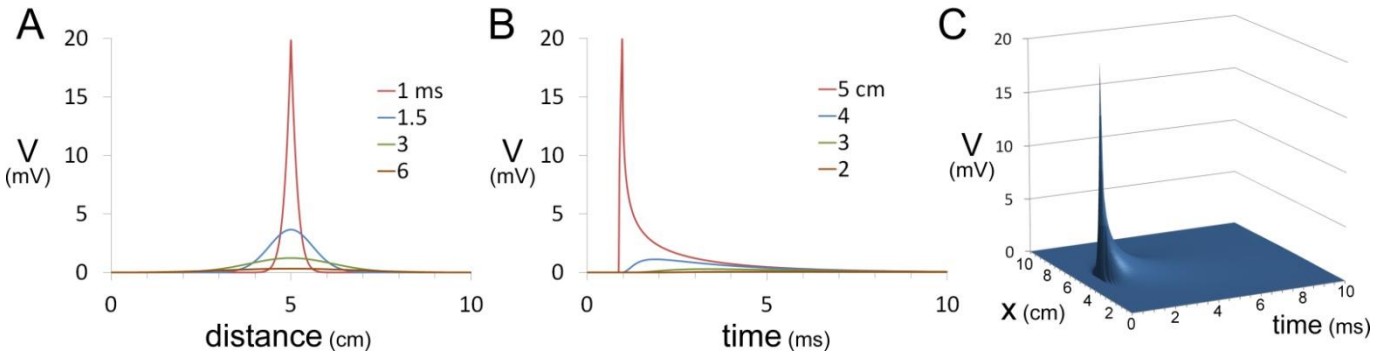

Figure 12. Effect of current injection in a passive cable. A. Voltage profile along the length of the axon at simulation times 1 (at the end of the current injection), 1.5, 3 and 6 ms. B. Voltage profile across the simulation time at 5 cm (the point of current injection), 4 cm, 3 cm and 2 cm along the cable. C. Voltage response plotted with respect to both time and location along the cable. The equivalent circuit was a model of the squid giant axon, 10 cm long with a radius of 238 μm. The cell membrane had a specific capacitance of 1 uF/cm^2, a specific leak conductance of 0.3 mS/cm^2 and the coupling resistance between compartments was 0.0354 kΩcm. Current injection was 10 μA for 0.1 ms, ending at time = 1 ms. Matlab program *BackEulerCable.m* was used for the simulation.

6. Action Potential Propagation in the Axon

To model an action potential travelling down an axon the model of the passive electrical properties of the axon is combined with the models of the two voltage-gated channels in the same way as was done for the spherical cell. It is assumed that the voltage-gated channels are uniformly distributed.

To simplify the notation and to better match the provided computer programs a non-standard notation for element-wise vector manipulation is used in this section e.g. $\mathbf{xy}$ is the vector whose elements are the products of the elements of vectors $\mathbf{x}$ and $\mathbf{y}$ (the Hadamard product), while $\mathbf{x}^4$ is four element-wise multiplications of itself. Addition and subtraction of scalars to vectors is also considered to be element-wise. Matrix multiplication retains its conventional meaning.

The individual gating probabilities are gathered into three vectors, $\mathbf{n}(t)$, $\mathbf{m}(t)$ and $\mathbf{h}(t)$, spanning the axon compartments. The gating probabilities are solved using the implicit Trapezoid method as was done for the spherical cell (equation 16), which is second order accurate.

$$\mathbf{n}_{j+1} = \frac{(1/\Delta t - (\boldsymbol{\alpha}(\mathbf{v}_j) + \boldsymbol{\beta}(\mathbf{v}_j))/2)\mathbf{n}_j + \boldsymbol{\alpha}(\mathbf{v}_j)}{1/\Delta t + \left(\boldsymbol{\alpha}(\mathbf{v}_j) + \boldsymbol{\beta}(\mathbf{v}_j)\right)/2} \qquad 34$$

The voltage dependent potassium and sodium currents associated with each compartment are incorporated into equation 28 in vector form.

$$C\frac{d\mathbf{v}}{dt} = \mathbf{i}(t) - G\mathbf{v}(t) - \mathbf{i}_{\mathrm{K}}(t) - \mathbf{i}_{\mathrm{Na}}(t) + \mathbf{M}\mathbf{v}(t)/R$$

Expanding using specific membrane and axial resistance values and equations 21 and 22 for the membrane currents gives.

$$(2\pi r\Delta x)C_m\frac{d\mathbf{v}}{dt} = \mathbf{i}(t) - (2\pi r\Delta x)G_L(\mathbf{v}(t) - V_L) - (2\pi r\Delta x)G_K\mathbf{n}^4(\mathbf{v}(t) - E_K)$$

$$-(2\pi r\Delta x)\mathrm{G}_{\mathrm{Na}}\mathbf{m}^3\mathbf{h}(\mathbf{v}(t) - E_{Na}) + \frac{\pi r^2}{\Delta x R_a}\mathbf{M}\mathbf{v}(t)$$

$$C_m\frac{d\mathbf{v}}{dt} = \mathbf{i}(t)/A - G_L(\mathbf{v}(t) - V_L) - G_K\mathbf{n}^4(\boldsymbol{v}(t) - E_K) - G_{Na}\mathbf{m}^3\mathbf{h}(\mathbf{v}(t) - E_{Na}) + \frac{r}{2R_a}\frac{1}{\Delta x^2}\mathbf{M}\mathbf{v}(t)$$

where, compartment membrane area $\mathrm{A} = 2\pi r\Delta x$.

Substitute in the matrix $\mathbf{S} = 1/\Delta\mathrm{x}^2\mathbf{M}$ and group terms dependent on $\mathbf{v}$(t):

$$C_m\frac{d\mathbf{v}}{dt} = \frac{\mathbf{i}(t)}{A} - (G_L + G_K\mathbf{n}^4 + G_{Na}\mathbf{m}^3\mathbf{h})\mathbf{v}(t) + (G_LV_L + G_K\mathbf{n}^4E_K + G_{Na}\mathbf{m}^3\mathbf{h}E_{Na}) + \frac{r}{2R_a}\mathbf{S}\mathbf{v}(t)$$

Substitute

$$\boldsymbol{B} = \frac{r}{2R_a}\mathbf{S}$$

$$\mathbf{d} = G_L + G_K\mathbf{n}^4 + G_{Na}\mathbf{m}^3\mathbf{h}$$

$$\mathbf{f} = \frac{\mathbf{i}(t)}{A} + G_LV_L + G_K\mathbf{n}^4E_K + G_{Na}\mathbf{m}^3\mathbf{h}E_{Na}$$

to give.

$$\frac{d\mathbf{v}}{dt} = (\,\mathbf{f} - \mathbf{d}\mathbf{v}(\mathrm{t}) + \mathbf{B}\mathbf{v}(\mathrm{t})\,)/C_m \qquad 35$$

To model the action potential requires the solution of four linked differential equations as was required for the spherical cell. At each time step Δt, the three gating probabilities are solved using the implicit Trapezoid method, as shown for the n probability in equation 34. The membrane voltage can then solved using Equation 35 using either the forward or backward Euler methods. The forward Euler method has the same stability problem as for the passive cable but will work for relatively small numbers of compartments (*ForEulerHHcable.m*).

The half-step backward Euler is the method of choice since it is unconditionally stable and second order accurate when used in combination with implicit Trapezoid method for the gating probabilities.

$$\mathbf{v}_{n+\frac{1}{2}} = \mathbf{v}_n + \frac{\Delta t}{2C_m}\left(\mathbf{f}_{\mathrm{n+1}} - \mathbf{d}_{\mathrm{n+1}}\mathbf{v}_{n+\frac{1}{2}} + \mathbf{B}\mathbf{v}_{n+\frac{1}{2}}\right)$$

Bring terms dependent on $\mathbf{v}_{n+1/2}$ to the LHS.

$$\frac{2C_m}{\Delta t}\mathbf{v}_{n+1/2} + \mathbf{d}_{n+1}\mathbf{v}_{n+1/2} - \mathbf{B}\mathbf{v}_{n+1/2} = \frac{2C_m}{\Delta t}\mathbf{v}_n + \mathbf{f}_{n+1}$$

$$\mathbf{v}_{n+1} = \mathbf{C}^{-1}\left(\frac{2C_m}{\Delta t}\mathbf{v}_n + \mathbf{f}(t)\right) \qquad 35$$

where $\mathbf{C} = \text{diag}\left(\frac{2C_m}{\Delta t} + \mathbf{d}_{n+1}\right) - \mathbf{B}$.

Matrix $\mathbf{C}$ is dependent on the values in vector $\mathbf{d}$, which change with each time step, so this matrix must be continuously updated.

The voltage vector $\mathbf{v}$ is then advanced linearly an additional half-step to complete the cycle for each Δt.

$$\mathbf{v}_{j+1} = 2\mathbf{v}_{j+1/2} - \mathbf{v}_j$$

This method is implemented in *BackEulerHHcable.m*.

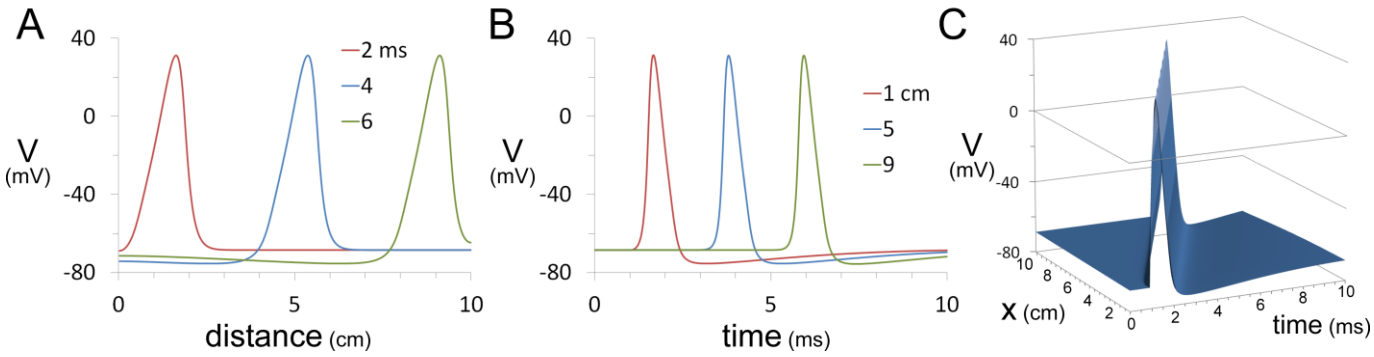

Figure 13. Action potential traversing an axon. A. Voltage profile along the length of the axon at simulation times 2, 4 and 6 ms, showing the wave of depolarization moving along the axon. B. Voltage profile in compartments 1, 5 and 9 cm along the cable. Action potentials arrive later with distance along the axon. C. Voltage plotted with respect to both time and location along the cable. The equivalent circuit was a model of the squid giant axon, 10 cm long with a radius of 238 μm. The cell membrane had a specific capacitance of 1 uF/cm^2, a specific leak conductance of 0.3 mS/cm^2, a specific sodium conductance of 120 mS/cm^2 and a specific potassium conductance of 36 mS/cm^2. The coupling resistance between compartments was 0.0354 kΩcm. Current injection was 20 μA for 0.1 ms, ending at time = 1 ms. Matlab program *BackEulerHHCable.m* was used for the simulation.

Additional Reading

'Mathematics for Neuroscientists" by F. Gabbiani and S. J. Cox gives a more complete and rigorous description of this material.

Problems

1. Using the Matlab file *ForEulerRC.m* as a template solve the RC circuit equation 4 using the Runge-Kutta 4th order and backward Euler methods.
2. For a 20 μm diameter cell for which the cell membrane has a specific capacitance of 1 uF/cm^2 and a specific leak conductance of 0.3 mS/cm^2.
   a. Determine the magnitude of the steady-state voltage response to a 50 pA current injection.

b. Using the Matlab file *ForEulerLeak.m* as a template use equation 12 and the Runge-Kutta 4th order method, plot the response of the cell to the following current injections: -0.1, -0.05, 0, 0.05 and 0.1 nA.

3. Solve the Hodgkin and Huxley rate equations using the backward Euler method. The Matlab file *VoltageClamp.m* can be used as a template.

4. Demonstrate that solution of the linked differential equations (equations 23-26) using a combination of the implicit Trapezoid method and the backward Euler method described in section 4 is in fact second order accurate with respect to voltage. Run simulations at Δt = 0.1, 0.01, 0.001, 0.0001 and 0.00001. Assume that the finest resolution time step is exact and derive errors for the other time steps relative to that solution. The Matlab file *HHcell.m* can be used as a template.

Appendix 2 Numerical Methods for First Order Differential Equations

Most differential equations cannot be solved analytically. As a consequence, an array of numerical methods have been developed to produce approximate solutions, typically by making successive stepwise approximations across some finite interval from a defined starting point. Although there are specialized software packages available for this purpose there are many occasions when it is necessary to produce a home-brew solution. It is also useful to understand the basic principles of these methods in order to understand the limitations of different packaged methods. This appendix provides the background necessary to solve common differential equation problems using numerical methods.

The goal is to approximate a solution for the differential equation,

$$\frac{dy}{dt} = f(t, y) \qquad \text{A2.1}$$

over the interval $0 \leq t \leq T$. Typically there will be an infinite number of solutions and in order to select a specific solution it is also necessary to define an initial condition.

$$y(0) = y_0$$

This combination of a differential equation, a fixed interval for solution and a defined initial condition is known as an initial value problem.

To make this a tractable problem for computation, the continuous differential equation is converted into a difference equation in discrete-time, which is equally-spaced points in time, separated by some finite time difference Δt. The first step is to convert the continuous interval $0 \leq t \leq T$ into a finite number of discrete steps. In the simplest case the steps are all of equal length so that,

$$\Delta t = \frac{T}{N}$$

where, N is the number of steps in the interval. This creates the series $t_0 = 0,\ t_1 = t_0 + \Delta t,\ t_2 = t_1 + \Delta t, \dots,\ t_{n+1} = t_n + \Delta t, \dots,\ t_N = T$ for which we wish to determine the corresponding y-values $y_0,\ y_1,\ y_2, \dots,\ y_{n+1}, \dots, y_N$.

There are two broad classes of numerical methods for the solution of differential equations known as explicit and implicit methods. Each has some advantages. Explicit methods are generally easier to program for a broad range of differential equations and are usually less computationally intensive. Implicit methods are generally more stable.

1. Explicit Methods

1.1 Forward Euler Method

The forward Euler method is the easiest numerical method to understand and to program. The method is inaccurate relative to more complex methods and can be unstable. These disadvantages can be minimized to some degree by using small step sizes but more complex algorithms are usually a better choice. Nonetheless, this method can be a good first choice to get some initial feedback on a particular problem because its inherent simplicity minimizes the chance of introducing inadvertent programming errors. There are several different ways to understand the forward Euler method.

The derivative is defined as,

$$\frac{dy}{dt} = \lim_{h \to 0} \frac{y(t+h) - y(t)}{h}$$

The discrete form of this equation is,

$$\frac{dy}{dt} \approx \frac{y(t+\Delta t) - y(t)}{\Delta t} \qquad \text{A2.2}$$

Using this approximation with equation A2.1 gives

$$\frac{y_{n+1} - y_n}{\Delta t} = f(t_n, y_n) \qquad \text{A2.3}$$

and rearranging gives the forward Euler method,

$$y_{n+1} = y_n + \Delta t \cdot f(t_n, y_n) \qquad \text{A2.4}$$

which is used to march across the interval $0 \le t \le T$.

$$\begin{aligned} y_0 &= y_0 \\ y_1 &= y_0 + \Delta t \cdot f(t_0, y_0) \\ y_2 &= y_1 + \Delta t \cdot f(t_1, y_1) \\ &\dots \\ y_N &= y_{N-1} + \Delta t \cdot f(t_{N-1}, y_{N-1}) \end{aligned}$$

It is an explicit method because at every step all of the variables on the right hand side of the equation are known, making computation of the next step trivial.

The geometric interpretation is illustrated in Figure 1A. The differential equation $dy/dt = f(t_n, y_n)$ gives the tangent or slope at any point along the curve,

$$\text{slope of curve at } t_n = f(t_n, y_n) = \frac{\text{rise}}{\text{run}} = \frac{y_{n+1} - y_n}{\Delta t}$$

which again gives equation A2.4.

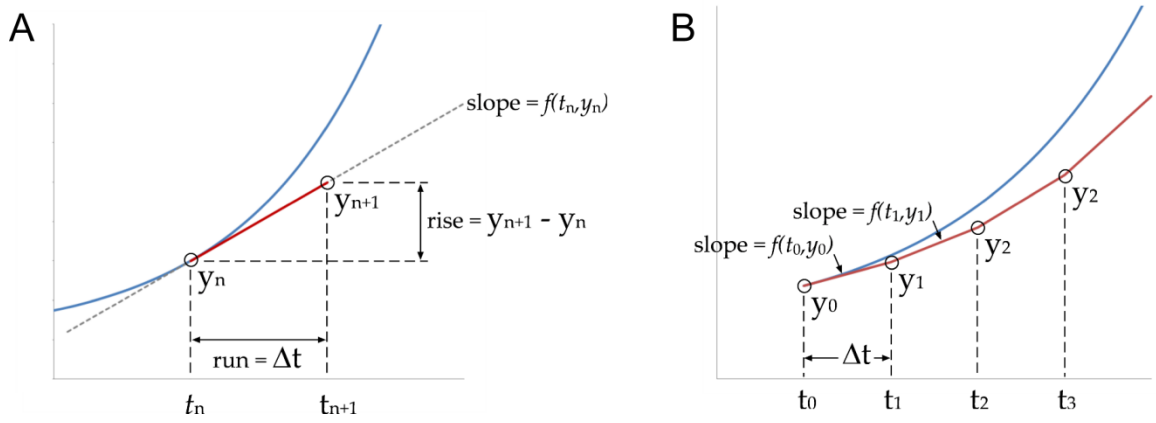

Figure 1. A) Forward Euler method. The exact solution is the blue line and the forward Euler estimate for one step Δt is shown in red. B) The forward Euler estimate for successive steps of Δt.

To begin the march across the entire time interval the tangent at t_0 is projected forward a distance of Δt to t_1 (Fig. 2). It is then assumed that y_1 is on or close to the curve at t_1 and the tangent $dy/dt = f(t_1, y_1)$ is evaluated again and the process repeated. Clearly errors in this process are unavoidable and they can accumulate.

A third way to derive the forward Euler method is from the Taylor series expansion of y about t.

$$y(t+\Delta t) = y(t) + \Delta t y'(t) + \frac{1}{2}\Delta t^2 y''(t) + \frac{1}{3!}\Delta t^3 y'''(t) + \cdots + \frac{1}{n!}\Delta t^n y^{(n)} + \cdots$$

Truncating the Taylor series at the second term, $\Delta t y'(t)$, and rearranging for $y'(t)$ gives,

$$y'(t) = \frac{y(t+\Delta t) - y(t)}{\Delta t} + O(\Delta t)$$

where $O(\Delta t)$ represents all the terms after the first term and is a measure of the error of the method.

1.2 Explicit Trapezoidal Method

This method has multiple names, it also known as Heun's method and the modified Euler method. The algorithm for the modified Euler method requires two evaluations of the function $dy/dt = f(t,y)$ for each Δt step, making it twice as expensive computationally as the forward Euler method.

$$y^*_{n+1} = y_n + \Delta t \cdot f(t_n, y_n) \qquad \text{A2.5}$$

$$y_{n+1} = y_n + \frac{\Delta t}{2}\left(f(t_n, y_n) + f(t_{n+1}, y^*_{n+1})\right) \qquad \text{A2.6}$$

The first equation is simply the forward Euler method, which produces an initial prediction of y_{n+1}, called y^*_{n+1}. The second equation produces the corrected estimate of y_{n+1}.

This method also has a simple geometric interpretation (Figure 2). The forward Euler method is used to make an initial prediction of y^*_{n+1}. The slope at point (t_{n+1}, y^*_{n+1}) is given by $f(t_{n+1}, y^*_{n+1})$. The corrected estimate of y_n uses a numerical average of these two measures of the slope.

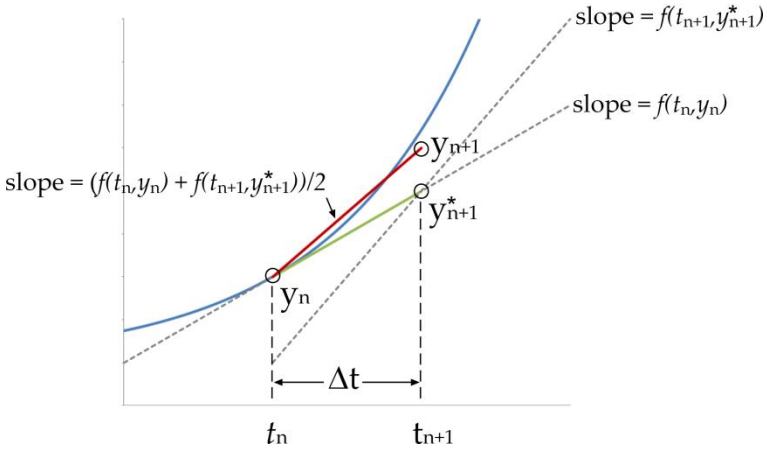

Figure 2. Modified Euler method. The exact solution (blue), forward Euler estimate (green) and modified Euler estimate (red) are shown. The modified Euler produces a notably improved estimate of y_{n+1} compared to the forward Euler method.

1.3 Runge–Kutta 4th order Method

The 4th order Runge-Kutta method or RK4 requires four evaluations of the function for each time step. The marching scheme is given by the following set of equations.

$$k_1 = \Delta t \cdot f(t_n, y_n)$$

$$k_2 = \Delta t \cdot f\left(t_n + \frac{1}{2}\Delta t, y_n + \frac{1}{2}k_1\right)$$

$$k_3 = \Delta t \cdot f\left(t_n + \frac{1}{2}\Delta t, y_n + \frac{1}{2}k_2\right)$$

$$k_4 = \Delta t \cdot f(t_{n+1}, y_n + k_3)$$

$$y_{n+1} = y_n + \frac{1}{6}(k_1 + 2k_2 + 2k_3 + k_4)$$

In this method $f(t_n, y_n)$ is the slope at the beginning of the interval $[t_n,\ t_n + \Delta t]$, $f(t_n + 1/2\,\Delta t,\ y_n + 1/2\,k_1)$ is the predicted slope in the middle of the interval, $f(t_n + 1/2\,\Delta t,\ y_n + 1/2\,k_2)$ is a corrected estimate of that slope and $f(t_{n+1},\ y_n + k_3)$ is the slope at the end of the interval. The four estimates of the slope are averaged, giving greater weight to the two center estimates.

1.4 Accuracy of explicit methods

The mathematical framework for analyzing the numerical error of ODE solution methods uses the Taylor Series expansion of the solution function, y.

$$y(t + \Delta t) = y(t) + \Delta t y'(t) + \frac{1}{2}\Delta t^2 y''(t) + \frac{1}{3!}\Delta t^3 y'''(t) + \cdots + \frac{1}{n!}\Delta t^n y^{(n)} + \cdots$$

This expansion is as a series of increasingly accurate approximations of the function y. The simplest approximation to y near t is simply $y(t)$. Addition of the second term, $\Delta t y'(t)$, forms the linear approximation to y. As noted earlier this is the approximation used in the Forward Euler Method. The local truncation error of the forward Euler method is $O(dt^2)$ (pronounced 'big-oh dt squared'). This is because the error term (i.e. the sum of the terms we ignored) is dominated by the term ½ $dt^2\, y''(t)$. The dt^2 term dominates because for very small dt, say $dt = 10^{-3}$, we have $dt^2 = 10^{-6}$, $dt^3 = 10^{-9}$, $dt^4 = 10^{-12}$ and so on. Hence, the dt^2 term is by far the largest of all the error terms.

The local accuracy of the Explicit Trapezoid Method and the Runge-Kutta 4th Order Method is determined similarly. Their local truncation errors are $O(dt^3)$ and $O(dt^5)$ respectively. This means that they match the Taylor Series expansion up to and including the dt^2 term for the Explicit Trapezoid Method and the dt^4 term for the RK4.

Generally we are more concerned with the global truncation error – the total accumulated error at the end of the simulation. Determination of the global truncation error relies on a theorem that roughly states , if the local truncation error is $O(dt^n)$ then the global truncation error is $O(dt^{n-1})$. This means that the Euler method is 1st order accurate $O(dt)$, the Explicit Trapezoid Method is 2nd order $O(\Delta t^2)$and the RK4 method is 4th order $O(dt^4)$.

There are two ways to gain accuracy in solving initial value problems, decrease the step size or use a higher order and more accurate method. The greatest accuracy for the least amount of computational effort is desirable, where the amount of computation is determined by the number of times the function, f, is evaluated. The Euler method is computationally inexpensive (only one function call per step) but has a low order of accuracy. The RK4 is more expensive (four function calls per step) but is accurate up to 4th order.

To decide how to strike this balance we will use the fact that if the error of an approximation is $O(dt^n)$ then the error is usually roughly equal to some constant multiplied by dt^n. For the Euler method if the step size is decreased by a factor of 4, making the computation four times as expensive, then the global

truncation error also decreases by a factor of four since the global truncation error is O(dt). However, for the same computational cost we could keep the original step size but switch to the RK4 method, which would reduce the error by a factor of h^3. For small h this is a much bigger improvement than we would get from decreasing the step size in the Euler method making the RK4 method a better choice.

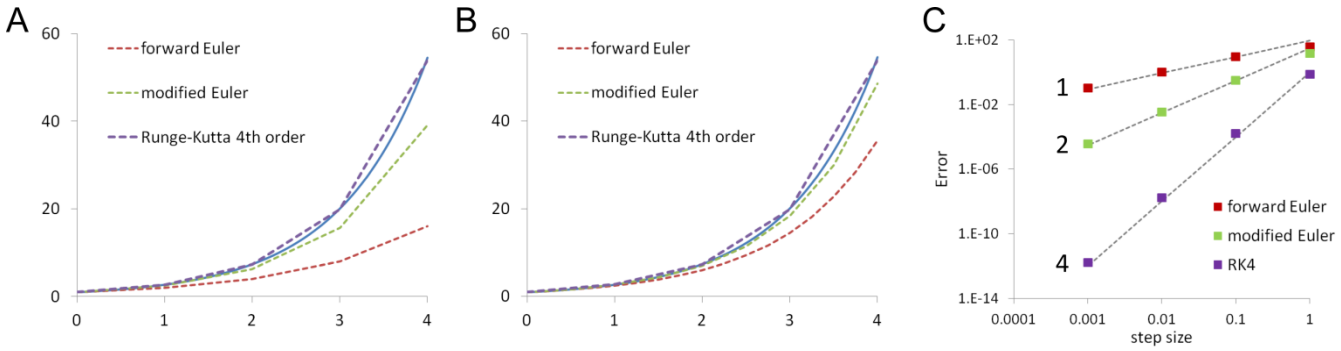

Figure 3. Comparison of forward Euler, modified Euler and Runge-Kutta 4th order methods with the exact solution of $dy/dt = y$. A. Equal step size. B. Equal number of function evaluations ie. the step size for the forward Euler is 4 and 2 times smaller than that for the modified Euler and Runge-Kutta method respectively. C. Effect of changing step size on error size for the three methods. Dashed lines are fits to the error values with exponents of 1, 2 and 4.

This is shown graphically in Figure 4.3. The 4th order Runge-Kutta method is remarkably accurate for large step sizes, much better than the other two methods (Fig. 3A). This advantage is retained when the comparison is controlled for equal computational effort (i.e. equal number of function evaluations) (Fig. 3B).

The effect of the order of accuracy of a solution method can be seen using a log-log plot of the global error against the step size, dt (Fig. 3C). If the method is $O(dt^n)$ then the errors should fall close to a straight line with gradient n. A plot of the error versus step size for the three methods (Fig. 3C) shows how much faster the error declines for the 4th order Runge-Kutta method with decreasing step size compared to the 1st order forward Euler method. The 4th order Runge-Kutta produces a better estimate for less computational cost. There are diminishing returns and increased complexity with even higher order methods and RK4 method is generally the method of choice amongst fixed step explicit numerical methods.

2. Implicit Methods

2.1 Backward Euler Method

The backward Euler method is given by the following formula

$$y_{n+1} = y_n + \Delta t \cdot f(t_{n+1}, y_{n+1}) \qquad \text{A2.7}$$

This has the same form as the forward Euler method, with $f(t_{n+1}, y_{n+1})$ substituted for $f(t_n, y_n)$. It has similar geometrical interpretation except that the slope is now calculated at the end of the time step rather than the beginning. For explicit methods all of the terms on the right hand side of the equation are known so that y_{n+1} can be determined explicitly. For the backward Euler method y_{n+1} appears on both sides of the equality, which means that some work must be invested to evaluate y_{n+1}. The amount of work required depends on the nature of the function.

This is best illustrated with an example. For,

$$\frac{dy}{dt} = -y$$

using the reverse Euler method (equation A2.7),

$$y_{n+1} = y_n + \Delta t \cdot (-y_{n+1})$$

rearranging gives,

$$y_{n+1} = \frac{y_n}{1 + \Delta t}$$

In this case it is easy to isolate an explicit solution for y_{n+1} in terms of y_n. In most cases this is not as straightforward and it will be necessary to use a numerical root-finding method to solve for y_{n+1}. This can add considerable computational overhead, making the method impractical. The advantage of using this implicit method is that it is more stable than the equivalent explicit method, as shown in Figure 4.

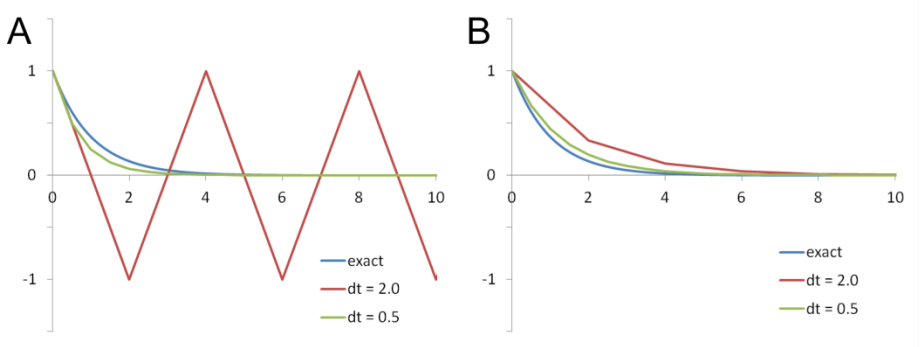

Figure 4. Comparison of forward Euler and backward Euler methods for the solution of $dy/dt = -y$. A. Forward Euler with exact and estimated solutions with Δt = 0.5 and 2.0. B. Backward Euler with exact and estimated solutions with Δt = 0.5 and 2.0. Exact solution is $y(t) = e^{-t}$.

Although the backward Euler method is 1st order and, like the forward Euler method, is slow to converge on the exact solution with decreasing step size, it behaves much more predictably than the forward Euler at large step sizes. While the forward Euler is prone to verge into instability the forward Euler remains stable (Fig. 4). This can be a significant advantage particularly when dealing with systems of differential equations in which rates of change for different variables can occur on widely varying times scales. Even if the solution for some variables is not especially accurate an implicit method will not blow up as easily as an explicit method. Systems of differential equations that are unstable when solved using explicit methods are generally known as stiff and are best solved using an implicit method.

2.2 Implicit Trapezoid Method

The implicit trapezoid method is also known as the Adams-Moulton One-Step method.

$$y_{n+1} = y_n + \frac{\Delta t}{2}\left(f(t_n, y_n) + f(t_{n+1}, y_{n+1})\right) \qquad \text{A2.8}$$

This is an implicit second-order method, requiring two function evaluations per step. It is a numerical average of the forward and backward Euler methods. It is the implicit analog of the explicit modified Euler method. Like the backward Euler method it can be converted to an explicit function for certain functions including the Hodgkin and Huxley rate equations, which are solved using this method in Chapter 5.

Additional Reading

'Numerical Analysis" by T. Sauer gives a much more complete and rigorous description of this material.

Examples and Problems

1. The best way to understand how these different methods work is to create a table for a series of steps to see how they evolve. Two examples are provided in the form of Excel files.

Example 1.xlsx

$$\frac{dy}{dt} = y$$
$$y_0 = 1$$
$$0 \le t \le 4$$

The exact solution is, $y(t) = e^t$.

Example 2.xlsx

$$\frac{dy}{dt} = t + y$$
$$y_0 = 0$$
$$0 \le t \le 4$$

The exact solution is, $y(t) = e^t - t - 1$.

Using these files as templates, solve the following problem using the forward Euler, modified Euler and Runge-Kutta 4th order methods.

$$f(t, y) = ty + t^3$$
$$y_0 = 1$$
$$0 \le t \le 4$$

The exact solution is, $y(t) = 3e^{t^2/2} - t^2 - 2$.

2. Solve problem 1, solve using Matlab. Two Matlab files (*example1.m* and *example2.m*) are provided as templates using the examples given above.

3. For the differential equation described in Question 1 show that the forward Euler, modified Euler and Runge-Kutta methods are 1st , 2nd and 4th order methods respectively by graphing the errors. Solve the differential equation over the range $0 \le t \le 4$ for dt = 1.0, 0.1 , 0.01, 0.001 and 0.0001. Determine the difference between the estimated value and the exact solution at $t = 4$ and plot on a log-log plot. For very small steps, $dt < 0.0001$, truncation errors within Matlab may produce inaccurate results. At large steps the errors may deviate from a straight line on the log-log plot. Fit the error values over the linear range.

4. Demonstrate the superior stability of an implicit method compared to the equivalent explicit method by solving the following stiff equation using both the forward and backward Euler methods.

$$\frac{dy}{dt} = 10(1 - y)$$
$$y_0 = 0.5$$
$$0 \le t \le 4$$

The explicit solution is $y = 1 - e^{-10t}/2$. Demonstrate what happens when the step size is larger than Δt = 0.1.